Sorbent characterization and application of the in-tube microextraction technique

Dissertation

zur Erlangung des akademischen Grades eines
Doktors der Naturwissenschaften
– Dr. rer. nat. –

vorgelegt von

Xochitli Libertad Osorio Barajas

geboren in Guadalajara, Jalisco, Mexiko

Institut für Instrumentelle Analytische Chemie
der
Universität Duisburg-Essen

2016

Die vorliegende Arbeit wurde im Zeitraum von Mai 2013 bis Juli 2016 im Arbeitskreis von Prof. Dr. Torsten C. Schmidt am Institut für Instrumentelle Analytische Chemie der Universität Duisburg-Essen durchgeführt.

Tag der Disputation: 13. Dezember 2016

Gutachter:	Prof. Dr. Torsten C. Schmidt
	PD Dr. Hans-Georg Schmarr
Vorsitzender:	Prof. Dr. Karin Stachelscheid

Summary

Extraction techniques are a key part of sample preparation. The miniaturization and automatization of these techniques provide the opportunity of a higher sample throughput with more precise results. Furthermore, solventless microextraction techniques are environmental friendly, in comparison to other extraction techniques. Nonetheless the selection of the sorbent for extraction is currently based on experience or via trial and error, which is time consuming and could lead to suboptimal choices. ITEX is a solventless microextraction where the headspace of samples is dynamically enriched on the chosen sorbent and thermodesorption is applied to proceed with the separation and detection of the sample. The analysis of the sorbent for the extraction of the sample needs a more detailed investigation to further understand and improve the ITEX technique.

Among the material characterization techniques, inverse gas chromatography was applied to investigate three commercial sorbents for ITEX. Inverse gas chromatography provides the parameters which are needed to be determined for the purpose of this thesis, such as sorption enthalpy (ΔHs), partitioning constant between the solid and gas phase (K_d) and kinetic parameters like the diffusion coefficient (D^{∞}), dispersion coefficient (D^*), and apparent permeability (P_{app}). PDMS, Tenax TA and Carbopack C were studied in this thesis. For the analyzed probes, Tenax TA proved to be the most suitable sorbent for extraction.

Due to the 160 µL available in the body of the stainless steel ITEX cannula, a manifold of materials can be packed and tested. Carbon based-nanomaterials and polymeric ionic liquids are gaining popularity and both materials are not commonly applied as sorbent in ITEX. To evaluate their analytical performance, polycyclic aromatic hydrocarbons were chosen as analytes for carbon based-nanomaterials, while for the polymeric ionic liquids short chained alcohols were selected. A HS-ITEX-GC/MS method was applied for both materials. The optimal parameters for the two applications were selected in different fashions. On one hand with a Box-Behnken design and on the other hand with parameters reported in literature. Once the suitable extraction parameters were established, then the method was validated.

Since five carbon based-nanomaterials and four extraction parameters at three levels were investigated, a response surface methodology was applied to determine the optimal parameters. A Box-Behnken design was set and from the results, fullerenes were the sorbent of choice to perform a full determination of the figures of merit. The linear range covered four orders of magnitude (from 0.25 to 250 µg L^{-1}), the method detection limit was comparable or improved in comparison to other sorbents (0.01 to 0.3 µg L^{-1}) and similar recovery values

were also obtained (45 to 103 %). For the analysis of larger polycyclic aromatic hydrocarbons with carbon based-nanomaterials, enough surface and active sites must be available to screen a large amount of them. Otherwise, only the small polycyclic aromatic hydrocarbons will be extracted. In comparison to Tenax GR as sorbent, carbon based-nanomaterials are a more suitable sorbent for extraction.

For the polymeric ionic liquids, to some extent the same extraction parameters as for a commercial material were set. By this, direct literature comparison was performed. The results were comparable, but the expected improvement was not achieved. A linear range from 0.55 to 5,500 µg L^{-1} and limits of detection from 0.3 to 15.1 µg L^{-1} were achieved. The recovery values obtained from spiked beer yielded a poor response (0.1 to 45 %). Nonetheless, with polymeric ionic liquids a lower thermodesorption was set and the extraction yield was comparable. A hydrophobic behavior of the polymeric ionic liquid could improve its analytical performance. This can be modified during its synthesis, by changing the anion and increasing the alkyl chain. Material characterization via inverse gas chromatography could be applied to confirm that for the one type of polymeric ionic liquid as sorbent in ITEX, derivatized aldehydes are a more suitable group of probe compounds for analysis than short chained alcohols. As well as to define that for the second polymeric ionic liquid, short chained alcohols are appropriate probe compounds for investigation. Finally, via inverse gas chromatography, it would be possible to further explain the differences between the polymeric ionic liquids applied in this thesis.

Kurzfassung

Extraktionstechniken sind ein Schlüsselprozess in der Probenvorbereitung. Die Miniaturisierung und Automatisierung von dieser Techniken erhöht den Probendurchsatz und ergibt präzisere Ergebnisse. Außerdem gelten lösungsmittelfreie Mikroextraktionstechniken als umweltfreundlicher im Vergleich zu anderen Anreicherungsmethoden. Ein Nachteil ist jedoch, dass die Entscheidung für ein geeignetes Sorbens meist auf Erfahrungswerten basiert und somit sehr zeitaufwendig ist. Außerdem können die Ergebnisse der Selektion möglicheriwese nicht optimal sein. ITEX ist eine lösungsmittelfreie Mikroextraktionstechnik, in der die Gasphase über einer Probe aktiv am Sorbens angereichert wird. Mittels Thermodesorption werden die angereicherten Analyten den Gaschromatograph überführt, in dem die Trennung und Detektion der Analyten erfolgt. Um die ITEX-Techniken besser zu verstehen und weiter zu entwickeln, ist eine detaillierte Analyse der Sorbenseigenschaften erforderlich.

Im Rahmen dieser Arbeit wurde inverse Gaschromatographie angewandt, um drei kommerziell verfügbare ITEX Sorbenzien zu charakterisieren. Die Sorptionsenthalpie (ΔHs), die Verteilungskonstante zwischen Festphase und Gasphase (K_d), der Diffusionskoeffizient (D^{∞}), der Dispersionskoeffizient (D^*) und die scheinbare Permeabilität (P_{app}) wurden bestimmt. PDMS, Tenax TA und Carbopack C wurden als Packungsmaterial untersucht. Bei den angewendeten Modellanalyten und Sorbenzien, erwies sich Tenax TA als das am besten geeignete Sorbens für die Extraktion.

Die ITEX Edelstahl Kanüle hat einen 160 µL Hohlraum, dadurch entsteht die Möglichkeit, eine große Vielfalt an Materialien zu packen und zu testen. Kohlenstoff-basierte Nanomaterialien und polymere ionische Flüssigkeiten sind interessante Materialien, die man als Sorbens in ITEX anwenden könnte. Da beide Materialien nicht üblicherweise als Sorbens für die Anreicherung aus der Gasphase von Proben genutzt wurden, ist ihre Untersuchung vielversprechend. Polyzyklische aromatische Kohlenstoffe wurden genutzt, um die Kohlenstoff-basierten Nanomaterialien zu validieren und kurzkettige Alkohole wurden verwendet, um die polymere ionische Flüssigkeiten zu analysieren. Für beide Methoden wurde eine HS-ITEX-GC/MS Methode angewendet. Die optimierten Extraktionsparameter wurden auf zwei verschiedenen Arten bestimmt. Einerseits mit einem Box-Behnken Versuchsplan, anderseits mit Exktraktionsparameter aus der Literatur. Anschließend, wurden beide Methoden mit den optimierten Extrakationsparameter validiert.

Fünf verschiedene Kohlenstoff-basierte Nanomaterialien mit vier Extraktionsparametern (je in drei Levels) wurden gemessen. Eine statistische Versuchsplanung wurde angewendet, um die optimalen Extraktionsparameter zu bestimmen. Das Box-Behnken Design ergab, dass Fulleren das am besten geeignete Sorbens war, so dass die nachfolgende Validierung damit durchgeführt wurde. Der lineare Bereich umfasste vier Größenordnungen (von 0.25 bis 250 µg L^{-1}) und die Nachweisgrenzen (0.01 zu 0.3 µg L^{-1}), sowie Wiederfindungsraten (45 zu 103 %) waren vergleichbar oder besser als bisher in der Literatur angegeben. Größere polyzyklische aromatische Kohlenstoffe benötigen eine größere Oberfläche, an der die Sorption stattfinden kann. Ansonsten werden nur die kleineren polyzyklischen aromatischen Kohlenstoffe angereichert. Im Vergleich zu dem kommerziell erhältlichen Sorbens, Tenax GR, haben sich Kohlenstoff-basierte Nanomaterialien als besser geeignete Sorbenzien herausgestellt.

Für polymere ionische Flüssigkeiten wurden die optimalen Extraktionsparametern von einem anderen Sorbens partiell übernommen. Ein direkter Literaturvergleich war möglich. Die Ergebnisse waren ähnlich, aber die erwartete Verbesserung wurde nicht bestätigt. Der lineare Bereich lag zwischen 0.55 und 5,500 µg L^{-1} und die erreichten Nachweisgrenzen lagen zwischen 0.3 und 15.1 µg L^{-1}. Die Wiederfindungsraten in dotierten Bierproben lieferten schlechte Ergebnisse (0.1 zu 45 %). Dennoch konnte gezeigt werden, dass trotz der niedrigeren Thermodesorptiontemperatur ähnliche Peakausbeuten erreicht wurden. Die analytische Leistung der polymere ionische Flüssigkeiten, könnte mittels einer hydrophobischen Eigenart gesteigert werden. Diese Merkmale können während der Synthese geändert werden, in dem man ein anderes Anion auswählt und eine längere Alkylkette einsetzt. Material Charakterisierung mittels inverse Gaschromatographie, würde hilfreich sein um zu beweisen, dass derivatisierte Aldehyde bessere Modellanalyten als kurzkettige Alkohole für die erste polymere ionische Flüssigkeiten sind. Auch, um zu bestaetigen, dass die kurzkettige Alkohole gute Modellanalyte für Analyse mit der zweiten polymere ionische Flüssigkeit sind. Abschließend, die Unterschiede zwischen den polymere ionische Flüssigkeiten, werden weiterhin mittels inverse Gaschromatographie erläutern.

Table of contents

Chapter 1 General Introduction

1.1 Microextraction techniques

In analytical chemistry a proper sample preparation before the introduction of the sample into the separation and analysis equipment is a requirement to obtain meaningful data. Sample preparation still accounts for the major inaccuracies and time consumption of the total analytical process [1], thus further development has huge potential for improvements. It is required to remove matrix components that could interfere with the separation, providing suitable analytes for analysis and enhancing its detection and separation. [2] An option to improve the sample preparation step, would be the transfer of traditional sample preparation methods to microextraction methods. [1] Drawbacks such as human error, amount of work, sample preparation and preconcentration in various steps, are issues that can be overcome nowadays, because most of these techniques can be automated and [3] miniaturized. [1] Microextraction techniques, such as solid phase microextraction (SPME), in-tube extraction (ITEX) and liquid phase microextraction (LPME) represent an improvement in this field and are characterized by the smaller extraction phase amount in comparison to the sample volume. [2] [4]

The extraction can be performed in a static or dynamic fashion, and the techniques are divided into solvent or solventless techniques. The main difference between static and dynamic mode is that in static analysis, a defined headspace volume of a sample at equilibrium (the sample is usually conditioned with temperature to establish equilibrium conditions) is extracted once, [5] thus mainly only the free concentration of the analytes is investigated. [1] While in the dynamic mode, the headspace above the liquid or solid sample is continuously removed (in Figure 1-1, t corresponds to each time the headspace is removed) and trapped, changing the concentration of the analyte in the HS (it decreases) and each time the equilibrium between sample and headspace is reestablished. [6] Higher sensitivity is achieved, [5] because a larger amount of analyte is extracted in a shorter time frame, in contrast to the static fashion where the extraction would take too long. Figure 1-1 exemplifies the situation that under static conditions the time required to extract the same amount would be longer in comparison to the dynamic mode.

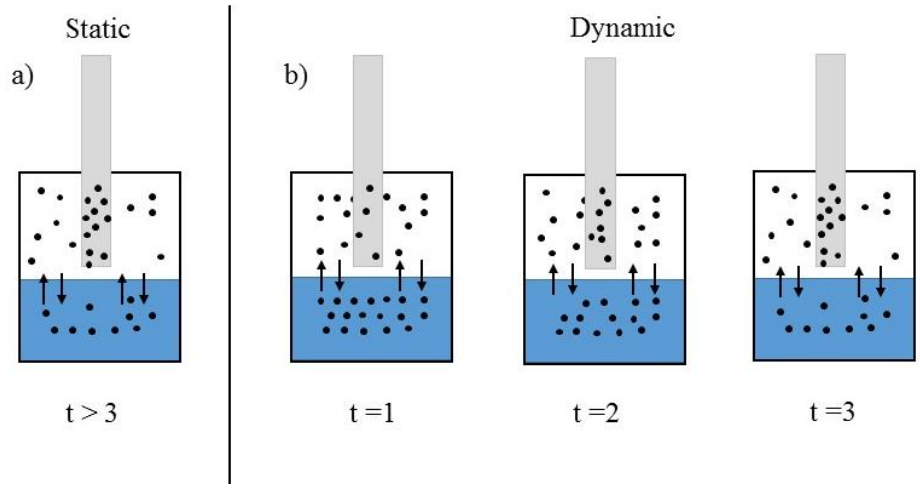

Figure 1-1. Static (a) and dynamic (b) extraction mode. Sorbent in grey and analytes in black. The time required to reach the same extraction efficiency under a static extraction, is longer than for the dynamic extraction (t > 3 and t =3, respectively).The concentration in the HS decreases and the equilibrium is reestablished on every step.

Examples for solvent microextraction techniques are LPME, single-drop LPME, [1] hollow-fiber LPME (HF-LPME), dispersive liquid-liquid microextraction (DLLME), electromembrane extraction (EME) and supported liquid membrane (SLM). [4] [7]

Solventless microextraction techniques can be classified into, i) application of a coating on the surface of a rod or needle ii) sorbent material packed in a tube or needle. [8] PAL SPME Arrow, SPME, high-capacity headspace sorptive extraction (HSSE), stir bar sorptive extraction (SBSE), and solid phase dynamic extraction (SPDE) are examples of type i). [2] [9] The extraction is usually performed in a static mode, with the exception of SPDE. In-tube extraction (ITEX) and needle trap (NT) are classified under type ii) and the extraction, in contrast to the above mentioned solventless microextraction techniques, is carried out in a dynamic mode.

ITEX is commercially available since 2006. It features a sorbent bed volume of 160 µL and is a fully automatable device. This void volume gives the opportunity to pack a great variety of materials to be used as sorbents in the extraction step for analysis of different compounds/samples. The stainless steel needle, packed with a sorbent, is surrounded by an external heater unit. The needle is connected to a 1.3-mL gas-tight syringe with a side-port. Enrichment is carried out by aspirating and dispensing the syringe several times (strokes) and pumping the sample headspace through the sorbent bed at a corresponding extraction flow. After extraction, the analytes are thermodesorbed into the injector of the gas chromatograph with a portion of the sample headspace or aspirated carrier gas from the injector. Finally, the syringe is withdrawn from the injector, the plunger is moved above the side port and the

heated trap is flushed with inert gas (N_2, He) to clean it and to avoid possible carryover. A schematic depiction of the steps in the ITEX procedure is given in Figure 1-2.

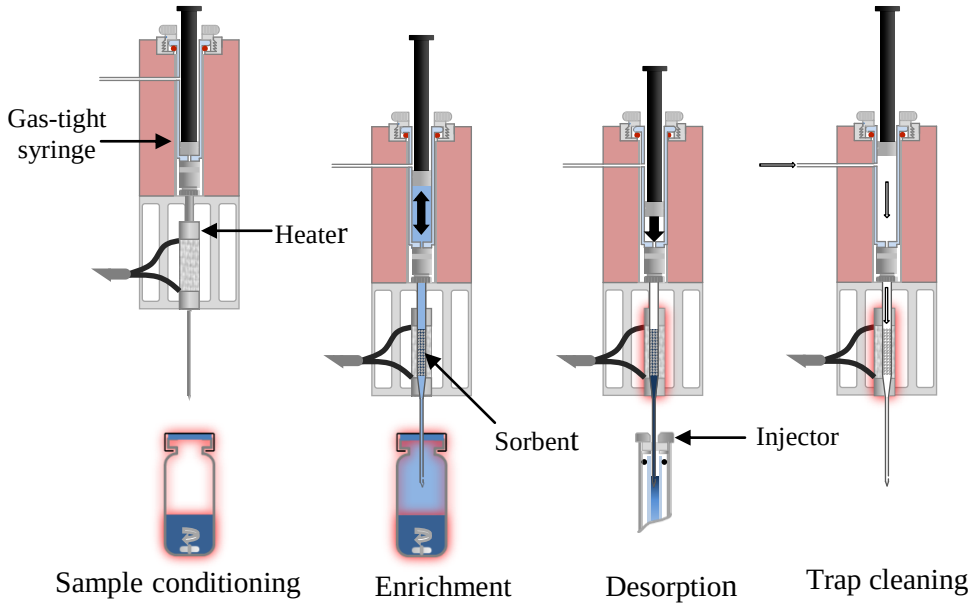

Figure 1-2. Dynamic extraction steps for ITEX. [3]

In comparison to common headspace (HS) methods, ITEX achieves a higher sensitivity and usually lower method detection limits than HS. [10] [11] Figure 1-3 demonstrates the advantage of applying an enrichment technique over a HS injection with the exemplary comparison of naphthalene intensities obtained A time difference is observed because after performing the extraction with ITEX, the polycyclic aromatic hydrocarbons (PAHs, in this example, naphthalene is depicted) were injected and focused with the help of a cryotrap unit for one minute. The column length difference also influenced the shift in time for the detection of naphthalene. For ITEX a 60 m long column was used, while for the HS experiments a 30 m long column was applied.

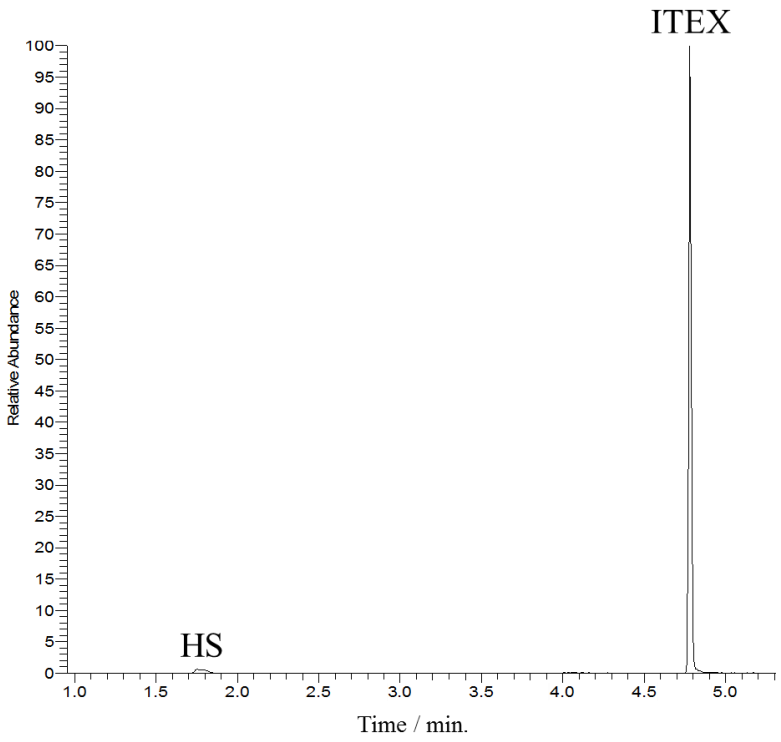

Figure 1-3. Overlap of two different naphthalene injections (HS and ITEX), depicted in one chromatogram for comparison porpuse. Normalized at max. intensity of ITEX = 1.88×10^{6}. *m/z* = 128. Fullerenes as sorbent in ITEX. For this example, the intensity ratio from ITEX/HS equals 145 times.

In the ITEX extraction procedure, several parameters must be optimized prior to a full method validation. The decisive factors are: type of sorbent for the corresponding analytes, number of strokes and its flow, temperature for sample extraction and desorption temperature. [12] The optimization step can then be performed either with the common one-variable-at-the-time approach or via design of experiments (DoE). [13] The main advantage of a DoE over a conventional optimization is the reduction of the necessary number of experiments to generate meaningful data for parameter optimization. Time and resources are saved. [14]

The first step for the proper selection of the optimization method is to define the factors (*k*) which significantly influence the response. [13] [14] Afterwards, a more elaborated model like Box-Behnken design (BBD), Central Composite design (CCD) or Doehlert Matrix is applied to generate the required data. [15] These methods belong to the class of response surface methodology (RSM), where the results are fitted to polynomial functions to describe the studied system. [13] The next step is the statistical analysis of the functions for the verification of the model and finally define the optimal conditions. [13]

The number of experiments/run (N) depends on the selected DoE method. Table 1-1 presents the equations for each:

Table 1-1. Number of experiments required according to the DoE applied.

DoE	Equation for the number of experiments [13]
BBD	$N = 2k(k-1) + c_p$
CCD	$N = k^2 + 2k + c_p$
Doehlert Matrix	$N = k^2 + k + c_p$

k = Factors. c_p = Central points

A BBD is an appropriate design when the response at the extreme conditions is not of interest, this means that the factors are not analyzed at their highest or lowest levels. [16] A BBD measures the factors at three levels (encoded as -, + and 0), by this maintaining a reduced number of experiments although the number of factors increases. [17]

A CCD requires five levels for each factor and combines the factors at their highest and lowest level, in contrast to a BBD where only three levels are needed. [14] Thus, the experiment time is increased. Taking the extraction time in ITEX as an example, if the extreme conditions (as in a CCD) are added to the DoE, then the extraction time required at the set conditions would range from 7 min. to 89 min. [12] While, if the parameters are only analysed close to the assumed optimal conditions (as in a BBD), the time would range from 7 to approx. 55 min., [12] thus reducing the sampling time required to run the DoE.

The two previous designs are symmetrical designs, since all of the factors are measured at the assigned levels. In a Doehlert Matrix, the levels for a factor can be varied. [16] Due to this variation, it is possible in Doehlert Matrix designs to introduce new factors during the course of an experimental study without losing the already measured data. [16]

The c_p are included to determine the experimental error. [18] The c_p are repeated between two to five times [16] and if a more precise estimation of the error is of concern, then more replicates of the c_p should be performed. [16] The number of c_p will increase, as the number of factors also increases. [19]

The BBD and Doehlert Matrix designs are mentioned to be more efficient than a CCD [15], but the choice of the design will depend on the goal of the study.

1.2 Material characterization

Material analysis yields information about the composition (elements present, type of bond), molecular structure, physical or physicochemical properties of the sample under investigation.

[20] [21] According to the type of information required, the corresponding technique should be applied.

Typical techniques for material characterization are contact angle measurements (based on geometry features), spectroscopic methods like x-ray photoelectron spectroscopy (XPS), x-ray diffraction (XRD), scanning electron microscopy (SEM) and transmission electron microscopy (TEM). Thermal gravimetric analysis (TGA) is another applied method as well as chromatographic methods such as inverse gas chromatography (IGC).

1.2.1 Inverse Gas Chromatography (IGC)

IGC is a technique applied for material characterization and was first mentioned by Kiselev in 1960. [22] The term "inverse" refers to the analysis of the stationary phase packed in the column and not the sample injected, as in conventional gas chromatography (GC). [22] The packed column is examined with known liquids or gases, called probes. An inert marker, like methane or nitrogen, is also injected. [22] The inert marker is characterized by its non-interaction with the stationary phase under analysis. [22] [23] It is applied to determine the dead volume of the system. [23] From the retention time difference between the probe and the inert marker, multiplied by the column flow and compressibility factor, the net retention volume (V_N) is obtained. From V_N, the specific retention volume (V_g) is calculated. V_g is the multiplication of V_N by a temperature factor and divided by the multiplication of the mass and the column temperature. The samples for IGC experiments can be prepared at a concentration approaching infinite dilution or at finite concentration. According to the type of concentration the equation of the net retention volume varies. [22] Eq. 1 and Eq. 2 are applied for samples prepared at a concentration approaching infinite dilution and Eq. 3 at finite concentration conditions:

$$V_N = jF\Delta t \qquad \text{Eq. 1 [24]}$$

$$V_g = \frac{273jF\Delta t}{mT} \qquad \text{Eq. 2 [24]}$$

$$V_N = A(1 - jy_0)\frac{d_q}{d_c} \qquad \text{Eq. 3 [22]}$$

j is the James-Martin compressibility factor, F is the column flow in mL min^{-1}, $\Delta t = t_r - t_0$ is the time difference between the probe (t_r) and the inert marker (t_0), m is the mass of the sorbent or stationary phase, T is the column temperature in K, A is the surface area of the sorbent, y_0 is the mole fraction of solute in the gas phase at the column inlet and $\frac{d_q}{d_c}$ is the slope of the adsorption isotherm at a corresponding concentration.

At infinite dilution, the retention follows the Henry´s law region (linear) and only sorbate-sorbent interactions happen. [22] Under this conditions, thermodynamic parameters like partitioning constant between solid and gas phase (K_d), [24] sorption enthalpy (ΔHs), molar free energy of sorption (ΔGs) and entropy of sorption (ΔSs) can be estimated. [25] The diffusion coefficient (D^{∞}), dispersion coefficient (D^*) as well as apparent permeability (P_{app}), which are kinetic parameters, can also be determined. [26-30]

At finite concentration (FC), three approaches are usually applied: frontal analysis (FA), frontal analysis by a characteristic point (FACP) and elution plateau (EP). [22] For FA, step gradients over time are used either in a staircase or rectangular pulse mode, as shown in Figure 1-4. [31] In the staircase mode, two solutions are mixed upstream the column and pumped through it at a constant flow rate. The first solution is the mobile phase and the second one a mixture of the studied compounds dissolved in the mobile phase. At corresponding times, the total concentration of the investigated solutes is increased stepwise (the concentration is increased at a constant relative composition) to generate the isotherm. In the rectangular pulse mode, the sample at the corresponding concentration is injected, then washed with the mobile phase off and then the next step is injected. [31] For FACP, a sample prepared at a high concentration is injected, once the equilibrium (plateau) has been reached, pure mobile phase is pumped to wash it off and the diffuse profile is recorded to estimate the isotherm. The diffuse profile at the rear of FA analysis can also be used for this purpose, as depicted in Figure 1-4. [32] [33]

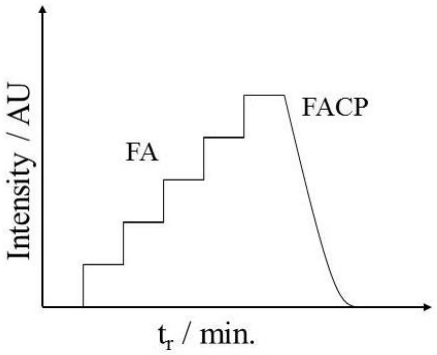

Figure 1-4. Finite concentration injection modi. Staircase (FA) or wash off with the mobile phase after a FA injection with a high concentration (FACP). [33]

For the EP approach (or pulse method), a steady-state concentration profile is established to generate a breakthrough curve. Then, a small disturbance is introduced (concentration change or mobile phase) and the time for the perturbation to propagate along the column is recorded (the elution time depends on the concentration, the higher the concentration of the stock solution, the shorter is the retention time of the perturbation). [34] The isotherm is obtained by

repeating the procedure with a concentration increase, depicted in Figure 1-5. [33, 34] The retention time of pulses measured with a column equilibrated with solutions of progressively increasing concentration, allow the calculation of the isotherm slopes at the different concentrations. [34] The goal of EP experiments is also to generate adsorption isotherms. [22] [33]

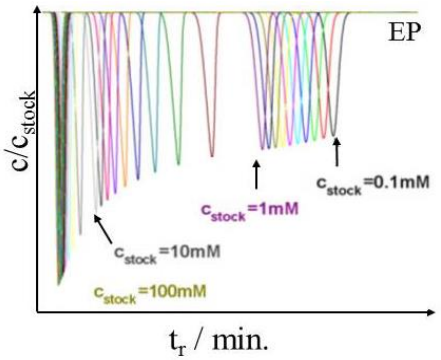

Figure 1-5. Elution plateau (EP) example for experiments run at finite concentration. [34]

IGC is a versatile material characterization technique applicable in many fields, like pharmaceuticals, fibers, polymers, food, cement and toner/ink. [22] [23, 35] For example, in the pharmaceutical industry, the dry material is packed in glass columns to investigate whether the material will remain as crystal or change to a rubbery consistency in dependence of the temperature and relative humidity (glass transition temperature). This is done to improve the fabrication of the pharmaceutical and avoid changes in the quality and performance of the product. [36] For example, salbutamol sulfate (applied for respiratory insufficiencies like asthma), was packed in glass columns and evaluated with IGC at infinite dilution to perform a quality test among the same batch. With the injection of several probe compounds (chloroform, acetone, ethyl acetate and tetrahydrofuran) the surface energy from the different salbutamol sulfate batches was estimated. As well as in the previous case, where the glass transition temperature of the material was investigated via IGC, if changes are detected then the quality, formulation and performance of the medicine might be inappropriately modified. [37]

Adsorption and desorption kinetics, slow mass transfer and small apparent plate numbers are some of the reasons for peak tailing, [38] which is a common feature of the peaks obtained via this technique. The peak area integration, i.e. the definition of the peak's start and endpoint, and the determination of the retention time, remains as a difficulty. [38] [39] Several approaches exist to evaluate the results.

The retention time can be interpreted via the maximum (apex), 1st moment or the median/half mass point method (50 % of the peak area). [38] [40] The apex retention time, as its name

specifies, is defined at the highest point of the peak. It can be applied, when small asymmetry values are found. The 1st moment is among the five statistical moments used for the description of asymmetric peaks in chromatography. It represents the mean retention time at the center of gravity of the peak. [41] The half mass point method, for the retention time estimation, corresponds to the integration of the peak area over time divided into two equal parts. [40] Figure 1-13 depicts an example from this work, for natural gas at 40 °C with PDMS as sorbent, when the retention time is evaluated with the half mass point method (grey line). In order to estimate the retention time according to the half mass point method, first with the help of software (e.g.: OriginPro), the peak area is integrated. The peak area and the time frame covered by it, as depicted in Figure 1-6 part a), is recorded. The peak area is then divided by two (554645/2 = 277322) in order to integrate only the half of the area and by this yielding the new limit value of the integral. One limit value is kept constant (the initial value at approx. 0.05 min.) and the second one (new limit value, which equals to the new retention time) is shifted until the calculated half of the peak area is reached. Occasionally, the software does not provide the exact half area calculated, rather one which is close to the estimated value, as in Figure 1-6 b). To control that new limit value/retention time is correct, the other half can also be integrated. Generally, the same time is obtained and in the case of a slight difference the average value is calculated. In Figure 1-6 c), the difference between the apex (dashed black line) and the half mass retention time (grey line) is demonstrated for a natural gas injection.

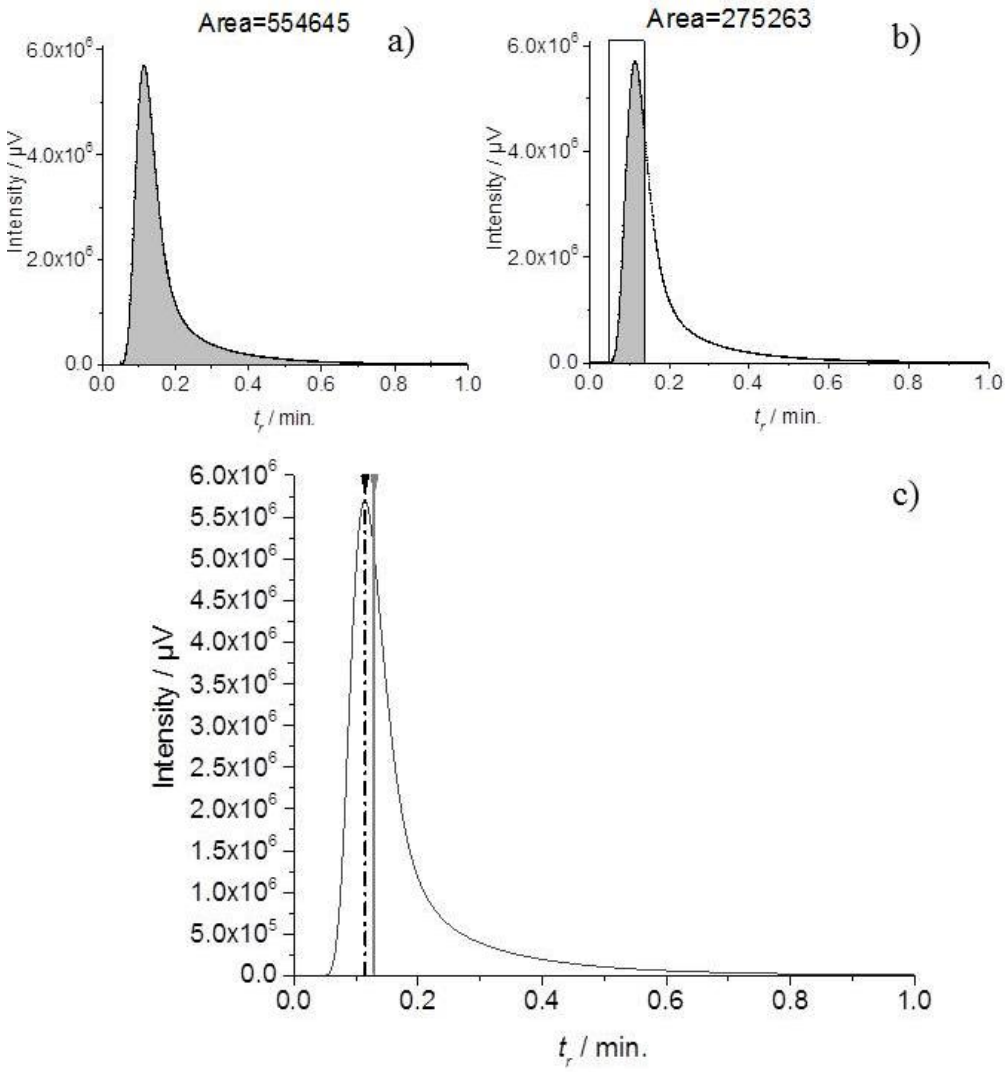

Figure 1-6. Explanation steps for the estimation of the retention time for tailing peaks via the half mass point method. a) Peak integration over time, b) Peak integration for the half, c) Comparison of the estimated retention time between apex (dashed black line) and half mass point method (grey).
IGC/FID measurement of natural gas at 40 °C, PDMS as sorbent and a column flow = 3 mL min^{-1}.

Moments are inaccurate when baseline drift, strong tailing or incomplete resolution happens, [40] thus making the half mass point method the method of choice for the retention time estimation, in particular when strongly tailing peaks are measured.

1.2.2 Contact angle measurement

This technique describes the interaction of a drop of pure liquid on a plane solid surface. Adhesive and cohesive forces are present, creating a contact angle. [42] This angle is formed by the intersection of the liquid-solid interface and the liquid-vapor interface. The shape of the drop depends on interfacial tension and further external forces, as visualized in Figure 1-7.

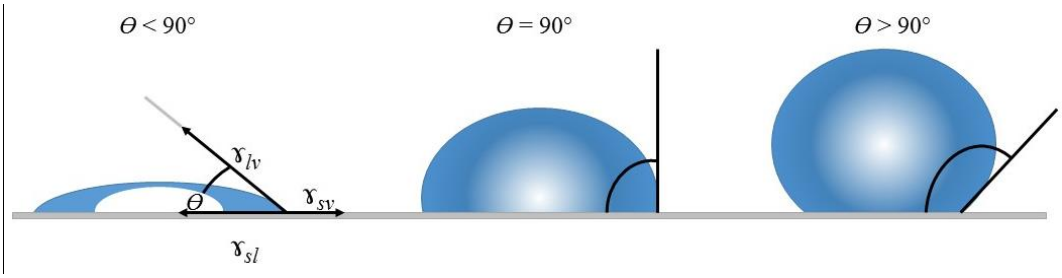

Figure 1-7. Contact angles formed by a sessile liquid drop's shape on a smooth homogeneous solid surface. [43]
Each angle is characteristic for a given system and the Young's equation describes the balance in the three-phase interface. [43]

$$\gamma_{lv} cos\theta_Y = \gamma_{sv} - \gamma_{sl}$$ Eq. 3 [43]

Where γ_{lv}, γ_{sv}, γ_{sl} are the liquid-vapor, solid-vapor and solid-liquid interfacial tensions, respectively. The contact angle θ is calculated from the inverse $cos\theta_Y$ in Eq. 3.

The techniques to determine the contact angle can be divided into direct optical and indirect force methods. [44] [45] Examples for direct measurement methods are telescope-goniometer, captive bubble and tilting plate method. [46] To perform these experiments, a liquid drop is deposited onto a flat surface. The profile of the drop is recorded with high resolution cameras to enable the examination of the intersection. The captive bubble method consists on inserting the sample in the testing liquid and form an air bubble beneath it. Similar to the captive bubble method, in the tilting plate method, the plate is immersed and a concave or convex meniscus is created. The plate is slowly slanted until the meniscus on one side of the plate is horizontal. [43] [45]

For indirect techniques, the Wilhelmy balance method, capillary penetration or capillary bridge method are usually applied. It is defined as an indirect method, because out of another parameter, such as pressure, height or weight difference, the angle is calculated. [43] [45]

The measured angle indicates whether a hydrophobic or hydrophilic surface is present, with angles larger than 90° or smaller than 90°, respectively. [43] The angle also depends on the nature of the liquid drop (water, hexane) applied. [42] Wettability, surface free energy and type of interaction like van der Waals forces, is the kind of information that can be gained when contact angle measurements are performed. [47] [48]

1.2.3 X-ray photoelectron spectroscopy (XPS) and x-ray diffraction (XRD)

XPS is a technique applied to investigate the occurrence of elements, their chemical state and types of bonds found at the surface of the sample, at no further than 10 nm depth. [49] The solid sample is positioned in the equipment and is irradiated with monochromatic x-rays.

Photoelectrons are ejected from the surface sample, [21] which are proportional to the number of atoms in a given state, over a range of kinetic energies. The excess kinetic energy released by the photoelectrons is the characteristic binding energy of an element, thus providing the chemical composition, chemical state and amount present in the material. [21] [49] The peaks obtained in a XPS spectra can be modelled from a set of Gaussian/Lorentzian shapes. The model requires input information, like intensity, peak position and other parameters. This procedure, called peak fitting, is an important issue in order to obtain relevant data. [49]

Another x-ray based technique applied for material characterization is XRD. It is mainly applied for crystalline materials. The x-ray beam impinges the sample and is scattered by its periodic atomic planes. The angle or energy at which the signal is detected is the diffracted x-ray. [50] A plot of diffraction angle against diffracted line intensity is created to generate a pattern. The pattern belongs to a characteristic specimen. [51] The signal XRD is capable of providing qualitative as well as quantitative information about the compounds present in the sample, as well as to calculate the material´s crystallite size, crystallinity and other features. [51] Both techniques require vacuum to perform the measurements.

1.2.4 Scanning electron microscopy (SEM) and transmission electron microscopy (TEM)

In contrast to light microscopes, where visible light is applied for imaging, SEM and TEM use electrons to create one. An approx. 100,000 times larger magnification is achieved. [52]

The electron beam is focused and positioned to the sample through scanning coils. Thus, electrons from the sample are emitted. High-energy (backscattered electrons) as well as low-energy electrons (secondary electrons) are generated. If the high-energy electrons are detected, then an “orientation image” describing the spatial variation is obtained. Effects such as texturing, recovery and recrystallization and material composition can be revealed. [21] At low incident beam energies (below 5 keV), information about the morphology of the sample is gained. [53] [54]

TEM provides an image by measuring the energy of an electron after it has passed through a transparent sample, analogous to a slide projector, but the source is an electron instead of light. [21] Sample preparation for TEM measurements is time consuming. They must be placed on special micromesh grids and it must be coated with a support material, as transparent as possible, that holds the sample in place. The image is projected onto a fluorescent screen, computer screen, photographic plate or charged-coupled device (CCD)

camera/monitor. Volatile samples are not recommended to be measured with this technique. [21] A meticulous sample preparation is required in order to reach a lateral spatial resolution of even 0.2 nm. [55] An improved image, in comparison to SEM, is obtained and also information about the chemical composition can be achieved.

1.2.5 Thermal gravimetric analysis (TGA)

In a TGA experiment, the weight change at different temperatures during a specific time frame is observed. [52] The atmosphere where the sample is measured is also controlled. [20] The sample is placed in a small container, attached to a microbalance. Afterwards, it is heated for the analysis time. The atmosphere surrounding the sample may be an inert gas at the beginning, but as the experiment proceeds, the gas can be switched to a reactive one (like oxygen). [52] The weight change can be associated to the volatile components in the sample, oxidation/reduction reactions, decomposition or gas absorption. [52] [20] The weight change (in percentage) is plotted against temperature and a thermogram is created. Weight-loss steps are depicted in the thermogram, yielding information about the composition of the material [20]

1.3 Materials for volatile organic compounds (VOC) extraction in ITEX

In ITEX several commercial materials are available for sampling, as shown in Table 1. Novel packing materials, like carbon based-nanomaterials (CNM) and polymeric ionic liquids (PIL), were tested to define and describe their potential application in this field. Characteristics of the materials are presented in Table 1. In this work, PDMS, Tenax TA, Carbopack C, five carbon CNM and two synthesized PIL (Sil. PIL 1 and Sil. PIL 2) were investigated. Therefore, only these materials will be described in more detail in the following.

Table 1-2. Characteristics of commercially available sorbents for ITEX (upper part) and newly materials to be applied in ITEX (below).

	Sorbent	Particle size	SSA / $m^2\ g^{-1}$	Pore size	Water affinity	Type of sorbent	Material
ITEX commercially available	PDMS	80/100 mesh[56]	/		Low[12]	Absorbent	Polydimethylsiloxane[57]
	Tenax TA	80/100 mesh[56]	35[12]	114×10^3 nm[a)][57]	Low[12]	Adsorbent	Poly-(2,6-diphenyl-)-*p*-phenylene oxide[57]
	Tenax GR	80/100 mesh[56]	24[12]	114×10^3 nm[a)][57]	Low[12]		70% porous organic polymer/30% graphitized carbon[12]
	Carbopack C	80/100 mesh[56]	10[12]		Relatively low[12]		Graphitized carbon black[57]
	Carboxen 1000	60/80 mesh[56]	1200[12]	1 to 1.2 nm for micropore[58]	Moderate[12]		Carbon molecular sieve[57]
	Carbosieve S III	60/80 mesh[56]	975[12]	0.4 to 1.1 nm for micropore[58]	Moderate[12]		Carbon molecular sieve[57]
	Molecular Sieve 5A	80/100 mesh[56]	800[59]	0.5 nm[60]	High[61]		Resin[60]
New sorbents in ITEX (investigated in this work)	Carbon nanohorns	5-150 nm[62]	200[62]	12 nm[62]	Relatively low	Adsorbent	> 95% carbon[62]
	Fullerenes	139 nm[63]	0.398[b)]	n.a.			≥ 99.5 % carbon[64]
	Graphene platelets	11-15 nm[65]	50-80[65]	3-11 nm[66]			> 99.5 % carbon[65]
	MWCNTs	> 1000 nm[67]	210[b)]	7-10 nm[66]			≥ 95 % carbon[67]
	MWCNTs-COOH	9.5 nm[68]	110[66]	n.a.			Carbon and COOH (>8%)[68]
	Sil. PIL 1	≤ 3000 nm			Depends mainly on the anion[69]		1-vinylimidazolium and AMPS
	Sil. PIL 2	≥ 3000 nm					1-vinylimidazolium and *p*-styrenesulphonate

a) Pore size calculated from the mentioned source [49]. b) BET measurement. SSA = Specific surface area. AMPS = 2-acrylamido-2-methylpropane sulphonic acid. n.a. = not available

1.3.1 PDMS

Polydymethylsiloxane (PDMS) is a silicone extensively used in the analytical chemistry field. It has multiple applications and has been well-characterized, due to its use as stationary phase in gas chromatography. [27] [57] Figure 1-8 depicts the structure of PDMS:

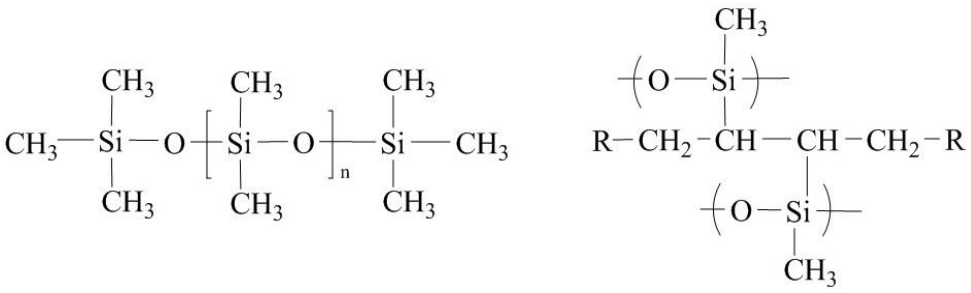

Figure 1-8. Linear PDMS structure on the left. Cross-linked PDMS on the right. [70]
Typical molecular weights range between 10,000 to 60,000 g mol^{-1}. [27] According to the molecular weight and the equation of the literature to estimate n, [71] n ranges from 135 to 810. R = Free-radical initiator for the cross-linking reaction.

It is primarily fabricated with a vinyl terminated PDMS group combined with a cross-linker. The specific ratio of each component (vinyl terminated PDMS group and cross-linker) yields the properties of the manufactured PDMS. It consists of a flexible Si-O backbone and the number of repeating $Si(CH_3)_2O$, defines the molecular weight and viscosity. [27] PDMS is highly hydrophobic, making it a suitable sorbent for the extraction of aqueous samples (the target analyte will be mainly enriched, but water will remain in the HS and not also be enriched in the sorbent), [27] [57]. Otherwise, when exposed to hydrophobic solvents, PDMS will tend to swell. [27] Absorption (partitioning and linear isotherms) is typically observed with PDMS. [57]

1.3.2 Tenax TA

Tenax TA is the commercial name of poly-(2,6-diphenyl-)-*p*-phenylene oxide, which is a porous organic polymer. [72]

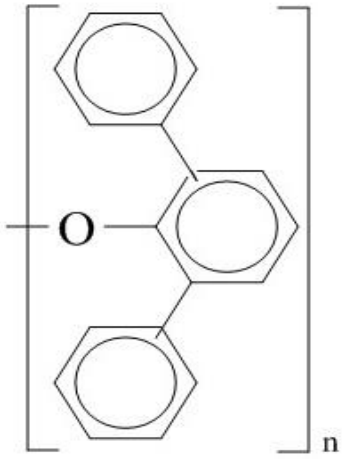

Figure 1-9. Tenax TA structure.
n is repeated between 37 to 595 times. n was calculated from the ratio of the Tenax TA molecular weight to the molecular weight of one repeating unit. [73]

Among the porous polymers, Tenax TA represents the most important sorbent for air analysis. [57] It is also a hydrophobic material, with high thermal stability. Tenax TA is generally utilized for the analysis of volatile organic compounds (VOC) [72] including hydrocarbons higher than four. [57] With aldehydes, such as *n*-Octanal, *n*-Nonanal and *n*-Decanal, its use is not recommended due to artifacts. [57] *n*-Nonanal and *n*-Decanal appear as artifact, [74] as well as benzaldehyde, acetophenone, phenol and benzonitrile. [74] [75] The type of sorption in this material is adsorption (pore filling) and in comparison to PDMS (where absorption takes place), a stronger sorption is generally found. [57] Non-linear isotherms are characteristic.

1.3.3 Carbopack C

This type of sorbent belongs to the graphitized carbon blacks. [72] The carbon black undergoes a thermal treatment at temperatures higher than 2,500 °C, where the spherical shape evolves to symmetric flat surfaces (basal planes), as shown in Figure 1-10. Non-porous carbon is generated. [76] [77] Due to the lack of micro-pores, its specific surface area is low (between 5 and 260 m^2 g^{-1}), turning it into unsuitable sorbents for small analytes (C_5 or smaller). [72] It is a non-polar adsorbent and enrichment takes place in the basal planes of the graphite crystallite (caused by non-specific interactions). The sorption strength is based on the molecule size, shape and degrees of polarization of the graphitized carbon black surface. [57]

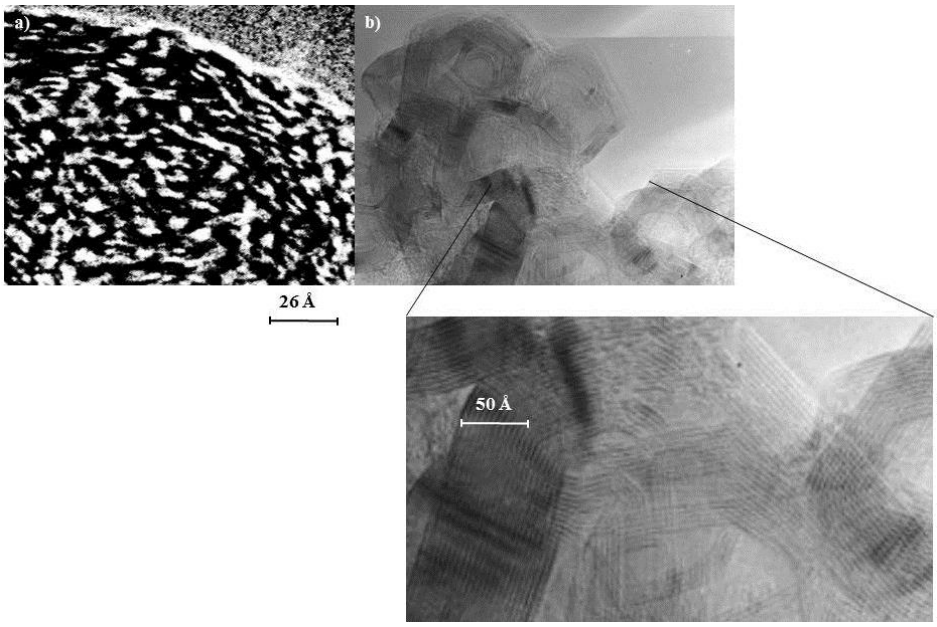

Figure 1-10. a) Carbon black. [78] b) Graphitized carbon black and its basal planes. [79]

1.3.4 Carbon based-nanomaterials

As previously mentioned, sample preparation and its improvement is of great importance for a successful analysis. The search for suitable and enhanced materials for sampling is latent. Carbon based-nanomaterials (CNM) seem a promising sorbent for the field. [80] Their unique characteristics, such as high-surface-to-volume ratio, easy derivatization procedures, unique thermal, mechanical and electronic properties, interaction with organic molecules and structure (hollow or layered) are the reasons why they have gained interest for investigation. [80] Five CNM have been utilized in this thesis and will be described briefly in the following.
Graphene is considered the basic building block of all graphitic forms. It has a two-dimensional (2D) structure of carbon atoms packed into a dense honeycomb crystal structure (sheet configuration) as shown in Figure 1-11. [80]

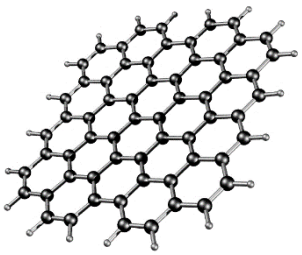

Figure 1-11. Graphene. [80]

The graphene family also comprises graphene oxide and reduced graphene oxide. [66]
Graphene is manufactured by two procedures. On the one hand, top-down, mechanical or electrochemical exfoliation of graphite to obtain single or multiple layer graphene is applied. It is an inexpensive technique, but only low quality of graphene sheets can be produced. On the other hand, the bottom-up procedure is applied for the synthesis of graphene. Organic compounds are broken down, under a hydrogen atmosphere, at high temperatures atop or within metals to afford atomic carbon structures, the procedure is called chemical vapor deposition. [81] The graphene sheets are produced defect free, but at an elevated cost. [66]
The pore size, distribution and surface area are influenced by their fabrication procedure. Typical surface area values range between 295 to 1206 $m^2 g^{-1}$. The specific surface area might decrease, if incomplete exfoliation, wrinkling and folding of the graphene sheets happen or a great number of graphene layers are present. [66]
Both sides of its planar sheets are available for adsorption. In addition, the delocalized π-electron system provides strong sorption via π -stacking for aromatic structures. [80]

Multi-walled carbon nanotubes (MWCNTs), Figure 1-12, together with single-walled carbon nanotubes (SWCNTs), until now have been the most used carbon nanotubes (CNTs) applied for sample preparation. They were discovered by Ijima in 1991. [82]

Figure 1-12. MWCNTs. [83]

They are considered a rolled graphene sheet capped by fullerene-like structures. [80] [84] Their structure consists of many concentric cylinders where van der Waal forces hold them together. [82]
Three methods are available for the synthesis of CNTs: arc discharge, laser ablation and chemical vapor deposition. Great attention to the impurities must be paid in order to produce high quality CNTs. [82] Usually interaction between organic molecules and MWCNTs are via π-π stacking, [85] electrostatic, van der Waals, hydrogen bonding and hydrophobic forces. [82] The analyte molecular size as well as the diameter and number of layers of the carbon-based nanomaterial to be applied, should be known for a proper sampling. Smaller molecules

have a greater number of sorption sites available than larger ones. [86] Larger molecules interact with the first couple of layers, leaving only space for the small molecules to interact at the groove areas causing condensation. [85] The groove areas are depicted in Figure 1-13.

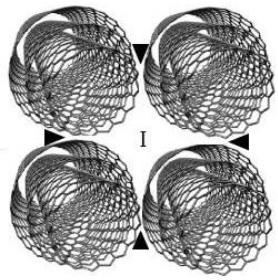

Figure 1-13. Groove (black triangles) and interstitial (I) areas for carbon nanotubes. [66]

MWCNTs can be functionalized to enhance or increase selectivity to favor the interaction with particular molecules. [84] Functional groups like –OH, -C=O and –COOH can be added by oxidation. [85]

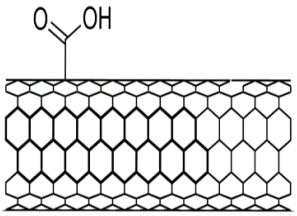

Figure 1-14. Functionalized MWCNTs. [68]

These groups change the sorption properties of the MWCNTs. For example, the wettability is modified, making them more hydrophilic and suitable for the adsorption of relatively low molecular weight and polar compounds. A disadvantage is that the available surface for large molecules is decreased. Also, observed from activated carbon, water molecules could also form hydrogen bonds, thus competing with the organic target analytes for adsorption sites. [85]

Fullerenes were discovered in 1985 by Kroto et al. [82] It consists of a closed-cage carbon, containing pentagonal and hexagonal rings. [80]

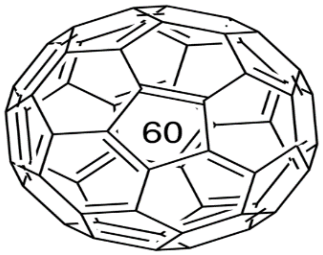

Figure 1-15. Fullerenes C_{60}. [87]

Homologous series and isomers of fullerenes also exist. They exhibit a relatively high electron affinity, hydrophobic surface and high surface to volume ratio. Also, C_{60} fullerenes show a low affinity for water and establishes π-π interactions with aromatic compounds like benzene. [88] These properties yield strong affinity for sorption of organic molecules, turning them suitable as a sorbent material. [80]

The affinity and selectivity for coplanar molecules, such as polychlorinated biphenyls (PCBs) pushed the investigation of fullerenes as stationary phase in high-performance liquid chromatography (HPLC). [89] It showed high column efficiency, wide temperature range operation, good thermal stability and selectivity. [90] These findings also encourage the application of fullerenes as sorbent material in solventless microextraction techniques.

Carbon nanohorns belong to the same family as SWCNTs. They consist of a single-graphene layer, wrapped and cone shaped. They form spherical aggregates forming either dahlia-like structures (the horns are clearly viewed, Figure 1-16) or bud-like structures (no protruding horns are visible which gives the impression of shorter horns). [91]

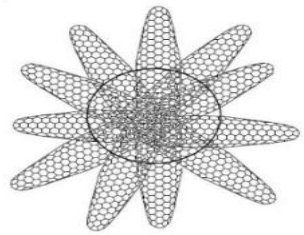

Figure 1-16. Carbon nanohorns, dahlia-like structure. [62]

For dahlia-like nanohorns, sorption on the outer surface of the individual horns, as well as in the interstitial sites has been observed. [91]

1.3.5 Polymeric ionic liquids (PIL)

Initial research on polymeric ionic liquids (PIL) began in the 1970´s, but only after 2000, PIL regained interest. [92] PIL are also called polymerized ionic liquids or polyionic liquids. [93] [92]

They are a subclass of polyelectrolytes and carry ionic liquid species in each of the repeating units. [92] Through a polymeric backbone they are connected, thus forming a macromolecular structure. [93] Examples for cations are: imidazolium, pyridinium, phosphonium and tetraalkylammonium. Typical anions applied for PIL synthesis are: halide, tetrafluoroborate, hexafluorophosphate, triflate etc. [94] [69]

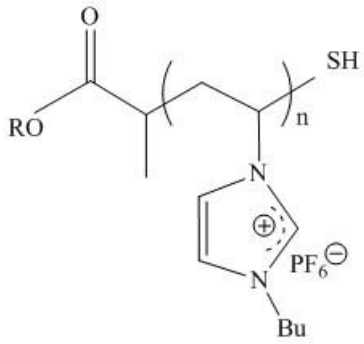

Figure 1-17. Example of a poly(N-vinyl-3-butylimidazolium) hexafluorophosphate PIL (imidazolium as cation and hexafluorophosphate as anion). Bu = Butyl, R = $-CH_3$. [95]

Direct polymerization of an IL monomer and chemical modification of an existing polymer are the two main pathways for PIL synthesis. [92] The first method requires several steps of organic synthesis, purification of the monomer, as well as control of the polymerization and more elaborated PIL can be synthesized. In contrast, in the second method, only one monomer purification step is required, but simpler PIL are produced. [96]

References

1. Pawliszyn, J. and S. Pedersen-Bjergaard, *Analytical microextraction: current status and future trends.* J. Chromatogr. Sci., 2006. **44**(6): p. 291-307.

2. Laaks, J., M.A. Jochmann, and T.C. Schmidt, *Solvent-free microextraction techniques in gas chromatography.* Anal. Bioanal. Chem., 2012. **402**(2): p. 565-571.

3. Laaks, J., et al., *In-tube extraction of volatile organic compounds from aqueous samples: an economical alternative to purge and trap enrichment.* Anal. Chem., 2010. **82**(18): p. 7641-7648.

4. Gjelstad, A., et al., *Kinetic aspects of hollow fiber liquid-phase microextraction and electromembrane extraction.* Anal. Chim. Acta., 2012. **742**: p. 10-16.

5. Handley, A.J. and E.R. Adlard, *Gas chromatographic techniques and applications*. 2001, England: Sheffield Academic Press. 337.

6. Majors, R.E., *Sample preparation fundamentals for chromatography the measure of confidence.* Agilent Technologies, Inc. , 2013. **5991-3326EN**.

7. Nuhu, A.A., C. Basheer, and B. Saad, *Liquid-phase and dispersive liquid–liquid microextraction techniques with derivatization: recent applications in bioanalysis.* J. Chromatogr. B, 2011. **879**(17–18): p. 1180-1188.

8. Jochmann, M.A., et al., *In-tube extraction for enrichment of volatile organic hydrocarbons from aqueous samples.* J. Chromatogr. A, 2008. **1179**(2): p. 96-105.

9. Kremser, A., M.A. Jochmann, and T.C. Schmidt, *PAL SPME Arrow—evaluation of a novel solid-phase microextraction device for freely dissolved PAHs in water.* Anal. Bioanal. Chem., 2015. **408**(3): p. 943-952.

10. David, F. and C. Devos, *Analysis of volatile organic compounds in beer using ITEX headspace sampling.* CTC Analytics. **ITEX Application Note #04**.

11. Rasanen, I., et al., *Headspace in-tube extraction gas chromatography–mass spectrometry for the analysis of hydroxylic methyl-derivatized and volatile organic compounds in blood and urine.* J. Anal. Toxicol., 2010. **34**(3): p. 113-121.

12. Laaks, J., et al., *Optimization strategies of in-tube extraction (ITEX) methods.* Anal. Bioanal. Chem., 2015. **407**(22): p. 6827-6838.

13. Bezerra, M.A., et al., *Response surface methodology (RSM) as a tool for optimization in analytical chemistry.* Talanta, 2008. **76**(5): p. 965-977.

14. Wu, L., et al., *Application of the Box–Behnken design to the optimization of process parameters in foam cup molding.* Expert Syst. Appl., 2012. **39**(9): p. 8059–8065.

15. Ferreira, S.L.C., et al., *Box-Behnken design: an alternative for the optimization of analytical methods.* Anal. Chim. Acta, 2007. **597**(2): p. 179–186.

16. Ferreira, S.L.C., et al., *Statistical designs and response surface techniques for the optimization of chromatographic systems.* J. Chromatogr. A, 2007. **1158**(1–2): p. 2-14.

17. Cavazzuti, M., *Design of experiments*, in *Optimization methods: from theory to design Scientific and technological aspects in mechanics*. 2013, Springer Berlin Heidelberg: Berlin, Heidelberg. p. 13-42.

18. Shen, X., G. Zhang, and B. Bjerg, *Assessments of experimental designs in response surface modelling process: estimating ventilation rate in naturally ventilated livestock buildings.* Energ. and Buildings, 2013. **62**: p. 570-580.

19. Draper, N.R., *Center points in second-order response surface designs.* Technometrics, 1982. **24**(2): p. 127-133.

20. Jansen, J.A., *Characterization of plastics in failure analysis.* p. 437-459.

21. Fahlman, B.D., *Materials characterization*, in *Materials Chemistry*. 2007, Springer Netherlands: Dordrecht. p. 357-432.

22. Butler, D. and D.R. Williams, *Particulate characterization: inverse gas chromatography*. 2000, Academic Press: London, UK. p. 3609-3614.

23. Segeren, L.H.G.J., et al., *Surface energy characteristics of toner particles by automated inverse gas chromatography.* J. Chromatogr. A, 2002. **969**(1-2): p. 215-227.

24. Boutboul, A., et al., *Use of inverse gas chromatography to determine thermodynamic parameters of aroma–starch interactions.* J. Chromatogr. A, 2002. **969**(1-2): p. 9-16.

25. Dritsas, G.S., K. Karatasos, and C. Panayiotou, *Investigation of thermodynamic properties of hyperbranched aliphatic polyesters by inverse gas chromatography*. J. Chromatogr. A, 2009. **1216**(51): p. 8979-8985.

26. Wijmans, J.G. and R.W. Baker, *The solution-diffusion model: a review.* J. Membr. Sci. , 1995. **107**(1-2): p. 1-21.

27. Seethapathy, S. and T. Górecki, *Applications of polydimethylsiloxane in analytical chemistry: a review.* Anal. Chim. Acta., 2012. **750 th anniversary volume**: p. 48-62.

28. Lonsdale, H.K., U. Merten, and R.L. Riley, *Transport properties of cellulose acetate osmotic membranes.* J. Appl. Polym. Sci. , 1965. **9**(4): p. 1341-1362.

29. Zhao, C., J. Li, and C. Zeng, *Determination of the infinite dilution diffusion and activity coefficients of alkanes in polypropylene by inverse gas chromatography.* J. Appl. Polym. Sci., 2006. **101**(3): p. 1925-1930.

30. Edwards, M.F. and J.F. Richardson, *Gas dispersion in packed beds.* Chem. Eng. Sci., 1968. **23**(2): p. 109-123.

31. Burger, D., et al., *Determination and comparison of competitive isotherms by frontal analysis and frontal velocity analysis.* Chromatographia, 2000. **51**(9): p. 517-525.

32. Golshan-Shirazi, S., S. Ghodbane, and G. Guiochon, *Comparison between experimental and theoretical band profiles in nonlinear liquid chromatography with a pure mobile phase.* Anal. Chem., 1988. **60**(23): p. 2630-2634.

33. Guiochon, G., A. Felinger, and D.G.G. Shirazi, *Fundamentals of preparative and nonlinear chromatography*. 2nd ed. 2006, San Diego, USA: Elsevier Science. 990.

34. Andrzejewska, A., K. Kaczmarski, and G. Guiochon, *Theoretical study of the accuracy of the pulse method, frontal analysis, and frontal analysis by characteristic points for the determination of single component adsorption isotherms.* J. Chromatogr. A, 2009. **1216**(7): p. 1067-1083.

35. Perruchot, C., et al., *Characterisation of the surface thermodynamic properties of cement components by inverse gas chromatography at infinite dilution.* Cem. Concr. Res., 2006. **36**(2): p. 305-319.

36. Surana, R., et al., *Determination of glass transition temperature and in situ study of the plasticizing effect of water by inverse gas chromatography.* Pharma. Res., 2003. **20**(10): p. 1647-1654.

37. Feeley, J.C., et al., *Determination of surface properties and flow characteristics of salbutamol sulphate, before and after micronisation.* Int. J. Pharm., 1998. **172**(1–2): p. 89-96.

38. Pápai, Z. and T.L. Pap, *Analysis of peak asymmetry in chromatography*. J. Chromatogr. A, 2002. **953**(1–2): p. 31-38.

39. Ng, L.L., C. Kumkumian, and R.L. Williams, *Reviewer guidance Validation of chromatographic methods*, A.m.t.c.o.t.c.m.c.c. committee, Editor. 1994: USA.

40. Bi, E., T.C. Schmidt, and S.B. Haderlein, *Practical issues relating to soil column chromatography for sorption parameter determination.* Chemosphere, 2010. **80**(7): p. 787-793.

41. *Evaluating system suitability CE, GC, LC and A/D chemstation Revisions: A.03.0x-A.08.0x*. Agilent Technologies.

42. Lamour, G. and A. Hamraoui, *Contact angle measurements using a simplified experimental setup.* J. Chem. Educ., 2010. **87**(12): p. 1403-1407.

43. Yuan, Y. and T.R. Lee, *Contact angle and wetting properties*, in *Surface Science Techniques*, G. Bracco and B. Holst, Editors. 2013, Springer Berlin Heidelberg: Berlin, Heidelberg. p. 3-34.

44. Mahyudin, F. and H. Hermawan, *Biomaterials and medical devices: a perspective from an emerging country*. Advanced structured materials. 2016, Switzerland: Springer International Publishing. XIV, 242.

45. Bezuglyi, B.A., O.A. Tarasov, and A.A. Fedorets, *Modified tilting-plate method for measuring contact angles.* Colloid J. **63**(6): p. 668-674.

46. Shang, J., et al., *Comparison of different methods to measure contact angles of soil colloids.* J. Colloid. Interf. Sci. , 2008. **328**(2): p. 299-307.

47. Żenkiewicz, M., *Methods for the calculation of surface free energy solids.* J. Achiev. Mater. Manuf. Eng, 2007. **24**(1): p. 137-145.

48. Van Oss, C.J., M.K. Chaudhury, and R.J. Good, *Interfacial Lifshitz-van der Waals and polar interactions in macroscopic systems.* Chem. Rev., 1988. **88**(6): p. 927-941.

49. XPS, C., *XPS spectra*. 2012. p. 77.

50. Huebschen, G., et al., *Materials characterization using nondestructive evaluation (NDE) methods*. 2016: Elsevier Science. 320.

51. Jenkins, R., *X-ray techniques: overview*, in *Encyclopedia of Analytical Chemistry*, R.A. Meyers, Editor. 2000, John Wiley & Sons, Ltd: Chichester. p. 13269-13288.

52. Materials Evaluation and Engineering, I., *Handbook of analytical methods for materials*. 2001: Plymouth, MN, USA.

53. Joy, D.C., *Scanning electron microscopy for materials characterization.* Curr. Opin. Solid State Mater. Sci., 1997. **2**(4): p. 465-468.

54. Joy, D.C. and C.S. Joy, *Low voltage scanning electron microscopy.* Micron, 1996. **27**(3): p. 247-263.

55. Brundle, C.R., C.A. Evans, and S. Wilson, *Encyclopedia of materials characterization: surfaces, interfaces, thin films*. 1992: Butterworth-Heinemann. 751.

56. *https://www.bgb-info.com/home.php?cat=17234 (accessed: July 13th 2016).*

57. Dettmer, K. and W. Engewald, *Adsorbent materials commonly used in air analysis for adsorptive enrichment and thermal desorption of volatile organic compounds.* Anal. Bioanal. Chem., 2002. **373**(6): p. 490-500.

58. Sigma-Aldrich, *Supelco specialty carbon adsorbents.* 2015(MQR 82950/T410081 1045).

59. Grace and G. Davison, *Sylobead adsorbents for process applications.* sylobead_br_E_2010 / studiohauck, 2010.

60. Sigma-Aldrich, *Product information molecular sieves.* 1999(SAG 03/01/99).

61. *https://www.sorbentsystems.com/desiccants_types.html (accessed: July 13th 2016).*

62. Molitor, N., T. Kitamura, and C. Javelle, *Status paper: background information on carbon nanohorns (cnh)*, T. GmbH, Editor. 2013: Germany.

63. Hu, X., et al., *Impact of some environmentally relevant parameters on the sorption of polycyclic aromatic hydrocarbons to aqueous suspension of fullerene.* Environ. Toxicol. Chem., 2008. **27**(9): p. 1868–1874.

64. Sigma-Aldrich, *Product specification fullerene C_{60}.* (Specification: PRD.1.ZQ5.10000033921).

65. GmbH, I.L.T., *Technical data sheet Graphene platelets, 11-15 nm, 99.5%*. 2012: Germany.

66. Machado Machado, F., et al., *Carbon nanoadsorbents*, in *Carbon nanomaterials as adsorbents for environmental and biological applications*. 2015, Springer: Switzerland. p. 122.

67. White, C.M., et al., *Characterisation of commercially CVD grown multi-walled carbon nanotubes for paint applications.* Prog. Org. Coat., 2016. **90**: p. 44-53.

68. Sigma-Aldrich, *Product specification Product Number: 755125*. 2015: USA.

69. Keskin, S., et al., *A review of ionic liquids towards supercritical fluid applications.* J. Supercrit. Fluid 2007. **43**(1): p. 150-180.

70. Mani, S., et al., *Cross-linking control of PDMS rubber at high temperatures using TEMPO nitroxide.* Macromolecules, 2009. **42**(21): p. 8460-8467.

71. Charmichael, N., *Linear polydimethylsiloxanes CAS No. 63148-62-9 (second Edition).* 2011, European Centre for Ecotoxicology and Toxicology of Chemicals: Brussels, Belgium. p. 155.

72. Dettmer, K. and W. Engewald, *Ambient air analysis of volatile organic compounds using adsorptive enrichment.* Chromatographia, 2003. **57**(Supplement 1): p. S339-S347.

73. *http://polymerdatabase.com/polymers/poly26-diphenyl-p-phenyleneoxide.html (accessed: August 10t^h 2016).*

74. Helmig, D. and J.P. Greenberg, *Automated in situ gas chromatographic-mass spectrometric analysis of ppt level volatile organic trace gases using multistage solid-adsorbent trapping.* J. Chromatogr. A, 1994. **677**(1): p. 123-132.

75. Rothweiler, H., P.A. Wäger, and C. Schlatter, *Comparison of Tenax TA and Carbotrap for sampling and analysis of volatile organic compounds in air.* Atmos. Environ. Part B, 1991. **25**(2): p. 231-235.

76. *Characterization of adsorbents for sample preparation processes*, in *T402026 EQG*. Supelco Sigma-Aldrich.

77. Dash, J.G., *Films on solid surfaces: the physics and chemistry of physical adsorption*. 2012, New York, USA: Elsevier Science. 286.

78. Ban, L.L. and W.M. Hess, *Orientation of graphite layers in standard and heat-treated carbon blacks,* in *9th bennial conference*. 1969, The american carbon society: Boston, MA, USA.

79. Spence, J.C.H., *High-resolution electron microscopy*. 2009, New York, USA: Oxford University Press. 424.

80. Zhang, B.T., et al., *Application of carbon-based nanomaterials in sample preparation: A review.* Anal. Chim. Acta, 2013. **784**: p. 1-17.

81. Tour, J.M., *Top-down versus bottom-up fabrication of graphene-based electronics.* Chemistry of Materials, 2014. **26**(1): p. 163-171.

82. Pyrzynska, K., *Carbon nanotubes as sorbents in the analysis of pesticides.* Chemosphere, 2011. **83**(11): p. 1407-1413.

83. Mauter, M.S. and M. Elimelech, *Environmental applications of carbon-based nanomaterials.* Environ. Sci. Technol., 2008. **42**(16): p. 5843-5859.

84. Valcárcel, M., et al., *Carbon nanostructures as sorbent materials in analytical processes.* Trends Anal. Chem., 2008. **27**(1): p. 34-43.

85. Pan, B. and B. Xing, *Adsorption mechanisms of organic chemicals on carbon nanotubes.* Environ. Sci. Technol., 2008. **42**(24): p. 9005-9013.

86. Peng, H.B., et al., *Organic contaminants and carbon nanoparticles: sorption mechanisms and impact parameters.* J. Zhejiang Univ. Sci. A, 2014. **15**(8): p. 606-617.

87. Sigma-Aldrich, *http://www.sigmaaldrich.com/catalog/product/aldrich/379646?lang=de&region=DE (accessed: April 18th 2016).*

88. Serrano, A. and M. Gallego, *Fullerenes as sorbent materials for benzene, toluene, ethylbenzene, and xylene isomers preconcentration.* J. Sep. Sci., 2006. **29**(1): p. 33-40.

89. Stalling, D.L., C.Y. Guo, and S. Saim, *Surface-Linked $C_{60}/_{70}$-polystyrene divinylbenzene beads as a new chromatographic material for enrichment of coplanar PCBs.* J. Chromatogr. Sci., 1993. **31**(7): p. 265-278.

90. Xiao, C.H., et al., *Use of polymeric fullerene as a new coating for solid-phase microextraction.* Chromatographia, 2000. **52**(11): p. 803-809.

91. Krungleviciute, V., A.D. Migone, and M. Pepka, *Characterization of single-walled carbon nanohorns using neon adsorption isotherms.* Carbon, 2009. **47**(3): p. 769-774.

92. Yuan, J. and M. Antonietti, *Poly(ionic liquid)s: polymers expanding classical property profiles.* Polymer, 2011. **52**(7): p. 1469-1482.

93. Yuan, J., D. Mecerreyes, and M. Antonietti, *Poly(ionic liquid)s: an update.* Prog. Polym. Sci., 2013. **38**(7): p. 1009-1036.

94. Yuan, J. and M. Antonietti, *Poly(ionic liquid) latexes prepared by dispersion polymerization of ionic liquid monomers.* Macromolecules, 2011. **44**(4): p. 744-750.

95. Panniello, A., et al., *Nanocomposites based on luminescent colloidal nanocrystals and polymeric ionic liquids towards optoelectronic applications.* Materials, 2014. **7**(1): p. 591.

96. Mecerreyes, D., *Polymeric ionic liquids: broadening the properties and applications of polyelectrolytes.* Prog. Polym. Sci., 2011. **36**(12): p. 1629-1648.

Chapter 2 Scope and Aim

Sample preparation in the analysis of a sample depends on the type of analytes and suitable extraction technique. The latter can be divided into solvent and solventless microextraction techniques. Among others, liquid phase microextraction (LPME), single-drop LPME, hollow-fiber LPME (HF-LPME) and electromembrane extraction (EME) are examples for solvent based microextraction. Solid phase microextraction (SPME), PAL SPME Arrow, stir bar sorptive extraction (SBSE), needle trap (NT) and in-tube extraction (ITEX) belong to solventless microextraction techniques.

Within this thesis, ITEX was selected for all investigations. Figure 2-1 shows in a general flow chart the steps to be taken after selection of a specific extraction technique, in this case ITEX. The next step is to define a suitable sorbent for extraction. Afterwards, the optimal extraction parameters should be set, to finally perform the method validation.

Sorbent selection in ITEX is up to now based mainly on experience/trial and error.

Thermodynamic and kinetic data would help to better understand the extraction procedure during ITEX and base the sorbent selection on more sound criteria. Inverse gas chromatography (IGC), among different material characterization techniques described in Chapter 1 (e.g.: x-ray photoelectron spectroscopy (XPS), x-ray diffraction (XRD) and thermal gravimetric analysis (TGA)), was applied for this purpose. The topic is covered in Chapter 3 (blue font in Figure 2-1). Three sorbents (PDMS –absorbent, polydimethylsiloxane-, Tenax TA –adsorbent, porous polymer- and Carbopack C –adsorbent, graphitized carbon black-) and probes with different polarities were tested. PDMS is a well-studied absorbent, thus it is a very useful material to set a common baseline one can compare other data with. A special feature from Chapter 3 is the simple and practical experiment set-up.

A wide spectra of materials can be packed in the ITEX cannula for investigation. In this thesis, carbon based-nanomaterials (CNM, Chapter 4, orange font in Figure 2-1) and polymeric ionic liquids (PIL, Chapter 5, purple font in Figure 2-1) were analyzed, both materials not currently used as sorbent. The latter, in a collaboration project with the University of Vienna and the University of Dhaka. The ITEX cannulas were also packed with textile fibers and characterized via IGC. The topic is not covered in this work, but shows the flexibility and versatility of the method.

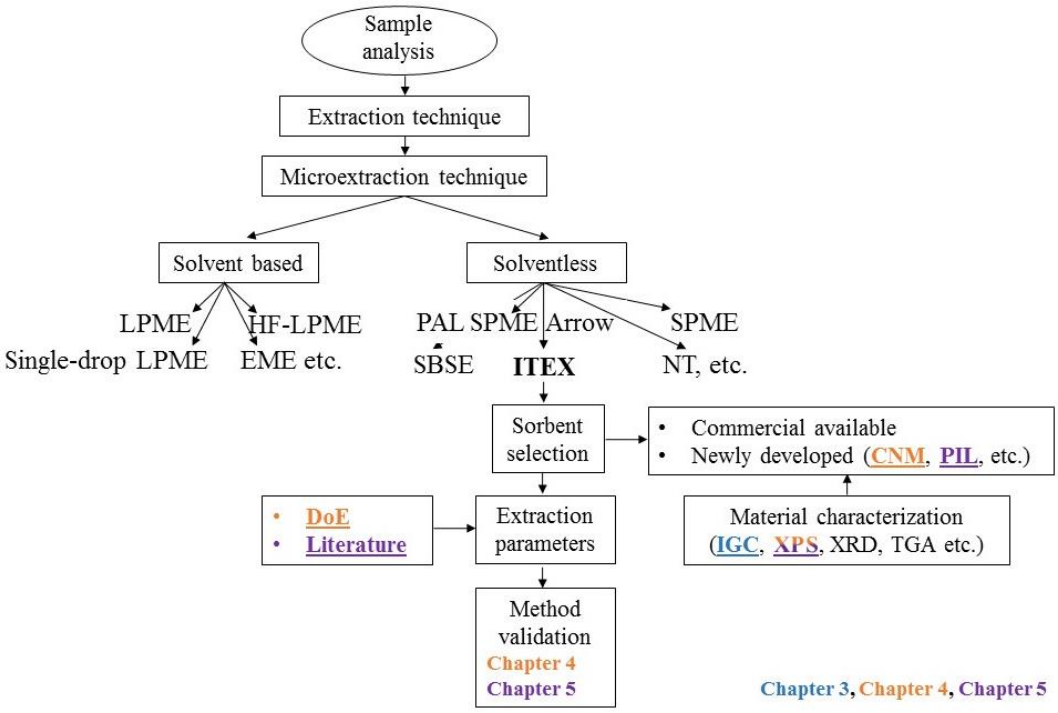

Figure 2-1. Thesis graphical overview. Items marked in colour refer to the chapters in which the corresponding topics are addressed.

Among the extraction parameters that highly influence this procedure are: incubation time, the number of aspirating and dispensing cycles (strokes), the flow for the aspirating and dispensing cycles, desorption temperature and injection volume. Optimal parameters should be determined to provide a proper extraction before method validation. In Chapter 4, a Box-Behnken design (design of experiments –DoE-) for the extraction of polycyclic aromatic hydrocarbons (PAHs) with five CNM was used. Three CNM were also characterized via XPS.

Another option for the extraction parameter selection, is to apply known ones from the literature, as well as the same chemical probe compounds. From the measured data, a direct comparison to the applied literature source is achieved. In Chapter 5, PIL were used as sorbent and the extraction parameters and probe compounds were selected from the literature. To characterize the synthesized PIL, XPS measurements were also performed.

Finally, Chapter 6. presents the overall conclusions from this thesis and an outlook on further developments of the different topics discussed during this work.

Chapter 3 Sorbent material characterization using in-tube extraction needles as inverse gas chromatography column

Abstract

The microextraction technique, in-tube extraction (ITEX) consists of a stainless steel needle, packed with sorbent material. The selection of the sorbent is merely based on empirical considerations than on experimental data. The reason is a lack of knowledge about the relevant physico-chemical properties. To overcome this issue, inverse gas chromatography using the ITEX needle directly as column was developed for sorbent characterization.
The ITEX needle was installed, via a short deactivated glass capillary, in the gas chromatograph. The probes, prepared at a concentration approaching the infinite dilution in the gas phase, were injected to characterize the sorbent. Natural gas was applied as inert marker. The thermodynamic parameters were determined at a constant column flow, while varying the column temperature. The kinetic parameters were determined at a constant temperature, while changing the column flow. Benzene, ethyl acetate and 3-methy-1-butanol were used to determine the thermodynamic parameters such as sorption enthalpy (ΔH_s), partitioning constant between the solid and gas phase (K_d) and kinetic parameters such as the diffusion coefficient (D^{∞}), dispersion coefficient (D*), and apparent permeability (P_{app}). As sorbent phases, PDMS, Tenax TA and Carbopack C were characterized, exemplarily.
ΔHs values for PDMS, Tenax TA and Carbopack C ranged from -64 to -4 kJ mol^{-1}. The ΔH_s is assumed to be constant within the temperature range measured. For PDMS, most of the probes analytes were measured from 40 to 150°C. For Tenax TA the range was smaller than PDMS, from 70 to 150°C. Experimental estimated K_d lay between 1 and 950. For literature comparison a power equation was fitted to calculate K_d at 25°C. The results for D^{∞} and D* were in the order of magnitude from as 10^{-8} to 10^{-9} m^2 s^{-1}, while P_{app} values ranged from 10^{-6} to 10^{-8} m^2 s^{-1}. According to the thermodynamic and kinetic data, among the three sorbents and probes, Tenax TA proved to be the most suitable sorbent for benzene and ethyl acetate, while PDMS for 3-methyl-1-butanol.

Introduction

Solventless microextraction techniques have been used for more than 15 years [1] and over this period sample preparation has been improved. [2] Former drawbacks, such as the amount of manual work, sample preparation and preconcentration in various steps, have been overcome as a result of the automatization. [3] Furthermore, higher extraction yields and more reproducible data as well as a smaller extraction phase to sample volume ratio in comparison to other enrichment techniques, are their major features. [2]

Solventless microextraction techniques can be classified into i) application of a coating on the surface of a rod or needle ii) sorbent material packed in a tube or needle. [1] Among the latter, in-tube extraction (ITEX) consists of a stainless steel needle with side port and the

microextraction technique in focus of this study. The needle body is packed with a sorbent material and is surrounded by an external heater for thermodesorption. Above the stainless steel needle, a gas tight Hamilton syringe (1.3 mL) is positioned. The analytes are enriched in the sorbent material by aspirating and dispensing the headspace (HS) volume from the sample. Following the extraction, thermodesorption is performed in the gas chromatograph injector.

ITEX has been utilized, e.g., for the quantification of halogenated hydrocarbons under abiotic and biotic conditions from microbially active and sterilized microcosms [4], for the analysis of hydroxylic methyl-derivatized and volatile organic compounds in blood and urine [5], for the investigation of alcoholic beverages, [6] [7] and as an efficient green analytical technique for geochemical evaluation of petroleum source rock. [8] In order to execute a successful analysis with ITEX, firstly the extraction parameters must be optimized, e.g., extraction strokes, incubation temperature, extraction flow. An approach to determine optimal parameters, is the application of design of experiments, which saves time and costs. [9] Nonetheless, the key point is the proper selection of the sorbent material. Generally, this decision is based on empirical considerations or simply on trial and error. [10] A targeted choice supported by thermodynamic and kinetic data, material characterization, will lead to a reduction in time for method optimization accompanied by an improved understanding of the system processes.

Inverse Gas Chromatography (IGC) is commonly applied for sorbent material characterization but not often in the field of microextraction techniques. The term “inverse” refers to the analysis of the stationary phase/packed material in the column and not the sample injected, as in conventional gas chromatography (GC). [11, 12] For IGC, the stationary phase is characterized using pure and known liquids or gases. These samples are prepared at a concentration approaching the infinite dilution (c^{∞}), where Henry’s law obeys. [13] Experiments performed at infinite dilution allow the investigation of interactions between the probe and the stationary phase and no probe-probe interactions have to be considered. [11, 14] From the retention time difference between a probe compound (t_r) and an inert marker (t_0) (e.g., methane), [15] multiplied by the column flow and a compressibility factor, the net retention volume (V_N) is calculated.[16] From this, thermodynamic data, the sorption enthalpy (ΔH_s), molar free energy of sorption (ΔG_s), entropy of sorption (ΔS_s) and the partitioning constant between solid and gas phase (K_d), can be calculated. [11, 17] Furthermore, IGC allows for the determination of kinetic data such as diffusion (D^{∞}) [18] and dispersion

coefficients (D^*). [19] The multiplication of the diffusion coefficient with the partitioning constant, yields the probes apparent permeability (P_{app}). [20-22]

These parameters can improve the process of identifying the optimal sorbent material for various analytes on a non-empirical/trial and error base. Different sorbent categories are available: graphitized carbons, carbon molecular sieves, porous polymers and miscellaneous. [23, 24] Here, an adsorbent from the graphitized carbon blacks (Carbopack C) and porous polymers (Tenax TA) were selected. Additionally, PDMS was investigated as the most widely used absorptive. The main task was to improve the selection of sorbent material based on determined thermodynamic and kinetic data by a fast inverse gas chromatography method using the originally packed ITEX needles directly.

Experimental

3.1.1 Reagents and materials

Natural gas obtained from an in-lab gas line was used as inert marker. It was stored in a one liter multi-layer foil gas sampling bag (Restek, Bad Homburg, Germany). Benzene (>99%), toluene (99.5%), ethyl acetate (>99.8%), 1,2-dichloroethane (>99.8%), methyl *tert*-butyl ether (MTBE) (>99.9%), ethyl *tert*-butyl ether (ETBE) (99%) and n-Pentane (99%) were purchased from Sigma-Aldrich. *o*-Xylene (>99.8%), 3-methyl-1-butanol (>99.8%) and 2-butanol (>99.8%), were purchased from Fluka (Sigma-Aldrich, Steinheim, Germany). All probes were prepared with reagent water from a PURELAB Ultra Analytic water purification system (ELGA LabWater, Celle, Germany).

3.1.2 Stock and Sample Preparation

Amber 20-mL screw cap headspace vials (BGB Analytik AG, Böckten, Switzerland) closed with rubber-PTFE septa screw caps (BGB Analytik AG, Böckten, Switzerland) were used for sample preparation. From the stock solutions (see concentrations in Table S.I.C3-1 of the Supplementary Information), benzene, toluene, *o*-xylene, ethyl acetate, 3-methyl-1-butanol, 1,2-dichloroethane, methyl *tert*-butyl ether, ethyl *tert*-butyl ether, 2-butanol and n-pentane samples were prepared at 3.49, 4, 3.51, 45.1, 101.12, 12.5, 14.8, 18.5, 500 and 1.01 mg L^{-1}, respectively. 10 mL were used as sample volume in the amber 20-mL headspace screw cap vial and closed with rubber-PTFE septa caps (BGB Analytik AG, Böckten, Switzerland). The stock and sample solutions were prepared daily. The samples were prepared at a concentration approaching the infinite dilution in the gas phase (around 0.3 to 1 mg L^{-1}).

3.1.3 Inverse Gas Chromatography

3.1.3.1 Column

Three ITEX needles packed with PDMS, Tenax TA and Carbopack C (CC) (BGB Analytik AG, Böckten, Switzerland) were used as column (further properties are found in the supplement Table S.I.C3-2). A 40 cm, 0.32 mm i.d. deactivated TSP FS-tubing (BGB Analytik AG, Böckten, Switzerland) was used to connect the column to the injector. On the side of the injector, the tubing was attached such as a usual GC column. The other side of the tubing was jointed to the ITEX needle (at the "top", not the cannula end) with a Swagelok connector containing a 1/8 " Teflon PTFE ferrule (Restek, Bad Homburg, Germany). The cannula from the ITEX was attached to the FID detector with the common ferrule and nut. The experimental set up is shown in Figure S.I.C3-1 of the Supplementary Information.

3.1.3.2 Apparatus and conditions

All measurements were performed using a Shimadzu 2014 gas chromatograph (GC) equipped with a flame ionization detector (FID) (Shimadzu, Duisburg, Germany). Injection was performed in a split/splitless (S/SL) injector at 200°C in split mode at a split ratio of 5. A VICI precision sampling pressure lok 0.5 mL (BGB Analytik AG, Böckten, Switzerland), was used to inject 20 µL of natural gas as inert marker, while a Hamilton syringe 1750 SL 500 µL Hamilton AG, Bonaduz, Switzerland) was utilized to inject 500 µL of the probe's HS volume. Both manually injected. N_2 of purity 5.0 (Air Liquide, Oberhausen, Germany) was used as carrier gas.

The thermodynamic parameters were determined at a constant column flow of 3 mL min^{-1} and the column temperature was varied from 313.15 to 423.15 K. The determination of the kinetic parameters was carried out at column flows from 1.4 to 4.2 mL min^{-1} and a temperature of 363.15 K or 423.15 K. The column flow was controlled with an FP-meter from Applied Instruments (Applied Instruments, The Netherlands). The FID temperature was set at 260°C with a sampling rate of 40 ms. Data reprocessing was performed with GCMS Solution, Microsoft Excel and Origin.

Each vial was used either for three temperature levels or three column flow settings, each level was measured in triplicates. Before injection into the S/SL injector, the syringe was cleaned with the probe headspace (HS) sample volume, afterwards another probe HS sample volume was injected for analysis.

Results and Discussion

3.1.4 Determination of thermodynamic parameters

To determine the thermodynamic parameters, the net retention volume (V_N) and the specific retention volume (V_g) were calculated (Eq. 1. and 2.). [17]

$$V_N = jF\Delta t \qquad \text{in mL} \qquad \text{Eq.1}$$

$$V_g = \frac{273Fj\Delta t}{mT} \qquad \text{in mL g}^{-1} \qquad \text{Eq.2}$$

Here, j is the James-Martin compressibility factor, F is the column flow in mL min^{-1}, $\Delta t = t_r - t_0$ is the time difference between the probe (t_r) and the inert marker (t_0), m is the mass of the sorbent or stationary phase and T is the column temperature in Kelvin. The details of the calculations are presented in Calculation S.I.1 of the Supplementary Information.

The difference in retention times between the probe (t_r) and the inert marker (t_0) were read from the chromatograms. Figure 3-1 shows an example of natural gas (20 µL injection volume) and benzene as probe (500 µL HS injection volume) at two different temperatures. As the column temperature decreases, the retention time t_r increases. The t_0 remains constant through the investigated temperature range, as long as the column flow is not changed.

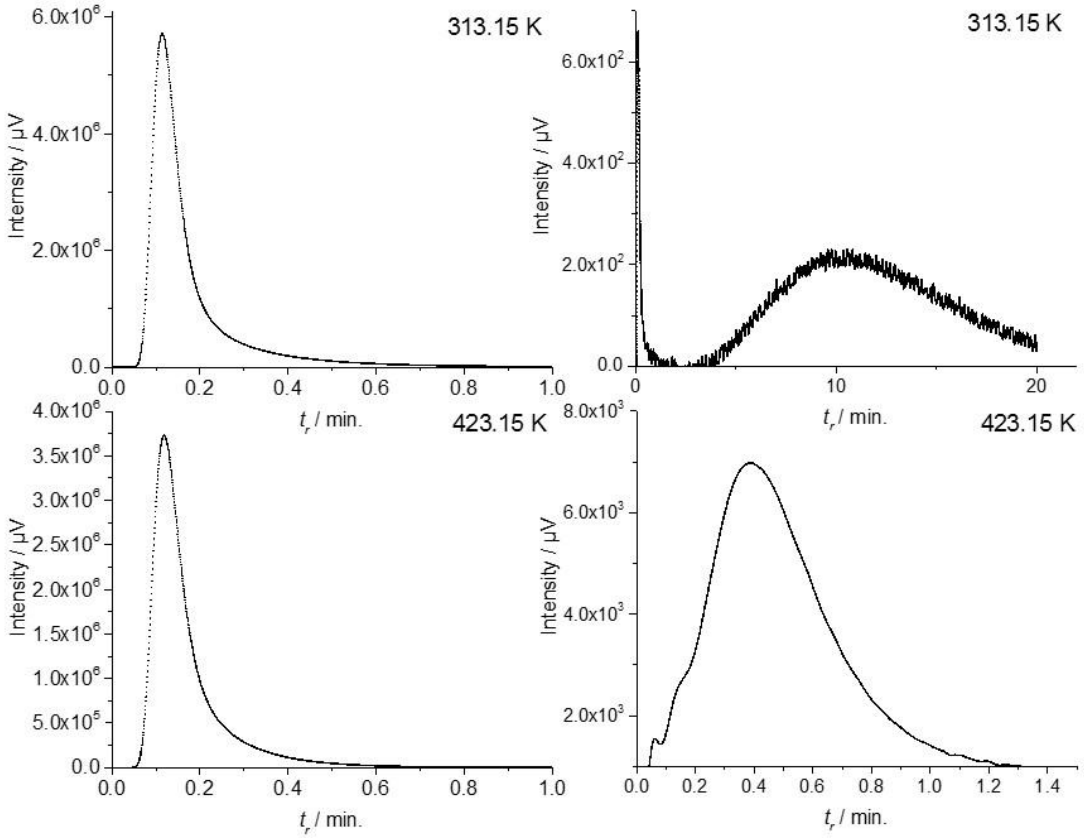

Figure 3-1. Breakthrough curves of natural gas and benzene by using an ITEX needle as IGC column. Here PDMS as sorbent was used and column flow was set to 3 mL min^{-1}. On the left side natural gas and on the right side benzene at 313.15 and 423.15 K, respectively, were measured.

The peaks shown in Figure 3-1 possess a certain degree of asymmetry, with tailing factors, e.g., for benzene of 1.5 or higher. The apex retention time, for the estimation of thermodynamic and kinetic parameters, is applied when symmetrical peaks (A_s = 0.9 to 1.1) [25] appear, which is not the case for this study. Further, the first moment analysis could not be applied for peak analysis because the method is susceptible for errors in case of strongly tailing peaks. For this reason, the retention times were determined using the half mass point method as proposed by Bi, E. et al. . [26] It consists in dividing the peak area into two equal parts and the retention time detected at the half is averaged and set as the retention time of the inert marker and probe. (See Table S.I.C3-3 for the coefficient of variation of the estimated retention time according to the half mass point method for three exemplary probes).

The natural logarithm of the specific retention volume (ln V_g) was calculated and plotted against the inverse temperature 1/T. From the slope, the sorption enthalpy (ΔH_s) can be determined. [11, 17, 27] In Figure 3-2 the sorption enthalpy determination is exemplarily shown for the probe compound benzene. The determination of the sorption enthalpy for the

other probe compounds and sorbents with corresponding, slopes, quadratic coefficient and temperature range where ΔH_s is constant, are presented in Table S.I.C3-4 of the Supplementary Information.

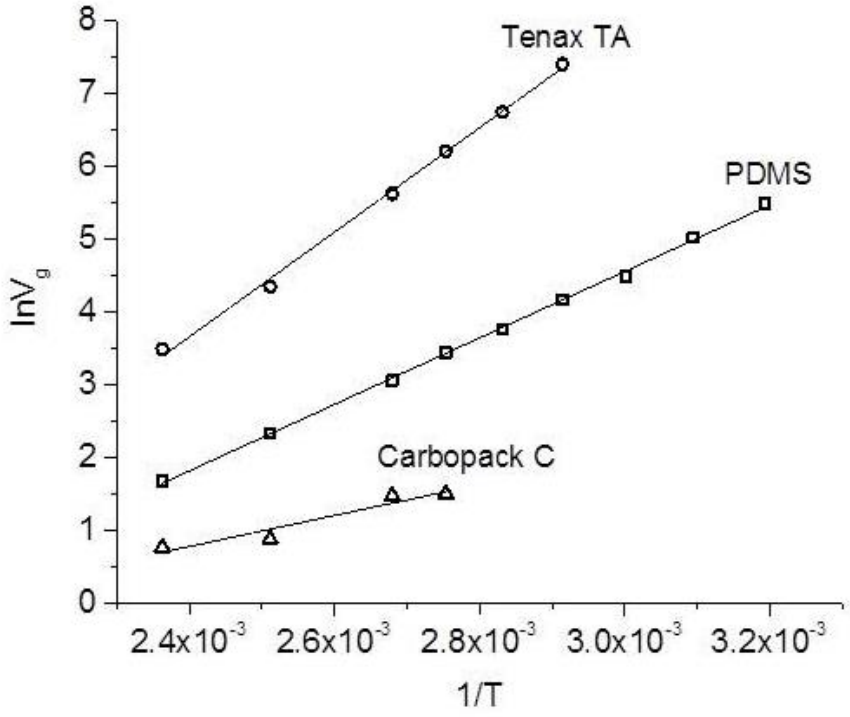

Figure 3-2. Graphical determination of ΔHs for benzene with three sorbents.
PDMS, Tenax TA and Carbopack C as sorbent were used and column flow was set to 3 mL min^{-1}. Benzene as probe compound (average of three replicates), with a sample concentration (c_{sample}) of 3.49 mg L^{-1} in the liquid and a headspace injection volume of 500 µL.

The negative sorption enthalpies ΔH_s indicate the release of heat during the exothermic sorption process. More negative ΔH_s indicate a stronger interaction between the probe and sorbent. [28] The more negative values were found for Tenax TA, which agrees to be the strongest material among the investigated sorbents and within the temperature range. [23] Adsorption and absorption are the types of mechanisms for sorption. In contrast for PDMS, absorption is the dominant sorption mode, which is weaker than adsorption and the release of probes can be hindered by the amount of fillers in PDMS. The fillers increase the tortuosity of the material. [21] Carbopack C is a non-polar, molecular shape dependent sorbent, recommended for the analysis of compounds larger than C_{12}. Benzene resembles the structure of Carbopack C, which explains the more negative ΔH_s. As presented in Table 3-1, the here measured ΔH_s values are in the same order of magnitude as with the literature values.

Table 3-1. Sorbent characterization with ΔH_s as parameter via IGC/FID.

	ΔH_s / kJ mol^{-1}					
	PDMS		Tenax TA		Carbopack C	
	This study	Literature	This study	Kroupa et al. [28]	This study	Karwa et al. [29]
Benzene	-38.0 ± 0.1		-59.7 ± 0.1	-48.8 ± 0.8	-17.7 ± 0.02	-16.0
Toluene	-44.8 ± 0.3	-33.4 [30]		-53.7 ± 1.2		
o-Xylene	-45.8 ± 8.6			-68.0 ± 1.7		
Ethyl acetate	-46.1 ± 0.3		-64.7 ± 0.3	-57.4 ± 1.9	-4.7 ± 0.01	
3-methyl-1-butanol	-49.3± 0.5		-56.0 ± 0.3		-16.8 ± 0.01	
2-butanol	-40.0 ± 0.1					
1,2-dichloroethane	-46.5 ± 0.4					
n-Pentane	-24.7 ± 0.01	-24.1 [15]		-38.0 ± 3.1		
MTBE	-38.2 ± 0.3					
ETBE	-49.6 ± 0.4					

Another approach to interpret sorption data is via descriptors for poly-parameter linear free-energy relationships. These descriptors yield information about a specific type of molecular interaction that occurs between the sorbent and sorbate and its contribution to overall sorption. Several types of non-specific and specific interactions are taken into account for sorption of non-ionic organic sorbates in these poly-parameter approaches.[31] Tenax TA only interacts via van der Waals forces/cavity formation, while PDMS interacts mainly also via van der Waals, but also via hydrogen bond basicity. Table S.I.C3-5 of the Supplementary Information contains the calculated values for interactions according to the descriptors.

To continue the analysis of the sorption phenomena, K_d values were calculated according to Eq.3. [17]

$$K_d = \frac{V_N}{V_P} \qquad \text{Eq.3}$$

Here, V_N is the net retention volume and V_P that of the sorption phase, respectively. Figure 3-3 presents K_d values for the probes and sorbents applied in this study. An example for the calculation of the V_P is given in the Calculation S.I.C3-2.

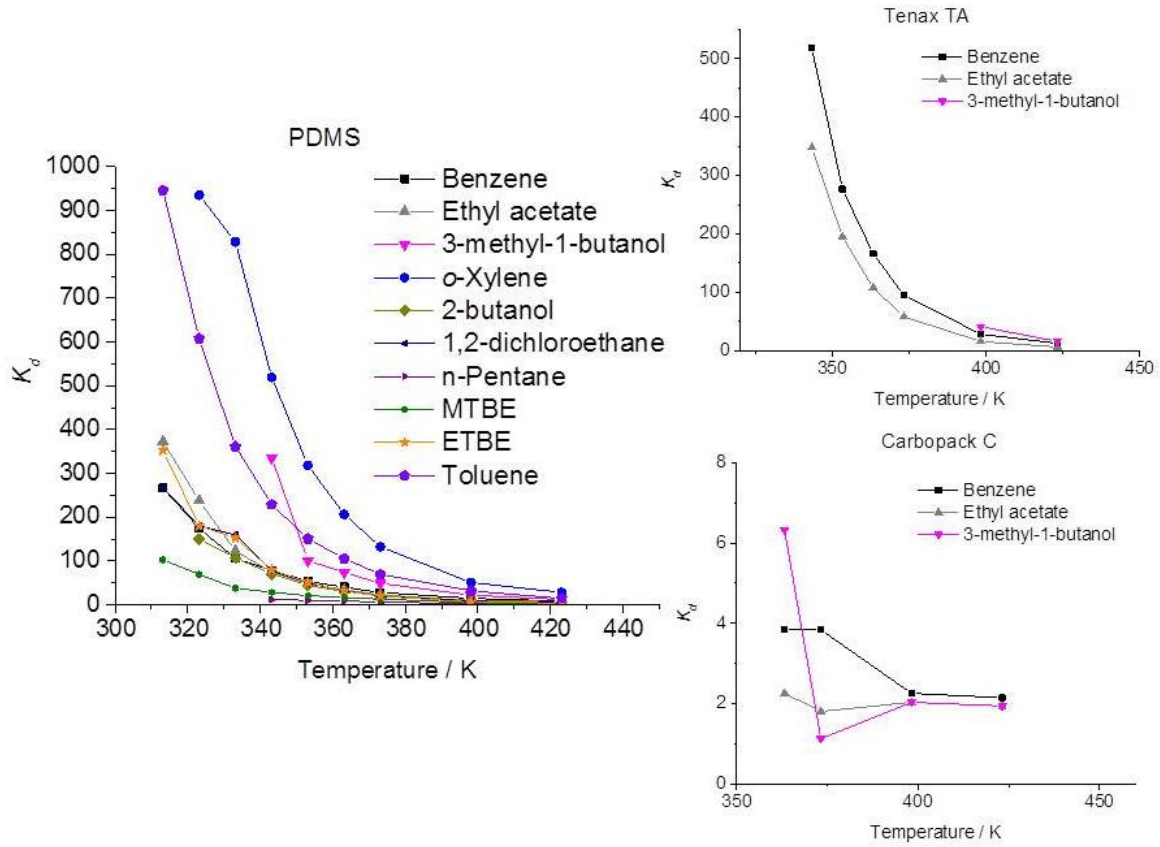

Figure 3-3. K_d values for three sorbents in ITEX.
PDMS, Tenax TA and Carbopack C as sorbent at a flow of 3 mL min^{-1}. Column temperature from 313.15 to 423.15 K or smaller depending on the probe.

To verify the measured data, in Table 3-2, the K_d values from the IGC measurements were fitted with a power equation and then extrapolated to 25 °C for literature comparison (an example calculation is presented in Calculation S.I.3 of the Supplementary Information).

Table 3-2. K_d literature comparison for PDMS and Tenax TA.

	K_d (PDMS at 25 °C)				K_d (Tenax TA)		
	This study	Sprunger et al. [32]	Pawliszyn [33]	UFZ [34]	This study[a)]	Kroupa et al.[a)] [28]	UFZ[b)] [34]
Benzene	444	537	423	338	5632	2675	8
Toluene	1519	776	818	888			27
o-Xylene	2863	1738	2800	2957			128
Ethyl acetate	518	270		240	4954	3598	4
3-methyl-1-butanol	1480	1380		1768	3493		9
2-butanol	383	575		501			2
1,2-dichloroethane	498	14		331			7
n-Pentane	32	59	77	47			0
MTBE	133			191			1
ETBE	556						

a) at 25 °C. b) at 40 °C.

According to the literature, if the predicted values are within a factor of two, a proper calculation can be assumed. [35] The experimentally determined K_d values were compared to literature values and values calculated by the UFZ pp-LFER calculator.[34]

With the exception of 1,2-dichloroethane our results match with literature and calculated data for PDMS. For Tenax TA, the here determined values fit with literature values[28] but show a discrepancy to the calculated pp-LFER K_d values.

In another study with a HS-ITEX-GC/MS method, Tenax TA was used as sorbent for ITEX measurements of benzene. [3] Two desorption temperatures were compared (200 and 300°C), yielding a peak area of 1.3 $x10^7$ and $1.8x10^7$, respectively. Assuming the peak yield at 300°C to be 100%, the peak yield at 200°C would represent 76%. If the power equation for benzene and Tenax TA established with the IGC/FID technique used in this study, is applied to calculate the amount of compound found in the gas phase at 200 and 300°C, then for 200°C 76% are calculated and 100% for 300 °C. This underlines that the measurements were performed correctly and useful data were generated. In order to apply the information gained from the K_d values to the ITEX technique, the K_d fitted equations were applied to calculate the amount of compound in the gas phase at 313.15 K (40 °C, usual extraction temperature), 473.15 and 573.15 K (200 and 300 °C, usual thermodesorption temperatures). In Table 3-3, data for the probe fraction in the gas phase (f_g) at the corresponding temperatures and K_d values are presented:

Table 3-3. Determination of f_g with fitted data for the comprehension of the ITEX extraction and thermodesorption procedure.

		PDMS			Tenax TA			Carbopack C		
	T / K	473.15	573.15	313.15	473.15	573.15	313.15	473.15	573.15	313.15
	T / °C	200	300	40	200	300	40	200	300	40
Benzene	K_d	2.1	0.2	251	1.5	0.0	2348	1.3	0.5	7.8
2*10^31 x^(-11.58)	f_g	0.703	0.956	0.020	0.769	0.990	0.002	0.799	0.903	0.392
Toluene	K_d	2.5	0.2	769						
3*10^37 x^(-13.86)	f_g	0.665	0.966	0.006						
o-Xylene	K_d	4.5	0.3	1443						
1*10^38 x^(-13.96)	f_g	0.524	0.941	0.003						
Ethyl acetate	K_d	0.7	0.0	257	0.6	0.0	1911	1.8	1.7	2.2
1*10^38 x^(-14.26)	f_g	0.875	0.991	0.019	0.887	0.997	0.003	0.731	0.747	0.693
3-methyl- 1-butanol	K_d	1.8	0.1	727	2.8	0.1	1638	1.0	0.5	5.4
1*10^39 x^(-14.48)	f_g	0.730	0.978	0.007	0.639	0.971	0.003	0.831	0.915	0.481
2-butanol	K_d	1.5	0.1	212						
2*10^32 x^(-12.01)	f_g	0.770	0.971	0.023						
MTBE	K_d	0.6	0.1	74						
1*10^31 x^(-11.67)	f_g	0.892	0.987	0.063						
ETBE	K_d	0.4	0.0	260						
1*10^41 x^(-15.46)	f_g	0.919	0.995	0.019						
1,2-dichloroethane	K_d	0.6	0.0	244						
3*10^38 x^(-14.46)	f_g	0.889	0.992	0.020						
n-Pentane	K_d	1.4	0.4	23						
2*10^18 x^(-6.786)	f_g	0.780	0.929	0.178						

According to the Henry constant, small f_g values suggest that most of the probe is found in the sorbent with the corresponding available fraction of compound in the gas phase. This is the case at 40 °C, which favors the extraction procedure in the ITEX technique. At larger temperatures (200 and 300 °C), the fraction of the compound in the gas increases. In ITEX, this is an advantage, because those are common thermodesorption temperatures. Therefore, if a larger amount of compound is present in the gas phase at higher thermodesorption temperatures, more analyte will be injected in the gas chromatograph.

3.1.5 Determination of the diffusion coefficient, dispersion coefficient, apparent permeability and significance for the ITEX system

In addition to the determination of the thermodynamic parameters, a kinetic examination of how the probe is flowing through the material is crucial for a comprehensive understanding of the processes occurring during ITEX. The diffusion (D^{∞}) and dispersion (D*) coefficient are used to determine how fast the equilibrium is reached. This information is of importance for the ITEX technique, because faster equilibration results in less extraction strokes required and

consequently saved time. The apparent permeability (P_{app}) yields information whether the compound will have a faster or slower transit through the material. This aspect is relevant for the ITEX technique, because at the moment of sample volume injection (the corresponding amount of gas passes through the sorbent) it is favorable if a large amount of the analyte is swept over and introduced in the gas chromatograph.

The diffusion coefficient (D^{∞}) was calculated according to Equation 4. [18]:

$$D^{\infty} = \frac{8 d_p^2 k}{\pi C (1+k)^2} \qquad \text{in } m^2 s^{-1} \qquad \text{Eq.4}$$

d_p is the particle diameter, k the partition ratio equal to the time difference between the probe (t_r) and the inert marker (t_0), divided by the retention time of the inert marker (t_0) and C is the slope from the van Deemter plot. The C term corresponds to the mass transfer processes during sorption and desorption. [36]

In order to calculate C, Equation 5, for the Plate Height Theory (H) was applied.

$$H = \left(\frac{l}{5.54}\right)\left(\frac{d}{t_r}\right)^2 \qquad \text{in m} \qquad \text{Eq.5}$$

l is the length of the packed sorbent material, d is the peak width at half the maximum of the height and t_r the probe's retention time.

A plot of H against the mobile phase velocity is generated and at high velocities a linear regression is set. The slope of the line accounts to the C term, Figure S.I.C3-2 of the Supplementary Information, depicts the van Deemter plot for benzene.

To determine whether dispersion is an important parameter or not, the Reynolds number was calculated[37]:

$$Re = \frac{\rho v_{cg} d_p}{\eta} \qquad \text{Eq.6}$$

Where ρ is the mobile phase density (nitrogen), vcg is the mobile phase velocity, d_p is the PDMS, Tenax TA or Carbopack C diameter (150 or 165 μm) and η the dynamic viscosity from nitrogen.

The calculated Reynolds numbers ranged between 0.004 and 0.09 (see Table S.I.C3-6 of the Supplementary Information for further information). Since the values are smaller than one, diffusion will predominate in the system and the dispersion coefficient will be similar to the diffusion coefficient. [19] As a consequence, Equation 7 can be used to calculate the dispersion coefficients.

$$D^{*} = \gamma D^{\infty} \qquad \text{in } m^2 s^{-1} \qquad \text{Eq.7}$$

γ is the tortuosity and a value of 0.69 was supposed for calculations. [19]

The apparent permeability (P_{app}) comes from the multiplication of the diffusion coefficient with K_d. [20, 21] In this study, either the K_d at 90 or 150°C was applied. These temperatures were chosen, according to the thermodynamic experiments. Table 3-4 presents the results for the kinetic parameters using three sorbents.

Table 3-4. Kinetic parameters at 90 °C for three sorbents using IGC/FID.

	D^{∞} / m^2 s^{-1}			D^* / m^2 s^{-1}			P_{app} / m^2 s^{-1}		
	Benzene	Ethyl acetate	3-methyl 1-butanol	Benzene	Ethyl acetate	3-methyl 1-butanol	Benzene	Ethyl acetate	3-methyl 1-butanol
CC	2.07E-08	-	1.08E-08	1.43E-08	-	1.01E-08	8.34E-08	-	3.25E-08
PDMS	1.54E-09	1.27E-09	1.25E-09	1.07E-09	8.78E-10	8.62E-10	6.98E-08	3.95E-08	1.06E-07
Tenax TA	7.79E-09	8.15E-09	1.50E-08[a)]	5.38E-09	5.62E-09	1.04E-08[a)]	1.31E-06	8.80E-07	2.37E-07[a)]

a) experiment run at 150 °C

Based on the data in Table 3-4, the most suitable sorbent for benzene and ethyl acetate is Tenax TA. It has the highest diffusion coefficients, as well as the highest apparent permeability. Initially, it could be selected as the most proper sorbent for the extraction of 3-methyl-1-butanol, but these experiments were performed at higher temperatures, where sorption is weaker, which facilitates the determination of the kinetic parameters. For 3-methyl-1-butanol, PDMS would be a more suitable option, since it is easily desorbed. Carbopack C does not represent a preferable option for any of the compounds. The diffusion coefficients in the present study were compared to previous studies to verify whether the application of ITEX as IGC column yielded similar results. A diffusion coefficient for benzene in PDMS, of 2.8E-10 m^2 s^{-1} at 298.15 K was reported in literature. [38] The diffusion coefficient varies to the temperature in a logarithmic fashion, it may vary five orders of magnitude from 25 to 160 °C, and is explained by the Arrhenius equation. [18] [39] For this reason the results vary within orders of magnitude.

The sorbent enrichment in ITEX is performed by aspirating and dispensing the headspace of the aqueous sample through the sorbent. Each time this cycle is run (aspirating and dispensing) is called stroke. According to the extraction flow, extraction volume set for each stroke, type of analytes and sorbent, the enrichment procedure may take around 50 minutes. For this reason a high diffusion and dispersion coefficient, as well as a high apparent permeability implies that equilibrium in the sorbent is faster reached and therefore less strokes for sorbent enrichment would be needed. As a consequence, time during the extraction procedure will be saved, reaching a larger sample throughput.

Conclusions

The practical experimental set-up presented in this work, allowed a fast and easy characterization of three commercial available sorbent materials applied in ITEX. The ITEX needle packed with PDMS, Tenax TA and Carbopack C were used as inverse gas chromatography column for the determination of thermodynamic parameters such as, enthalpy of sorption, partitioning coefficient as well as kinetic parameters like diffusion coefficient, dispersion coefficient and apparent permeability.

The partition constants allowed the estimation of the amount of compound found in equilibrium at the gas and solid phase, which is valuable information for the comprehension of the extraction and thermodesorption procedures in ITEX. With the kinetic parameters, it was possible to gather information concerning which sorbent will reach a faster equilibrium and by this decreasing the number strokes needed for sorbent enrichment.

In summary, the variation of data yields an investigation field to gather information and create a proper database according to sorbent, probe and other parameters.

Acknowledgement

We thank Beat Schilling, Dr. Maik Jochmann and Dr. Thorsten Hüffer, for their valuable comments and help. As well as Nova Maulani and Iradani Katalia for their contributions.

Nomenclature

C	Slope from the linear section of the van Deemter plot
d	Peak width at half height maximum
d_p	Particle diameter
D^{∞}	Diffusion coefficient in the sorbent
D^*	Dispersion coefficient
F	Column flow
H	Plate Height
HS	Headspace
j	James-Martin compressibility factor
k	Partition ratio
K_d	Partitioning constant between the solid and gas phase
l	Length of the packed sorbent material
m	Mass of the sorbent or stationary phase

P	Ratio between inlet and outlet pressure
P_{app}	Apparent permeability
p_0	Outlet pressure (atmospheric)
T	Column temperature
t_0	Inert marker retention time
t_r	Probe retention time
vcg	Mobile phase velocity
V_g	Specific retention volume
V_N	Net retention volume
V_P	Volume of the stationary phase.
ΔHs	Sorption enthalpy
$\Delta t = t_r - t_0$	Time difference between the probe (t_r) and the inert marker (t_0)
η	Dynamic viscosity of the mobile phase
ρ	Density of the mobile phase

References

1. Jochmann, M.A., et al., *In-tube extraction for enrichment of volatile organic hydrocarbons from aqueous samples.* J. Chromatogr. A, 2008. **1179**(2): p. 96-105.

2. Laaks, J., M.A. Jochmann, and T.C. Schmidt, *Solvent-free microextraction techniques in gas chromatography.* Anal. Bioanal. Chem., 2012. **402**(2): p. 565-571.

3. Laaks, J., et al., *In-tube extraction of volatile organic compounds from aqueous samples: an economical alternative to purge and trap enrichment.* Anal. Chem., 2010. **82**(18): p. 7641-7648.

4. Ruecker, A., et al., *Predominance of biotic over abiotic formation of halogenated hydrocarbons in hypersaline sediments in western Australia.* Environ. Sci. Technol., 2014. **48**(16): p. 9170-9178.

5. Rasanen, I., et al., *Headspace in-tube extraction gas chromatography– mass spectrometry for the analysis of hydroxylic methyl-derivatized and volatile organic compounds in blood and urine.* J. Anal. Toxicol., 2010. **34**(3): p. 113-121.

6. Salanţă, L.C., et al., *Determination of the volatile compounds from hop and hop products using ITEX/GC-MS technique.* J. Agroaliment. Proc. Technol., 2012. **18**(2).

7. David, F. and C. Devos, *Analysis of volatile organic compounds in beer using ITEX headspace sampling.* CTC Analytics. **ITEX Application Note #04**.

8. Akinlua, A., et al., *Microwave-assisted nonionic surfactant extraction of aliphatic hydrocarbons from petroleum source rock.* Anal. Chim. Acta, 2011. **691**(1-2): p. 48-55.

9. Hüffer, T., et al., *Multi-walled carbon nanotubes as sorptive material for solventless in-tube microextraction (ITEX2)—a factorial design study.* Anal. Bioanal. Chem., 2013. **405**(26): p. 8387-8395.

10. Laaks, J., et al., *Optimization strategies of in-tube extraction (ITEX) methods.* Anal. Bioanal. Chem., 2015. **407**(22): p. 6827-6838.

11. Dritsas, G.S., K. Karatasos, and C. Panayiotou, *Investigation of thermodynamic properties of hyperbranched aliphatic polyesters by inverse gas chromatography.* J. Chromatogr. A, 2009. **1216**(51): p. 8979-8985.

12. Perruchot, C., et al., *Characterisation of the surface thermodynamic properties of cement components by inverse gas chromatography at infinite dilution.* Cem. Concr. Res., 2006. **36**(2): p. 305-319.

13. Voelkel, A., et al., *Inverse gas chromatography as a source of physiochemical data.* J. Chromatogr. A, 2009. **1216**(10): p. 1551-1566.

14. Hamieh, T. and J. Schultz, *New approach to characterise physicochemical properties of solid substrates by inverse gas chromatography at infinite dilution I. Some new methods to determine the surface areas of some molecules adsorbed on solid surfaces.* J. Chromatogr. A, 2002. **969**(1-2): p. 17-25.

15. Yampolskii, Y. and N. Belov, *Investigation of polymers by inverse gas chromatography.* Macromolecules, 2015. **48**(19): p. 6751–6767.

16. Segeren, L.H.G.J., et al., *Surface energy characteristics of toner particles by automated inverse gas chromatography.* J. Chromatogr. A, 2002. **969**(1-2): p. 215-227.

17. Boutboul, A., et al., *Use of inverse gas chromatography to determine thermodynamic parameters of aroma–starch interactions.* J. Chromatogr. A, 2002. **969**(1-2): p. 9-16.

18. Zhao, C., J. Li, and C. Zeng, *Determination of the infinite dilution diffusion and activity coefficients of alkanes in polypropylene by inverse gas chromatography.* J. Appl. Polym. Sci., 2006. **101**(3): p. 1925-1930.

19. Edwards, M.F. and J.F. Richardson, *Gas dispersion in packed beds.* Chem. Eng. Sci., 1968. **23**(2): p. 109-123.

20. Wijmans, J.G. and R.W. Baker, *The solution-diffusion model: a review.* J. Membr. Sci. , 1995. **107**(1-2): p. 1-21.

21. Seethapathy, S. and T. Górecki, *Applications of polydimethylsiloxane in analytical chemistry: A review.* Anal. Chim. Acta., 2012. **750 th anniversary volume**: p. 48-62.

22. Lonsdale, H.K., U. Merten, and R.L. Riley, *Transport properties of cellulose acetate osmotic membranes.* J. Appl. Polym. Sci. , 1965. **9**(4): p. 1341-1362.

23. Dettmer, K. and W. Engewald, *Adsorbent materials commonly used in air analysis for adsorptive enrichment and thermal desorption of volatile organic compounds.* Anal. Bioanal. Chem., 2002. **373**(6): p. 490-500.

24. Dettmer, K. and W. Engewald, *Ambient air analysis of volatile organic compounds using adsorptive enrichment.* Chromatographia, 2003. **57**(Supplement 1): p. S339-S347.

25. Supelco, *Capillary GC troubleshooting guide: How to locate problems and solve Them.* Bulletin 853B.

26. Bi, E., T.C. Schmidt, and S.B. Haderlein, *Practical issues relating to soil column chromatography for sorption parameter determination.* Chemosphere, 2010. **80**(7): p. 787-793.

27. Kunaver, M., et al., *Inverse gas chromatography - a different approach to characterization of solids and liquids.* Acta Chim. Slov., 2004. **51**(3): p. 373-394.

28. Kroupa, A., et al., *Breakthrough characteristics of volatile organic compounds in the −10 to +170 ◦C temperature range on Tenax TA determined by microtrap technology.* J. Chromatogr. A, 2004. **1038**(1-2): p. 215-223.

29. Karwa, M. and M. Somenath, *Gas chromatography on self-assembled, single-walled carbon nanotubes.* Anal. Chem., 2006. **78**(6): p. 2064-2070.

30. Cankurtaran, Ö. and F. Yilmaz, *Determination of exchange enthalpy and entropy parameters of the equation-of-state theory for poly(dimethyl siloxane) and some aromatic solvents by inverse gas chromatography.* Polym. Int., 2000. **49**(1): p. 99-102.

31. Schneider, M. and K.U. Goss, *Systematic investigation of the sorption properties of Tenax TA, Chromosorb 106, Porapak N, and Carbopak F.* Anal. Chem., 2009. **81**(8): p. 3017-3021.

32. Sprunger, L., et al., *Characterization of the sorption of gaseous and organic solutes onto polydimethyl siloxane solid-phase microextraction surfaces using the Abraham model.* J. Chromatogr. A, 2007. **1175**(2): p. 162-173.

33. Pawliszyn, J., *Solid phase microextraction theory and practice*. 1997, Canada: Wiley-VCH. 1-247.

34. Endo, S., et al., *UFZ-LSER database v 2.1 [Internet], Leipzig, Germany, Helmholtz Centre for Environmental Research-UFZ. 2015. Available from https://www.ufz.de/index.php?en=31698&contentonly=1&m=0&lserd_data[mvc]=Public/start (accessed: June 4th 2016).*

35. Arp, H.P.H., K.U. Goss, and R.P. Schwarzenbach, *Evaluation of a predictive model for air/surface adsorption equilibrium constants end enthalpies.* Environ. Toxicol. Chem., 2006. **25**(1): p. 45-51.

36. Spangenberg, B., C.F. Poole, and C. Weins, *Quantitative thin-layer chromatography a practical survey*. 2011, Germany: Springer.

37. Cramers, C.A., J.A. Rijks, and C.P.M. Schutjes, *Factors determining flow rate in chromatographic columns.* Chromatographia, 1981. **14**(7): p. 439-444.

38. Newns, A.C. and G.S. PARK, *The Diffusion coefficient of benzene in a variety of elastomeric polymers.* J. Polym. Sci.: Part C, 1969. **22**(2): p. 927-937.

39. Chandak, M.V., et al., *Sorption and diffusion of volatile organic compounds in polydimehtylsiloxane membranes.* J. Appl. Polym. Sci., 1998. **67**(1): p. 165-175.

C3 Supplementary Information

Table S.I.C3-1 Stock solution concentrations.

Probe	c_{stock} / mg L^{-1}
Benzene	87.4
Toluene	86.5
o-Xylene	87.9
Ethyl acetate	451
3-methyl-1-butanol	404.5
2-butanol	1000
1,2-dichloroethane	125
n-Pentane	1096.5
Methyl *tert*-butyl ether	148
Ethyl *tert*-butyl ether	370

Table S.I.C3-2 Sorbent properties.

	Density / g cm^3	Mesh	Specific surface area / m^2 g^{-1}	Type of sorbent	Material
Carbopack C	0.64	80/100	10	Adsorbent	Carbon
PDMS	0.965	80/100	/	Absorbent	Polydimethyl- siloxane
Tenax TA	0.25	80/100	35	Adsorbent	Poly-(2,6-diphenyl-)-*p*-phenylene oxide

Figure S.I.C3-1 ITEX as IGC column.

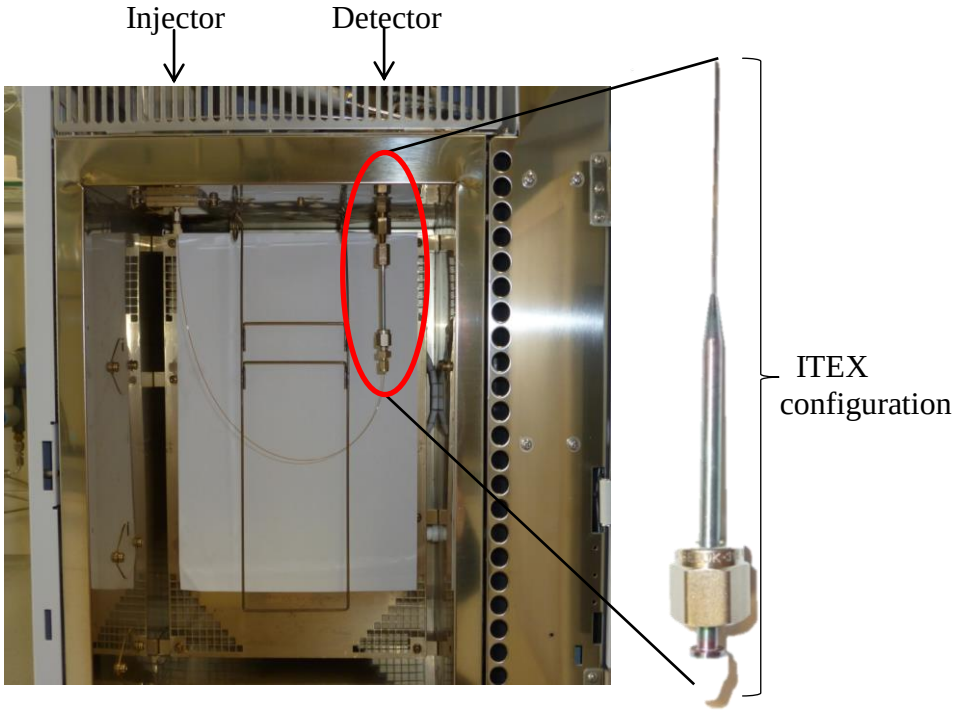

Experimental set-up.
GC/FID, ITEX as IGC column.

Calculation S.I.C3-1 James-Martin compressibility factor.

Exemplary calculation of the James-Martin compressibility factor $j = \frac{3}{2}\left(\frac{\left(\frac{\Delta p + p_0}{p_0}\right)^2 - 1}{\left(\frac{\Delta p + p_0}{p_0}\right)^3 - 1}\right) j$ [1]

where $\Delta p = p_o - p_i$, p_o = 101320 Pa, p_i = 50000 Pa $\therefore j = 0.79$

Table S.I.C3-3 Statistical data for the retention time of the peaks analyzed with the half mass point method.

Estimation of the peak retention time via the half mass point method. Integration performed with Origin software.
PDMS as sorbent material packed in ITEX. Column flow= 3 mL min^{-1}. Column temperature according to probe. Natural gas as inert marker and 20 µL as injection volume. Benzene, ethyl acetate and 3-methyl 1-butanol as probes, with a c_{sample}= 3.49, 45.1, 101.12 mg L^{-1} respectively, in the liquid phase. 500 µL as injection volume from the HS.

	Benzene						Ethyl acetate						3-methyl-1-butanol					
	Inert			Probe			Inert			Probe			Inert			Probe		
Temp. / K	Ret. time / min.	Std. dev.	CV / %	Ret. time / min.	Std. dev.	CV / %	Ret. time / min.	Std. dev.	CV / %	Ret. time / min.	Std. dev.	CV / %	Ret. time / min.	Std. dev.	CV / %	Ret. time / min.	Std. dev.	CV / %
313.15	0.13	0.00E+00	0.00	11.42	4.31E-01	3.77	0.13	1.53E-03	1.18	15.86	6.45E-01	4.07	-	-	-	-	-	-
323.15	0.13	1.53E-03	1.18	7.51	1.07E-01	1.42	0.13	2.08E-03	1.58	10.19	9.48E-01	9.31	-	-	-	-	-	-
333.15	0.13	5.77E-04	0.44	4.60	4.17E-02	0.91	0.13	2.31E-03	1.82	5.33	6.88E-01	12.92	-	-	-	-	-	-
343.15	0.13	1.53E-03	1.18	3.46	1.95E-01	5.64	0.13	0.00E+00	0.00	3.29	4.90E-02	1.49	0.11	5.77E-04	0.52	14.32	1.03E+00	7.18
353.15	0.13	1.15E-03	0.89	2.40	2.12E-01	8.84	0.13	1.15E-03	0.90	2.18	2.63E-02	1.21	0.10	1.15E-03	1.15	4.36	1.21E+00	27.67
363.15	0.13	1.00E-03	0.77	1.83	2.04E-01	11.16	0.13	1.53E-03	1.18	1.58	1.21E-02	0.77	0.11	5.77E-04	0.52	3.23	2.56E-01	7.93
373.15	0.13	3.06E-03	2.35	1.32	1.22E-02	0.93	0.13	5.77E-04	0.45	1.08	4.58E-03	0.42	0.10	0.00E+00	0.00	2.17	1.41E-01	6.49
398.15	0.13	1.00E-03	0.77	0.75	1.66E-02	2.22	0.12	4.58E-03	3.82	0.51	2.08E-03	0.41	0.10	3.06E-03	3.06	1.04	5.77E-02	5.54
423.15	0.13	3.00E-03	2.31	0.47	6.03E-03	1.28	0.12	4.04E-03	3.32	0.36	7.64E-03	2.11	0.10	1.15E-03	1.17	0.60	4.71E-02	7.80

Table S.I.C3-4 Slope values for the sorption enthalpy determination and temperature range.

PDMS, Tenax TA and Carbopack C (CC) as sorbents for material characterization via inverse gas chromatography/FID.

	PDMS		Tenax TA		CC		PDMS	Tenax TA	CC
	m	R^2	m	R^2	m	R^2	Temp. range / °C		
Benzene	4565.1	9.99E-01	7607.5	9.996E-01	2126.3	9.240E-01	40-150	70-150	90-150
o-Xylene	5511.1	9.92E-01	-	-	-	-	50-150	-	-
Toluene	5388.1	1.00E+00	-	-	-	-	40-150	-	-
Ethyl acetate	5543.8	9.95E-01	7778.3	9.98E-01	568.3	5.624E-01	40-150	70-150	90-150
3-methyl-1-butanol	5923.5	9.52E-01	6738.8	1.00E+00	2023.0	2.208E-01	70-150	125 and 150	90-150
2-butanol	4811.3	9.93E-01	-	-	-	-	50-150	-	-
1,2-dichloroethane	5595.1	9.92E-01	-	-	-	-	40-150	-	-
n-Pentane	2975.2	9.43E-01	-	-	-	-	70-150	-	-
MTBE	4592.9	9.94E-01	-	-	-	-	40-150	-	-
ETBE	5965.2	9.93E-01	-	-	-	-	40-150	-	-

Table S.I.C3-5 Molecular interactions according to sorbent and sorbate descriptors.

	Molecular interactions							
	Tenax TA				PDMS			
	Hydrogen bond acidity	Hydrogen bond basicity	Influence hydrogen bond	van der Waals/cavity	Hydrogen bond acidity	Hydrogen bond basicity	Influence hydrogen bond	van der Waals/cavity
	a*A	b*B	a*A+b*B	l*L	a*A	b*B	a*A+b*B	l*L
Benzene	0	0	0	2.54	0	0.08	0.08	2.20
Toluene	0	0	0	3.59	0	0.09	0.09	3.11
o-Xylene	0	0	0	2.12	0	0.26	0.26	1.84
Ethyl acetate	0	0	0	2.12	0	0.26	0.26	1.84
3-methyl-1-butanol	0	0	0	2.73	0.42	0.28	0.70	2.37
2-butanol	0	0	0	2.13	0.38	0.32	0.70	1.85
1,2-dichloroethane	0	0	0	2.34	0.11	0.06	0.18	2.03
n-Pentane	0	0	0	1.97	0	0	0	1.71
MTBE	0	0	0	2.15	0	0.32	0.32	1.87

Calculation S.I.C3-2 Stationary phase volume (*Vp*) example PDMS.

- Assuming a spherical shape for PDMS

$$\emptyset_{PDMS} = 150\ \mu m = 0.015\ cm$$

$$V = \frac{4}{3}\pi r^3 = \frac{4}{3}\pi\left(\frac{0.015\ cm}{2}\right)^3 = 1.76 \times 10^{-6} cm^3 = volume\ one\ PDMS\ sphere$$

- Volume available in ITEX needle

$$\emptyset_{ITEX} = 0.25\ cm, \qquad h = 3\ cm$$

$$V = \pi r^2 h = \pi\left(\frac{0.25\ cm}{2}\right)^2 \times 3\ cm = 0.147\ cm^3$$

- Number of PDMS spheres in the available ITEX volume

$$PDMS_{spheres} = \frac{0.147\ cm^3}{1.76 \times 10^{-6} cm^3} = 83333$$

Since only 68 % can be occupied

$$V_p = \frac{4}{3}\pi r^3 = \frac{4}{3}\pi\left(\frac{0.015\ cm}{2}\right)^3 \times 83333 \times 0.68 = 0.1\ cm^3$$

Calculation S.I.C3-3 *fg* example for benzene as probe with PDMS as sorbent.

$$K_d = \frac{C_s}{C_g} = \frac{C_1}{C_2} = K_{12}$$

$$f_g = f_{\overline{2}} = \frac{1}{1 + r_{12}K_{12}}$$

$$r_1 = \text{vol. PDM Sin ITEX} = 0.1 cm^3$$

$$r_2 = \text{injection volume} = 0.5 cm^3$$

$$\text{At } 300\,^{\circ}\text{C} = 573.15\,\text{K}$$

$$\text{Apply eq. benzene } y = 2 \times 10^{31} x^{-11.58}$$

$$y = 2 \times 10^{31} (573.15\,\text{K})^{-11.58} = 0.22$$

$$f_g = f_{\overline{2}} = \frac{1}{1 + r_{12}K_{12}} = \frac{1}{1 + \left(\frac{0.1 cm^3}{0.5 cm^3}\right)0.22} = \underline{\underline{0.95}}$$

Figure S.I.C3-2 Graphical estimation of the *C* term for the diffusion coefficient calculation. PDMS as sorbent and benzene as probe.

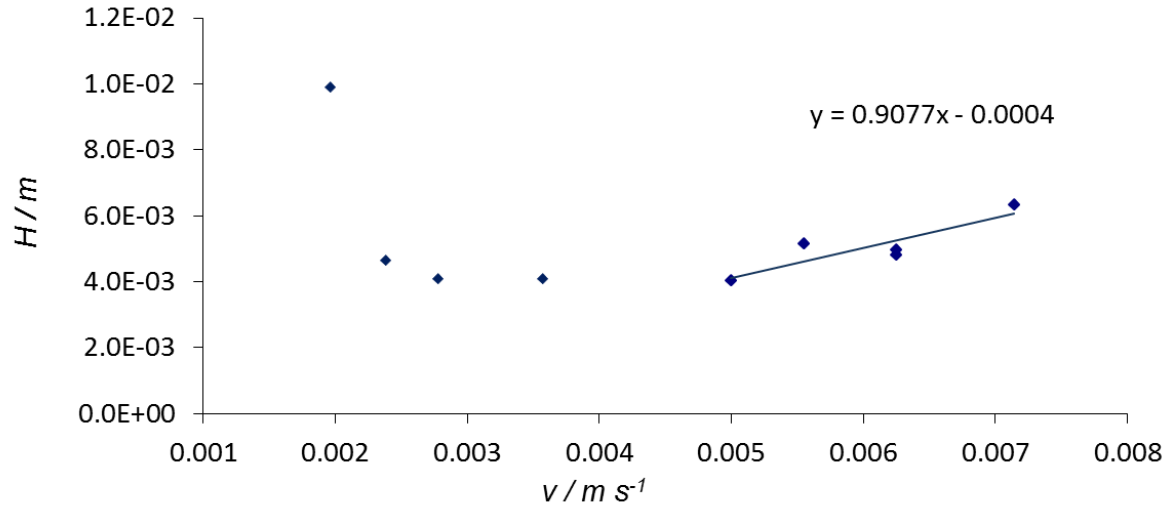

Table S.I.C3-6 Reynolds number.

Re number for analysis of diffusion and dispersion coefficients.
PDMS, Tenax TA and Carbopack C as sorbent material, packed in ITEX. N_2 as carrier gas.

Re		
PDMS	Tenax TA	Carbopack C
0.008	0.010	0.004
0.011	0.017	0.006
0.016	0.024	0.007
0.018	0.023	0.009
0.020	0.025	0.010
0.025	0.032	0.013
0.033	0.044	0.020
0.048	0.057	0.025
0.044	0.062	0.028
0.053	0.093	0.028
0.053	0.068	0.032

S. I. C3 References

1. Hamieh, T. and J. Schultz, *New approach to characterise physicochemical properties of solid substrates by inverse gas chromatography at infinite dilution I. Some new methods to determine the surface areas of some molecules adsorbed on solid surfaces.* J. Chromatogr. A, 2002. **969**(1-2): p. 17-25.

Chapter 4 DoE application for the investigation of carbon based-nanomaterials as sorbent via headspace in-tube extraction

Abstract

Carbon based-nanomaterials (CNM) possess unique properties, such as high surface-to-volume ratios, thermal stabilities and non-covalent interactions with organic molecules. These interactions are believed to increase sorption on CNM. Due to these properties, they represent promising materials for the application as sorbents in micro- and other extraction devices.
Some research has been performed to extract polycyclic aromatic hydrocarbons (PAHs) from water samples via headspace (HS) solid phase microextraction (SPME), but few via headspace in-tube extraction (HS-ITEX) and CNM as sorbent. To elucidate the performance of CNM as sorbent materials for HS-ITEX, the extraction of eight PAHs (naphthalene, acenaphthylene, acenaphthene, fluorene, phenanthrene, anthracene, fluoranthene and pyrene) with five CNM (MWCNTs, fullerenes, MWCNTs-COOH, graphene platelets and carbon nanohorns) was evaluated with a headspace HS-ITEX-GC/MS method. The optimal extraction parameters were defined using a Box-Behnken experimental design. From the extraction yield response, c_p analysis and physicochemical properties, fullerenes were selected as a suitable sorbent for method validation in ITEX purposes.
In the following, the analytical performance of fullerenes as HS-ITEX sorbent, was evaluated according to its performance in terms of linear range, limit of detection, precision and recovery. The method detection limit ranged from 10 to 300 ng L^{-1}. In this study, sorbent enrichment was performed via HS, in contrast to solid phase extraction or direct immersion of a solid phase microextraction fiber. Nonetheless, except for anthracene, similar recovery values between 45% to 103% were achieved. Finally, Tenax GR was tested for extraction yield comparison, demonstrating that CNM represent a better option than this widely used commercial material as sorbent in ITEX for PAH analysis.

Introduction

Carbon based-nanomaterials (CNM) have gained wide attention as sorbents in several analytical techniques, such as nano liquid chromatography (nano LC), [1] solid phase microextraction (SPME) fibers covered with nanomaterials, [2-5] solid phase membrane tip extraction (SPMTE), [6] solid phase extraction (SPE) [7-10]or as stationary phase in gas chromatography (GC) and liquid chromatography (LC). [11] Material characteristics, such as high surface to-volume ratios, high thermal stability, formation of non-covalent interactions with organic molecules, are the reasons why the application of CNM has increased in analytical chemistry. [12] π-π interactions and hydrogen bonding are among the non-covalent interactions and these type of interactions are believed to increase the sorption affinity

between CNM and organic pollutants. [13] Depending on the synthesis process applied on the carbon, either multi-walled carbon nanotubes (MWCNTs), fullerenes, graphene platelets, carbon nanohorns can be created. [6] [12] Their interactions and hollow/layered structures make them interesting candidates for use as sorbents of organic pollutants or heavy metals. [14] CNM surfaces can be modified with oxygen-containing groups such as carboxylic, carbonyl and hydroxyl, resulting in e.g.: MWCNTs-COOH. [11] Such modifications turn them into a more hydrophilic sorbents, suitable for relatively low molecular weight and polar compounds. [6] Their application in SPE and SPME has shown higher extraction and improved thermal stability compared to other commercial available commercial materials such as polydimethylsiloxane (PDMS) and PDMS/divinylbenzene (PDMS/DVB), respectively, thus improving the sample preparation step. [12]

Polycyclic aromatic hydrocarbons (PAHs) are ubiquitously found in the environment, mainly caused by incomplete combustion processes. They have been well studied and turns them into an appropriate model analyte for the evaluation of analytical methods. [15]

The most common methods to analyze PAHs from aqueous matrices is via solid phase extraction (SPE) with high performance liquid chromatography (HPLC) coupled to an ultraviolet (UV) detector [16] or via SPE-GC/MS. [17] To decrease the solvent amount, solid phase nanoextraction (SPNE) was introduced using gold nanoparticles as sorbent. [18]

Microextraction techniques have been developed as a solventless option and the extraction can be performed in a static or dynamic fashion. One approach is the direct immersion of the SPME fiber into the sample, but depending on the matrix, fiber fouling could arise and the lifetime of the fiber can be decreased. [19] [20] More recently, the application of PAL SPME Arrow (which provides a higher extraction phase volume compared to traditional SPME fibers), in combination with freely dissolved PAHs as probe compounds in water was evaluated. The technique yielded limits of detection in the ng L^{-1} range. [15] Another alternative is to enrich PAHs from the headspace (HS) above the water samples to a SPME fiber and finally analyze them with GC/MS or FID. [2] [21] [22] Further dynamic solventless microextraction technqiues could yield higher extraction efficiencies, which is an interesting approach to expand this field of investigation. Therefore, this study presents the application of in-tube extraction (ITEX) packed with CNM as sorbent for the HS enrichment out of aqueous samples containing PAHs.

ITEX is a fully automated technique, which consists of a stainless steel needle containing a side port. The needle body is packed with sorbent material and is surrounded by an external heater for thermodesorption. Above the stainless steel needle, a gas tight Hamilton glass

syringe (1.3 mL) is placed. The analytes are enriched in the sorbent material by aspirating and dispensing the HS volume from the sample. Following the extraction, thermodesorption is performed in the GC injector. Finally, the trap is cleaned. In order to execute a successful analysis with ITEX, firstly the extraction parameters must be optimized, e.g., extraction strokes, incubation temperature and extraction flow. [23] [24]

To determine the suitable extraction parameters the typical one-variable-at-the-time optimization [25] can be an option, but it is rather time consuming and may not necessary result in the optimal combination of parameters. A more systematic approach for optimization is to apply design of experiments (DoE). [26] [27] Due to a large number of experiments that need to be run when many influence factors are tested, it is recommended to use a response surface model (RSM) to reduce labor intensity. Central composite design (CCD), Doehlert Matrix or Box-Behnken design (BBD) are examples of RSM. Since no extreme conditions are tested in this work and the number of runs is maintained small, a BBD is well suited to fit a quadratic surface, which is usually designed for process optimization. [28] [29] [30]

The purpose of this study was to evaluate the performance of five CNM as sorbent material (MWCNTs, fullerenes, MWCNTs-COOH, graphene platelets and carbon nanohorns) for a HS-ITEX-GC/MS method with PAHs (naphthalene, acenaphthylene, acenaphthene, fluorene, phenanthrene, anthracene, fluoranthene and pyrene) as model analytes. The PAHs were prepared in an aqueous solution and the HS was extracted. A BBD with four factors, three levels and five central points was performed for each sorbent. Fullerenes were chosen for parameter optimization and method validation. To confirm that CNM represent an option as sorbent, PAHs in water samples were also extracted with a commercially available material (Tenax GR) and the extraction yield from the sorbents was compared.

The affinity towards a chemical by a sorbent can be observed by the surface energy, like sorption enthalpy, of the material in concern. [31] Since the application of CNM is gaining popularity and limited information concerning their thermodynamic properties is available, material characterization is needed to gain new insights regarding the surface chemical properties of the CNM. [32] Inverse gas chromatography (IGC) is a useful technique to investigate the strength of the interaction of the molecules with the carbon surface. [32] Thus, IGC coupled to flame ionization detector (FID) with benzene as probe compound was applied as a first approach to determine the sorption enthalpy (ΔHs) and partitioning constant between the solid and gas phase (K_d) of fullerenes as sorbent.

Experimental

4.1.1 Reagents and materials

Graphene platelets were purchased from IoLiTec (IoLiTec Ionic Liquids Technologies GmbH, Heilbronn, Germany). Fullerenes and carboxylic acid functionalized multi-walled carbon nanotubes (MWCNTs-COOH) were bought from Sigma-Aldrich (Sigma-Aldrich, Steinheim, Germany). Multi-walled carbon nanotubes (MWCNTs) Baytubes C150P were received from Bayer (Bayer AG, Leverkusen, Germany), and carbon nanohorns from TIE (TIE GmbH, Griesheim, Germany). Each sorbent was packed in an ITEX needle, with 20 mg, 115 mg, 34 mg, 52 mg and 20 mg, respectively. An ITEX needle packed with Tenax GR was purchased from BGB Analytik (BGB Analytik AG, Böckten, Switzerland).

Acetone (> 99.9 %) for preparation of standard solutions was obtained from Sigma-Aldrich (Steinheim, Germany). The SV Calibration Mix #5/610 PAH Mix (2,000 µg mL^{-1} each, > 99 %) was purchased from Restek (Restek GmbH, Bad Homburg, Germany). Water was obtained from a PURELAB Ultra Analytic water purification system (ELGA LabWater, Celle, Germany).

4.1.2 Stock and Sample Preparation

From the calibration mix, an acetonic stock solution at 50 mg L^{-1} (each PAH), was produced. From the stock solution a working concentration, dissolved in water, at 50 µg L^{-1} was prepared.

For the linear range determination, a secondary aqueous stock solution at 50 µg L^{-1} (from the acetonic stock solution at 50 mg L^{-1}) was prepared. This to prepare the concentration range between 0.1 to 2.5 µg L^{-1}. For the lowest concentrations, from 0.01 to 0.075 µg L^{-1}, a third aqueous stock solution at 0.1 µg L^{-1} from the secondary stock solution was used. Finally the range from 5 to 1000 µg L^{-1} was directly prepared from the acetonic stock solution at 50 mg L^{-1}. For the limit of detection measurements a 1 mg L^{-1} solution was used to prepare the concentration range from 0.1 to 5 µg L^{-1}.

For recovery determination, tap water was spiked to reach 50 µg L^{-1}.

10 mL sample volume were used in amber 20-mL headspace screw cap vials, including a magnetic stirrer (VWR International GmbH, Darmstadt, Germany) and closed with rubber-PTFE septa caps (BGB Analytik AG, Böckten, Switzerland).

The stock solutions were prepared every 2-3 months and stored at 4 °C. The samples were prepared daily.

4.1.3 GC/MS instrument parameters and injection

All samples were analyzed using a Thermo Scientific TRACE GC Ultra™ gas chromatograph coupled to a Thermo Scientific DSQ™ II mass spectrometer single quadropole (S+H Analytik, Mönchengladbach, Germany).

An Rxi®-5ms column (30 m × 0.25 mm × 0.25 μm) from Restek (Restek GmbH, Bad Homburg, Germany) was used. The GC was equipped with a CombiPal autosampler (Axel Semrau, Sprockhövel, Germany), a split/spliteless injector (S/SL) and an Optic 3 programmed temperature vaporization injector with a cryofocusing unit (Axel Semrau, Sprockhövel, Germany). It was additionally equipped with a TrayCooler for 20-mL headspace vials and a single magnet mixer (SSM; Chromtech, Idstein, Germany). The ITEX option for the CombiPal was obtained from CTC Analytics (Zwingen, Switerzerland) and consists of a heated syringe holder, a 1.3 mL gas tight Hamilton glass syringe with side port (Hamilton, Bonaduz, Switzerland) and a trap heater around the ITEX needle.

The S/SL injector was set at 220°C and operated in splitless mode. The Optic 3 was set to 250°C and the cryotrap unit at -50°C for 60 s. 500 μL of helium was aspirated as desorption gas and injected at 50 μL s^{-1} for analysis. After the transfer time, the split was opened at 10 mL min^{-1} and the cryotrap was heated to 250°C at a ramp of 30°C s^{-1}. Helium was used as carrier gas and a constant flow of 1.0 mL min^{-1} (Air Liquide, Oberhausen, Germany) was maintained. The initial oven temperature was 80°C, held for 1 minute, subsequently ramped at 25°C min^{-1} to reach 250 °C, held for 6 minutes. In a second ramp the oven was heated up to 300 °C with a rate of 10 °C min^{-1}, which was held for 15 minutes.

The temperature of the MS transfer line and ion source, were 300 and 220 °C, respectively. The MS was set to electron ionization (EI), with an ionization energy of 70 eV in full scan (m/z from 45 to 300) and with a scan rate of 500 amu per second.

For the control of the instruments, management and evaluation of the data the Xcalibur 1.4 data system was used (S+H Analytik, Mönchengladbach, Germany).

4.1.4 ITEX parameters: Box-Behnken design

After the samples were placed on the TrayCooler, the vials were transported to the SMM, where the samples were heated and stirred at 500 rpm for 15 min. For the optimization of the extraction and desorption procedure, four factors (i.e., extraction temperature, extraction strokes, extraction flow, and desorption temperature), at three levels where set according to a BBD. In Table 4-1 the codification of the factors and levels is presented:

Table 4-1. Factors and levels for the Box-Behnken design used for ITEX optimization.

Factor	Setting	Unit	Low / -	Medium / 0	High / +
T	Extraction temperature	°C	40	55	70
S	Extraction strokes	-	20	50	80
F	Extraction flow	$\mu L\ s^{-1}$	30	50	70
D	Desorption temperature	°C	200	250	300

The experimental block was measured three times and each setting in triplicate. On Table S.I.C4-1 from the Supplementary Information, the sequence of the experiment block is presented. The temperature of the ITEX syringe always matched the extraction temperature (factor T from Table 4-1) to avoid condensation in the needle during extraction. After extraction, the sample was injected into the GC and the trap was cleaned by flushing nitrogen for 5 min at 280 °C. All CNM sorbents plus Tenax GR (for Tenax GR, the experiment block was measured only once –with each setting in triplicates-, because the observed extraction yield was smaller than for most of the CNM) were investigated under these conditions.

To estimate the optimal extraction parameters, a Box-Cox transformation was first performed. Afterwards, the fitness of the full quadratic approximation of the BBD response surface model was estimated and statistically evaluated with an analysis of variance (ANOVA). This mathematical procedure was only applied to fullerenes, since in comparison to the rest of the sorbents, it yielded the most suitable response. The results of naphthalene, acenaphthene, phenanthrene and pyrene (as representative probes for the eight PAHs present in the sample) from the BBD were selected to feed the mathematical model applied for optimization. The optimized parameters were applied to all PAHs for method validation.

The statistical analysis of the DoE was conducted with MiniTab16 software (ADDITIVE GmbH, Friedrichsdorf, Germany).

2.5 IGC/FID

The information is described in the methods section of the Supplementary Information (Methods S.I.C4-1 and Figure S.I.C4-1).

Results and Discussion

4.1.5 Extraction yield with CNM as sorbent

Based on previous studies, the extraction temperature, extraction strokes, extraction flow, and desorption temperature were chosen as the most influent parameters for the ITEX extraction procedure. [27] Due to the number of sorbent materials and analytes to be studied, a fast screening approach for method optimization which provides significant data (e.g., BBD) was chosen.

Sorption to CNM is affected by the physical properties of the sorbent (e.g., surface area, number of layers, pore diameter, structure), attached functional groups (e.g., –OH, -COOH) as well as on the physicochemical properties of the sorbate (e.g., molecular size, planarity, presence of functional groups). [33] As a result, various types of molecular interactions may occur, such as hydrophobic, π-π, hydrogen bond and electrostatic interactions. Nonetheless, the sorption of organic molecules on CNM is known to be mainly influenced by π-π interactions. [34]

Figure 4-1 depicts a chromatogram of the eight extracted PAHs from the HS out of the aqueous samples with the five CNM and a commercial sorbent for ITEX (Tenax GR) studied in this work. The highest intensity (by MWCNTs-COOH) was set as the maximum for comparison of the sorbents. Among the CNM, MWCNTs-COOH yielded the largest intensity for naphthalene, but not for the rest of the compounds. Functionalization of the CNM surface increases the affinity/selectivity for low molecular weight and polar compounds. [6] The addition of the functional group makes the CNM an electron acceptor and electron-donor-acceptor π-π interactions occur. [33] As side-effect, the functionalization of the CNM surface may result in a decrease of surface area available for sorption of larger planar molecules. This could explain the lower extraction yield for MWCNTs-COOH, in comparison to MWCNTs, for the other seven PAHs in this study.

To investigate which sorbent is more suitable for the extraction of PAHs, as a first step, the peak areas of naphthalene and pyrene (exemplary) for all the 29 BBD settings and for the five CNM are depicted in Figure 4-2 and Figure 4-3, respectively. (Tables S.I.C4-2 and S.I.C4-3 from the Supplementary Information contain the numerical data). The affinity of the PAHs towards fullerenes is appreciated.

As a next step, the amount of analyte in the gas phase at equilibrium for the different extraction temperatures, was calculated. Table S.I.C4-4 from the Supplementary Information provides the calculated data for the eight PAHs. At an extraction temperature of 40 °C, the concentration ranges from 1.6 to 12.4 μg L^{-1}, (the highest concentration corresponding to

naphthalene and the lowest to pyrene). At 55 and 70 °C the concentration of the eight PAHs is similar, from 47.6 to 49.9 μg L^{-1}. From these concentrations, the smallest peak areas would be expected at the settings where 40 °C were applied as extraction temperature. The corresponding settings are 5, 7, 13, 14 and 17 and when analysed in Figures 4-2 and 4-3, the peak areas confirm the information. Under these conditions, the three sorbents, among the five CNM, which yielded larger peak areas were fullerenes, MWCNTs and MWCNTs-COOH. At more suitable conditions (with higher extraction temperatures), where a larger amount of analyte is present in the gas phase at equilibrium, a similar trend for the sorbent performance should be observed.

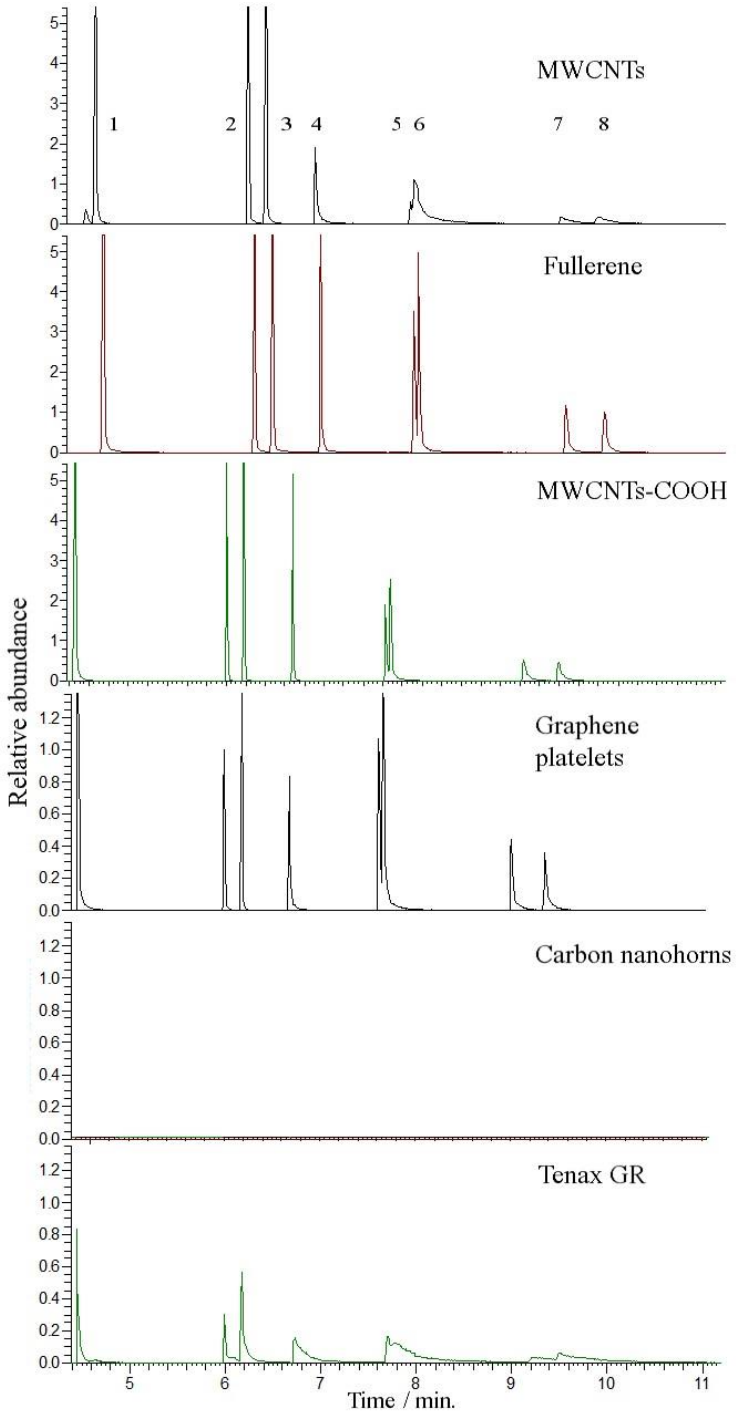

Figure 4-1. PAHs intensity with 5 CNM and Tenax GR as sorbent via HS-ITEX-GC/MS. Setting 20 from the BBD, c_{PAHs} = 50 µg L^{-1}, normalized to max. intensity from the MWCNTs-COOH at 2.92×10^{8}, *m/z*: 128,152, 154, 166, 178, 202.
1) Naphthalene 2) Acenaphthylene 3) Acenaphthene 4) Fluorene 5) Phenanthrene 6) Anthracene 7) Fluoranthene 8) Pyrene.
A shift in the chromatograms of the MWCNTs-COOH, graphene platelets and Tenax GR is present, because the GC-column was shortened.

For this reason, the analysis of the five central points (c_p) in the BBD was performed. The c_p are included in the RSM to determine the experimental error. [35] To this end the peak areas of the five c_p from the BBD together with the coefficient of variation (CV) were analyzed to

define a suitable CNM as sorbent in ITEX with PAHs as model analytes (see Table S.I.C4-5 in the Supplementary Information). Fullerenes yielded the smallest CV and largest peak areas, in comparison to the other CNM applied, which supports the decision of using fullerenes as sorbent in the subsequent work (parameter optimization and method validation).

The physical properties of the CNM were also investigated to study the sorption behavior observed by the materials. From the mass of the CNM packed in the ITEX needle and the specific surface area, the surface for each material was calculated. Table 4-2 presents the data.

Table 4-2. CNM physical properties and calculated area packed mass in ITEX needle.

	Specific surface area / $m^2\ g^{-1}$	Particle size	Pore size / nm	*m* / g	Area / m^2
Carbon nanohorns	200 [36]	5-150 nm [36]	12 [36]	0.02	4
Fullerenes	0.398[a)]	139 nm [37]	n.a.	0.115	0.05
Graphene platelets	50-80 [38]	11-15 nm [38]	3 to 11[39]	0.02	1 to 1.6
MWCNTs	210 [a)]	> 1 μm [40]	7 to 10 [39]	0.052	11
MWCNTs-COOH	110 [39]	9.5 nm [41]	n.a.	0.034	3.7

a) BET measurement. n.a = not available.

Despite the fact, that fullerenes only provide 0.05 m^2 (the smallest area among the CNM sorbents) a greater affinity to this material by the PAHs is observed, thus a stronger sorption proceeds.

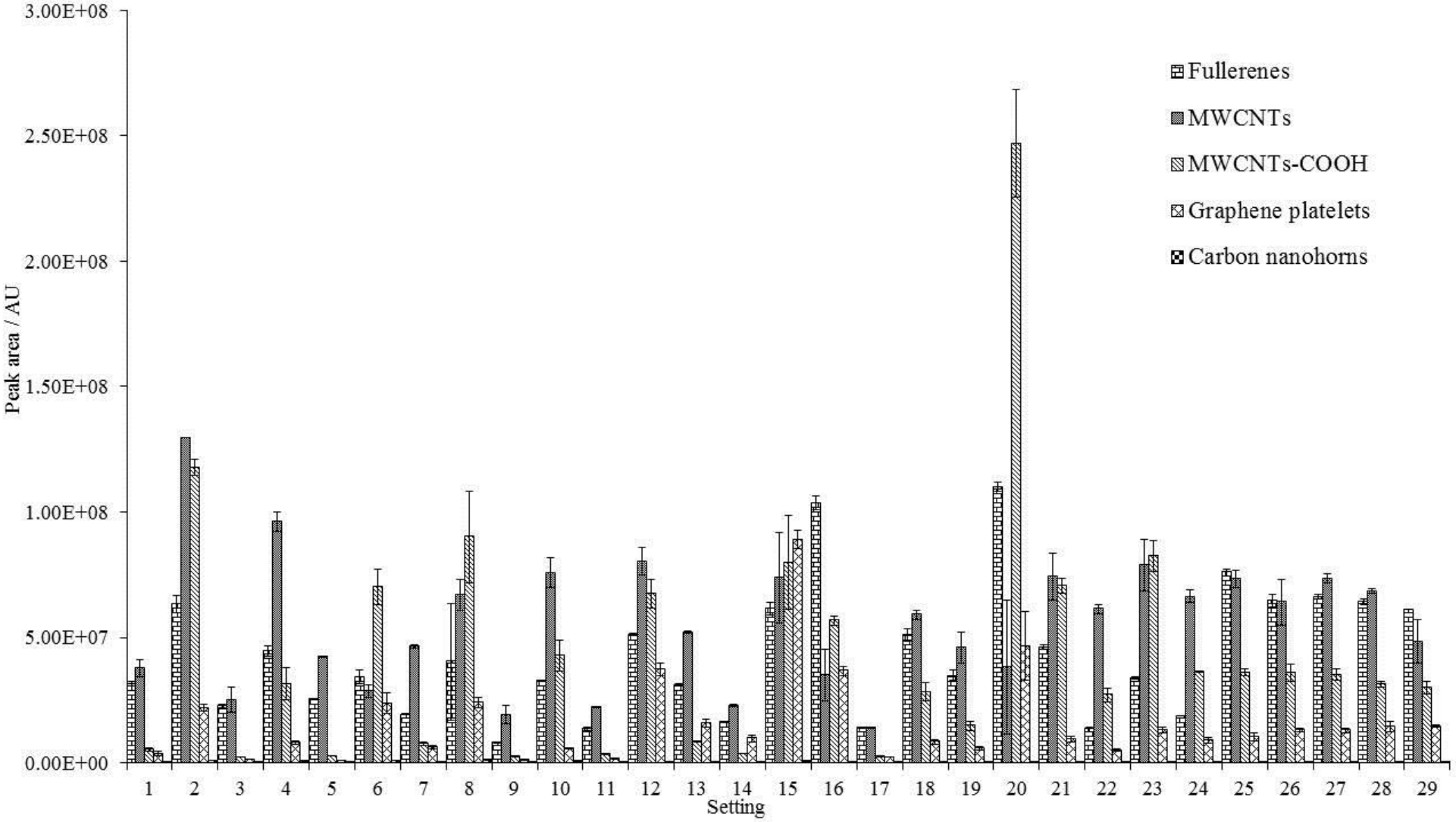

Figure 4-2. Extraction yield comparison, CNM as sorbents, naphthalene as probe, via a HS-ITEX-GC/MS method and a BBD, $c_{PAHs} = 50\ \mu g\ L^{-1}$.

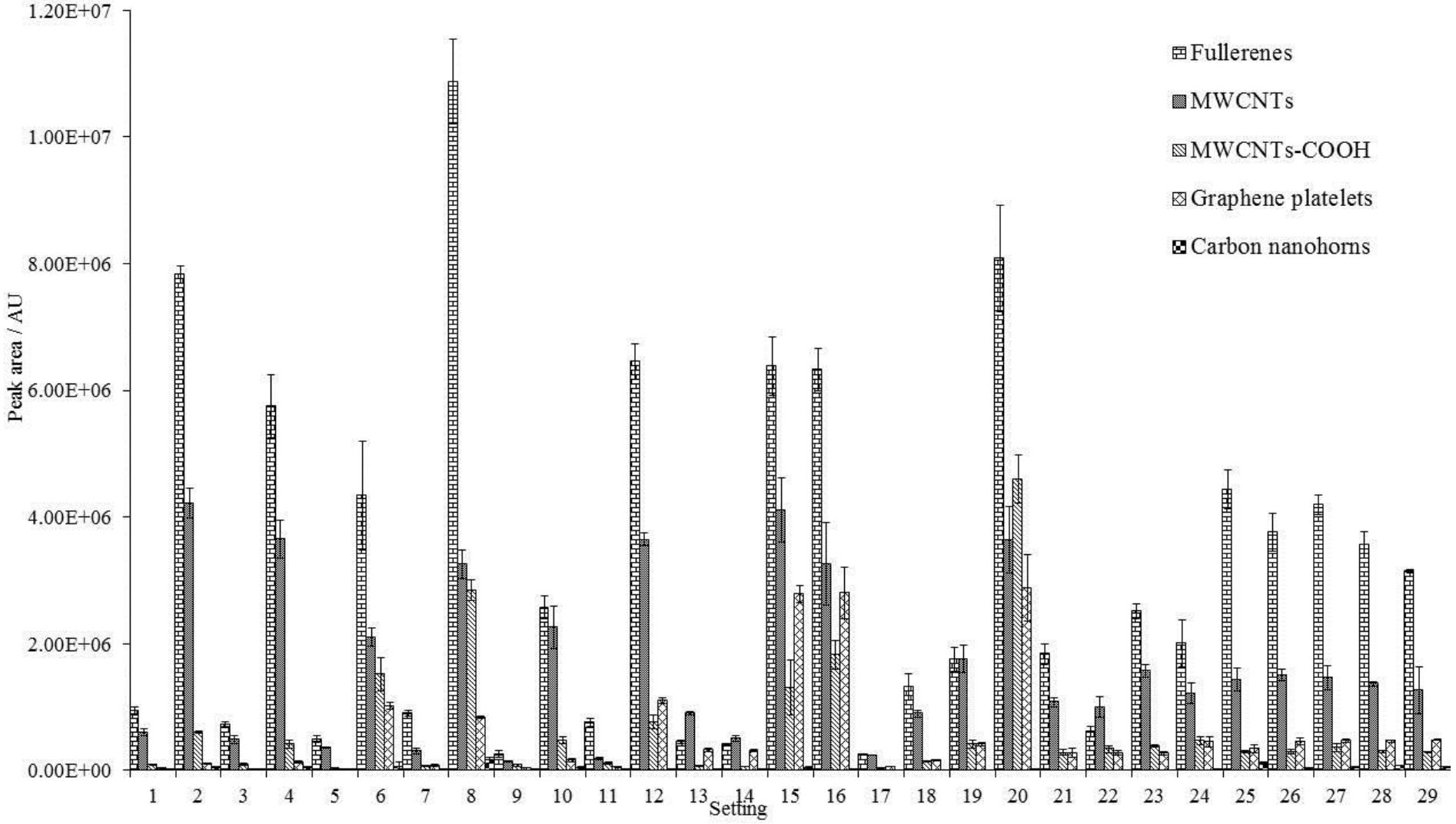

Figure 4-3. Extraction yield comparison , CNM as sorbents, pyrene as probe, via a HS-ITEX-GC/MS method and a BBD, c_{PAHs} = 50 µg L^{-1}.

Graphene platelets and carbon nanohorns had the lowest PAHs extraction yields. This may be due to capillary condensation of the analytes in meso- or macropores, pore deformation (the pathways for adsorption and desorption change), [42] or pore and particle size of the CNM.

To further investigate the low extraction yield of the graphene platelets and carbon nanohorns, X-ray photo-electron spectroscopy measurements (XPS) for these two materials and for MWCNTs were performed. The XPS parameters are given in the methods section of the Supplementary Information (M.S.I.C4-2). The XPS spectra for the MWCNTs, carbon nanohorns and graphene platelets are also depicted in the Supplementary Information, Figures S.I.C4-2 to S.I.C4-4, respectively. Table 4-3 shows the atomic percentage found at the surface (no deeper than 10 nm), for the tested CNM and per m^2 (according to the specific surface area and mass packed in the ITEX needle of the CNM). All the materials contained a similar percentage of carbon and oxygen.

Table 4-3. XPS measurements for sorption comparison according to the elements present at the surface of three CNM for the application as sorbent in a HS-ITEX-GC/MS method. Normalization of O % according to the CNM mass packed and its specific surface area.

	Elements / %		
	C	O	O / m^2
MWCNTs	75	17	1.6
Carbon nanohorns	74	20	5.0
Graphene platelets	77	18	11.3
Fullerenes	97[a)]	3[a)]	65.5[b)]

a) Raw data obtained from the authors. [43] b) The O / m^2 was calculated according to the estimated O % and mass of packed fullerenes for this study.

The oxygen percentage for fullerenes and MWCNTs-COOH was obtained from the literature (estimated also via XPS measurements). For fullerenes, an oxygen percentage ranging between 1.3 to 20 % was reported. [44] [45] The amount of oxygen in the MWCNTs-COOH corresponds to at least 8 % (reported by the supplier [41]). As in Table 4-3, the oxygen percentage per m^2 for fullerenes and MWCNTs-COOH was calculated. For fullerenes an oxygen percentage per m^2 of 26 to 176 was estimated, while for the MWCNTs-COOH only 2.1 O / m^2.

MWCNTs-COOH in comparison to the MWCNTs yielded a higher extraction for naphthalene. This behavior agrees with the literature, when a CNM is functionalized a better affinity towards less polar and low molecular weight compounds is observed. [6] For the rest of the CNM, the sorption was not influenced, since fullerenes yielded the largest peak areas with the highest O % per m^2. The affinity towards fullerenes is possibly due to its cage structure and hydrophobic feature. [46] During the extraction in ITEX, the compounds in the HS from the aqueous samples are enriched on the sorbent. A hydrophobic material is of

advantage during the extraction procedure, because the affinity towards the PAHs instead to water will be increased, by this also increasing the extraction yield.

From the extraction yield response, c_p analysis and physicochemical properties, fullerenes were selected as a suitable sorbent for method validation in ITEX.

4.1.6 Extraction parameter optimization and figures of merit

The results of the Box-Behnken design (peak area) with fullerenes as sorbent of four PAHs were selected for modeling and to determine the optimal extraction conditions. The four compounds were, naphthalene (two rings), acenaphthene (three rings), phenanthrene (three rings) and pyrene (four rings) representative for all of the PAHs measured in this study. Table 4-4 exemplarily shows the ANOVA results for naphthalene and pyrene (see Table S.I.6 for acenaphthene and phenanthrene):

Table 4-4. ANOVA for the Box-Behnken design using HS-ITEX-GC/MS. Fullerenes as sorbent.

	Naphthalene				Pyrene			
	DF	*Adj. SS*	*F*-Value	*p*-Value	*DF*	*Adj. SS*	*F*-Value	*p*-Value
Model	14	11.0643	9.45	0.000	14	3.2691	19.12	0.000
Linear	4	6.5721	19.65	0.000	4	2.9764	60.92	0.000
T	1	2.3018	27.52	0.000	1	1.5758	129.01	0.000
S	1	3.6277	43.38	0.000	1	1.1575	94.77	0.000
F	1	0.5753	6.88	0.02	1	0.3258	2.67	0.125
D	1	0.0673	0.81	0.385	1	2.1054	17.24	0.001
Square	4	3.9926	11.94	0.000	4	2.6988	5.52	0.007
T^2	1	0.1267	1.51	0.239	1	0.9236	7.56	0.016
S^2	1	0.8679	10.38	0.006	1	1.2370	10.13	0.007
F^2	1	0.3872	4.63	0.049	1	0.6101	5	0.042
D^2	1	3.6063	43.12	0.000	1	1.3745	11.25	0.005
2-Way interaction	6	0.4996	1	0.465	6	0.2281	0.31	0.921
T×S	1	0.0056	0.07	0.8	1	0.0037	0.03	0.863
T×F	1	0.3367	4.03	0.065	1	0.0010	0.01	0.93
T×D	1	0.0487	0.58	0.458	1	0.0233	0.19	0.669
S×F	1	0.0001	0	0.972	1	0.0005	0	0.952
S×D	1	0.0019	0.02	0.881	1	0.0059	0.05	0.829
F×D	1	0.1066	1.27	0.278	1	0.1937	1.59	0.228
Error	14	1.1708			14	1.7100		
Lack-of-Fit	10	1.1441	17.16	0.007	10	1.6367	8.93	0.025
Pure Error	4	0.0267			4	0.0733		
Total	28	12.2351			28	3.4401		

DF = Degrees of freedom. *Adj. SS* = Adjusted sum of squares. *F*-Value = Fisher´s value. *p*-Value = Result from the *F*-test for a lack of fit. T = Extraction temperature. S = Extraction strokes. F = Extraction flow. D = Desorption temperature.

The number of strokes and the extraction temperature are the two parameters, which have the highest influence on the extraction yield. This can be observed by the high *F*-values and low *p*-values on Table 4-4, also confirmed by the literature. [27] The extraction flow and desorption temperature are in comparison less decisive for the extraction yield. Nonetheless, the extraction flow will determine, together with the number of strokes, the extraction time. A combination of a high number of strokes (e.g. 80 strokes) with a slow extraction flow (e.g. 30 µL s^{-1}) results in long sampling time, [47] which is not favorable for prompt/practical applications. A decrease in the extraction yield is reported, [47] when a high extraction flow (e.g. 100 µL s^{-1}) is applied. Thus, a suitable extraction flow for initial trials would be 50 µL s^{-1}. For its proper determination, a BBD can be applied. Concerning the desorption temperatures, high temperatures (between 250 or 300 °C) would be suitable to obtain a high extraction yield and avoid carry-over. Inverse gas chromatography (IGC) could be applied for material characterization to determine the thermodynamic parameters of the sorbent and by this establish a more suitable thermodesorption temperature for the sorbent under investigation. The quadratic fitting of the RSM with the BBD can be applied to predict maximum or minimum responses, [30] which is the goal of this study to maximize the extraction yield under the set experimental conditions. The optimal parameters were, 70 °C as extraction temperature, 71 strokes for extraction at 54 µL s^{-1} and a desorption temperature of 257 °C.

For method validation, the linear range, method detection limit (MDL), precision and recovery were determined. The linear range determination consisted of a 16 point calibration, with each point measured in triplicate. The precision was calculated as the average of the RSD within the calibration range. [47] The MDL was obtained according to Eq. 1.:

$$MDL = t_{(N-1,1-\alpha=99\%)}\, s_c \qquad \text{Eq.1. [49]}$$

Where *t* is the student's t value for the one-tailed test with a confidence level of 99% and six degrees of freedom multiplied by the standard deviation of seven replicates (s_c) at a concentration that corresponds to an instrument signal to noise (S/N) in the range of 2.5 to 5. [48]

All validation data are given in Table 4-5:

Table 4-5. Figures of merit via HS-ITEX-GC/MS. Fullerenes as sorbent.

Compound	Linear range / µg L^{-1}	MDL[a] / µg L^{-1}	Precision / %	Recovery tap water[a),b)] / %
Naphthalene	0.07-50	0.07	16	54
Acenaphthylene	0.08-50	0.08	6	45
Acenaphthene	0.06-50	0.06	10	50
Fluorene	0.04-50	0.04	7	57
Phenanthrene	0.31-500	0.31	6	103
Anthracene	0.01-250	0.01	10	66
Fluoranthene	0.27-250	0.27	8	62
Pyrene	0.06-250	0.06	7	68

a) n = 3, b) Spike level = 50 µg L^{-1}.

The linear range covered four orders of magnitude. Phenanthrene and fluoranthene yielded high MDLs. The strong sorption of phenanthrene and fluoranthene by fullerenes is due to the fact that they contain a partial similar structure to that of fullerenes. The π-electron pair confined in the middle ring of phenanthrene resembles an alkene, by this increasing the sorption with fullerenes. [5] The strong sorption could hinder the amount of compound released when thermodesorption in ITEX proceeds.

An explanation for the higher naphthalene MDL obtained in this work compared to the literature, [27] could be related to the larger molecular size sampled in this study. Since all PAHs in the gas phase under equilibrium conditions at the optimal extraction conditions (70 °C) are present in similar concentrations (Table S.I.C4-4 from the Supplementary Information), the larger PAHs with a stronger sorption to fullerenes, could have displaced naphthalene and by this resulting in higher MDL, compared to the reported data. [27] .

The enrichment of the analytes out of the HS on a CNM as sorbent from water samples, reached recovery values similar to SPE. [12] Confirming, that this method represents an option for sampling small PAHs, over SPE, with the further advantage of having a fully automatized technique like ITEX, feature not offered by SPE.

The comparison of MDL values in Table 4-6, shows that the application of CNM as sorbent for the extraction of PAHs in water sample via HS, in comparison to common materials like PA, [22] significantly improved the quantitative detection. As well as the importance of the proper MDL comparison, according to the method applied for its estimation. Only the MDL obtained with a microwave HS assisted-SPME-GC/FID technique and commercial PDMS/DVB coating in SPME, yielded better MDL than the fullerenes and MWCNTs as sorbent.

Table 4-6. Sorbent comparison between CNM and commercially available sorbents for the extraction of PAHs with microextraction techniques.

	MDL / µg L^{-1}						
	This study		Hüffer et al. [27]	Maghsoudi et al. [2]	Xiao et al. [5]	Zuazagoitia et al. [22]	Wei et al. [21]
Technique	HS-ITEX-GC/MS			HS-SPME-GC/FID			Assisted HS-SPME-GC/FID
Sorbent	Fullerenes a)	Fullerenes b)	MWCNTs a)	MWCNTs b)	Fullerenes/ Polysilicone b)	PA b)	PDMS/ DVB b)
Naphthalene	0.07	0.004	0.002	0.06	0.04	0.2	0.1
Acenaphthylene	0.08	0.005	-	0.05	-	0.17	0.07
Acenaphthene	0.06	0.001	-	-	-	0.11	0.1
Fluorene	0.04	0.063	-	0.04	-	0.15	0.08
Phenanthrene	0.31	0.577	-	0.03	-	0.09	0.04
Anthracene	0.01	0.750	-	-	-	0.08	0.03
Fluoranthene	0.27	0.005	-	0.07	-	0.14	0.03
Pyrene	0.06	0.01	-	-	-	0.13	0.03

a) Calculated with Eq. 1. b) Calculated with S/N = 3.

Except for the carbon nanohorns, CNM do represent a more suitable option as sorbent than the usual commercial materials. A higher affinity with CNM for the PAHs than with Tenax GR (Figure 4-1) was observed, which confirms the promising application of the CNM as sorbent in the technique.

4.1.7 Fullerenes material characterization

The available literature for thermodynamic data, like partitioning constants from CNM to gas or enthalpy of sorption, is limited for the CNM and would be relevant to obtain for the visualization of the sorbent affinity towards a compound, thus defining its suitable application. Inverse gas chromatography (IGC) is a technique applied for material characterization. [32] [50] As a first approach to test whether IGC could offer valuable thermodynamic data, only one sorbent and one probe compound were investigated. Since fullerenes were selected as the sorbent for the determination of the figures of merit of this work, it was decided to start the analysis with this sorbent and benzene as probe.

The Methods S.I.C4-1 section and Chapter 3, describe the experimental set-up and thermodynamic calculations. ΔHs of -40.9 kJ mol^{-1} was estimated and K_d ranged from 50 to 250. For single-walled carbon nanotubes (SWCNTs) and benzene as probe, a sorption enthalpy of -55.9 kJ mol^{-1} was found. [51] For other carbon based-nanomaterials and high-

surface-area graphites, the ΔHs ranged from -52.5 to -33.7 kJ mol^{-1}. [32] The results are in good agreement with the one reported in this study.

Conclusions

CNM applied as sorbent in a HS-ITEX-GC/MS method for the extraction of PAHs in water samples were tested, successfully validated and yielded promising results for screening of these compounds. With the help of a BBD it was possible to analyze five sorbents and generate valuable data to determine which CNM to use for method validation as well as to establish the optimal parameters in a relatively short time frame.

The material characterization of fullerenes with benzene as probe via IGC, was successfully applied, gaining thermodynamic parameters of the material not before available in the literature. The experiment showed the potential of the technique to characterize further CNM with more probe compounds.

Carbon based-nanomaterials, fullerenes specifically, represent a better sorbent material for the extraction of PAHs out of the headspace than Tenax GR.

Acknowledgement

We thank the German Science Foundation, DFG Project SCHM1372/10-1, for funding and CTC Analytik AG (Zwingen, Switzerland) for cooperation and support with the ITEX 2 system. We thank Dr. Thorsten Hüffer, Dr. Maik Jochmann, Beat Schilling and Prof. Karl Molt for their valuable comments. Pascal Mettig for his intensive work in the laboratory as well as Promise A. Dzandu for the IGC measurements and Dr. Ulrich Hagemann for the XPS measurements.

Nomenclature

ΔHs	Sorption enthalpy
S_c	Standard deviation
t	Student's t value
V_g	Specific retention volume

References

1. Asensio-Ramos, M., et al., *Multi-walled carbon nanotubes–dispersive solid-phase extraction combined with nano-liquid chromatography for the analysis of pesticides in water samples.* Anal. Bioanal. Chem., 2011. **400**(4): p. 1113–1123.

2. Maghsoudi, S. and E. Noroozian, *HP-SPME of volatile polycyclic aromatic hydrocarbons from water using multiwalled carbon nanotubes coated on a steel fiber through electrophoretic deposition.* Chromatographia, 2012. **75**(15): p. 913–921.

3. Xiao, C.H., et al., *Use of polymeric fullerene as a new coating for solid-phase microextraction.* Chromatographia, 2000. **52**(11): p. 803-809.

4. Wang, J.X., et al., *Multiwalled carbon nanotubes coated fibers for solid-phase microextraction of polybrominated diphenyl ethers in water and milk samples before gas chromatography with electron-capture detection.* J. Chromatogr. A, 2006. **1137**(1): p. 8-14.

5. Xiao, C., et al., *Application of the polysilicone fullerene coating for solid-phase microextraction in the determination of semi-volatile compounds.* J. Chromatogr. A, 2001. **927**(1-2): p. 121-130.

6. Pyrzynska, K., *Carbon nanotubes as sorbents in the analysis of pesticides.* Chemosphere, 2011. **83**(11): p. 1407-1413.

7. Serrano, A. and M. Gallego, *Fullerenes as sorbent materials for benzene, toluene, ethylbenzene, and xylene isomers preconcentration.* J. Sep. Sci., 2006. **29**(1): p. 33-40.

8. Cai, Y., et al., *Multiwalled carbon nanotubes as a solid-phase extraction adsorbent for the determination of bisphenol A, 4-n-Nonylphenol, and 4-tert-octylphenol.* Anal. Chem., 2003. **75**(10): p. 2517-2521.

9. Vallant, R.M., et al., *Development and application of C_{60}-fullerene bound silica for solid-phase extraction of biomolecules.* Anal. Chem., 2007. **79**(21): p. 8144-8153.

10. Huang, K.J., et al., *Spectrofluorimetric determination of glutathione in human plasma by solid-phase extraction using graphene as adsorbent.* Spectrochim. Acta A, 2011. **79**(5): p. 1860– 1865.

11. Valcárcel, M., et al., *Carbon nanostructures as sorbent materials in analytical processes.* Trends Anal. Chem., 2008. **27**(1): p. 34-43.

12. Zhang, B.T., et al., *Application of carbon-based nanomaterials in sample preparation: A review.* Anal. Chim. Acta, 2013. **784**: p. 1-17.

13. Georgakilas, V., et al., *Functionalization of graphene: covalent and non-covalent approaches, derivatives and applications.* Chem. Rev., 2012. **112**(11): p. 6156-6214.

14. D'Souza, F. and K.M. Kadish, *Handbook of carbon nano naterials: volume 7: synthetic developments of graphene and nanotubes*. 2015, Singapore: World Scientific Publishing Company. 500.

15. Kremser, A., M.A. Jochmann, and T.C. Schmidt, *PAL SPME Arrow—evaluation of a novel solid-phase microextraction device for freely dissolved PAHs in water.* Anal. Bioanal. Chem., 2015. **408**(3): p. 943-952.

16. Corporation, W., *EPA Method 550.1 Polycyclic aromatic hydrocarbons (pahs) Determination of polycyclic aromatic hydrocarbons in drinking water by liquid-solid extraction and high performance liquid chromatography with ultraviolet detection*. 2008. p. 1-15.

17. Munch, J.W., *Method 525.2, Revision 2.0: Determination of organic compounds in drinking water by liquid-solid extraction and capillary column gas chromatography/mass spectrometry*, O.o. water, Editor. 1995, EPA: Cincinnati, Ohio, U.S.A.

18. Wang, H. and A.D. Campiglia, *Determination of polycyclic aromatic hydrocarbons in drinking water samples by solid-phase nanoextraction and high-performance liquid chromatography.* Anal. Chem., 2008. **80**(21): p. 8202–8209.

19. Pawliszyn, J., *Sampling and sample Preparation for field and laboratory: fundamentals and new directions in sample preparation*. Vol. 37. 2002, The Netherlands: Elsevier Science B.V. 1131.

20. Namieśnik, J. and P. Szefer, *Analytical measurements in aquatic environments*. 2009, United Kingdom: CRC. 503.

21. Wei, M.C. and J.F. Jen, *Determination of polycyclic aromatic hydrocarbons in aqueous samples by microwave assisted headspace solid-phase microextraction and gas chromatography/flame ionization detection.* Talanta, 2007. **72**(4): p. 1269–1274.

22. Zuazagoitia, D., E. Millán, and R. Garcia, *A screening method for polycyclic aromatic hydrocarbons determination in water by headspace SPME with GC-FID.* Chromatographia, 2007. **66**(9-10): p. 773-777.

23. Laaks, J., et al., *In-tube extraction of volatile organic compounds from aqueous samples: an economical alternative to purge and trap enrichment.* Anal. Chem., 2010. **82**(18): p. 7641-7648.

24. Laaks, J., M.A. Jochmann, and T.C. Schmidt, *Solvent-free microextraction techniques in gas chromatography.* Anal. Bioanal. Chem., 2012. **402**(2): p. 565-571.

25. Bezerra, M.A., et al., *Response surface methodology (RSM) as a tool for optimization in analytical chemistry.* Talanta, 2008. **76**(5): p. 965-977.

26. Lou, H., et al., *Systematic investigation on parameters of solution blown micro/nanofibers using response surface methodology based on Box-Behnken Design.* J. Appl. Polym. Sci., 2013. **130**(2): p. 1383-1391.

27. Hüffer, T., et al., *Multi-walled carbon nanotubes as sorptive material for solventless in-tube microextraction (ITEX2)—a factorial design study.* Anal. Bioanal. Chem., 2013. **405**(26): p. 8387-8395.

28. Wu, L., et al., *Application of the Box–Behnken design to the optimization of process parameters in foam cup molding.* Expert Syst. Appl., 2012. **39**(9): p. 8059–8065.

29. Ferreira, S.L.C., et al., *Box-Behnken design: an alternative for the optimization of analytical methods.* Anal. Chim. Acta, 2007. **597**(2): p. 179–186.

30. Ferreira, S.L.C., et al., *Statistical designs and response surface techniques for the optimization of chromatographic systems.* J. Chromatogr. A, 2007. **1158**(1–2): p. 2-14.

31. *http://surfacemeasurementsystems.com/learning-center/webinars/webinars-2015/surface-characterization-nanomaterials-inverse-gas-chromatography/ (accessed: August 16th 2016).*

32. Díaz, E., S. Ordóñez, and A. Vega, *Adsorption of volatile organic compounds onto carbon nanotubes, carbon nanofibers, and high-surface-area graphites.* J. Colloid Interf. Sci., 2007. **305**(1): p. 7-16.

33. Pan, B. and B. Xing, *Adsorption mechanisms of organic chemicals on carbon nanotubes.* Environ. Sci. Technol., 2008. **42**(24): p. 9005-9013.

34. Peng, H.B., et al., *Organic contaminants and carbon nanoparticles: sorption mechanisms and impact parameters.* J. Zhejiang Univ. Sci. A, 2014. **15**(8): p. 606-617.

35. Shen, X., G. Zhang, and B. Bjerg, *Assessments of experimental designs in response surface modelling process: estimating ventilation rate in naturally ventilated livestock buildings.* Energ. and Buildings, 2013. **62**: p. 570-580.

36. Molitor, N., T. Kitamura, and C. Javelle, *Status paper: background information on carbon nanohorns (cnh)*, T. GmbH, Editor. 2013: Germany.

37. Hu, X., et al., *Impact of some environmentally relevant parameters on the sorption of polycyclic aromatic hydrocarbons to aqueous suspension of fullerene.* Environ. Toxicol. Chem., 2008. **27**(9): p. 1868–1874.

38. GmbH, I.L.T., *Technical data sheet Graphene platelets, 11-15 nm, 99.5%*. 2012: Germany.

39. Machado Machado, F., et al., *Carbon nanoadsorbents*, in *Carbon nanomaterials as adsorbents for environmental and biological applications*. 2015, Springer: Switzerland. p. 122.

40. White, C.M., et al., *Characterisation of commercially CVD grown multi-walled carbon nanotubes for paint applications.* Prog. Org. Coat., 2016. **90**: p. 44-53.

41. Sigma-Aldrich, *Product specification Product Number: 755125*. 2015: USA.

42. Yang, K. and B. Xing, *Desorption of polycyclic aromatic hydrocarbons from carbon nanomaterials in water.* Environ. Pollut., 2007. **145**(2): p. 529-537.

43. Hüffer, T., et al., *How redox conditions and irradiation affect sorption of PAHs by dispersed fullerenes (nC_{60}).* Environ. Sci. Technol., 2013. **47**(13): p. 6935-6942.

44. Kadish, K.M., R.S. Ruoff, and E.S.F. Group, *Proceedings of the Symposium on Recent Advances in the Chemistry and Physics of Fullerenes and Related Materials*. 1996: Electrochemical Society.

45. Li, Q. and P.J. Alvarez, *2010 progress report: interactions of natural organic matter with C_{60} fullerene and their impact on C_{60} transport, bioavailability and toxicity*. 2010, EPA.

46. Cheng, X., A.T. Kan, and M.B. Tomson, *Naphthalene adsorption and desorption from aqueous C_{60} fullerene.* J. Chem. Eng. Data, 2004. **49**(3): p. 675-683.

47. Laaks, J., et al., *Optimization strategies of in-tube extraction (ITEX) methods.* Anal. Bioanal. Chem., 2015. **407**(22): p. 6827-6838.

48. Laaks, J., et al., *In-tube extraction-GC-MS as a high-capacity enrichment technique for the analysis of alcoholic beverages.* J. Agric. Food Chem., 2014. **62**(14): p. 3081-3091.

49. Glaser, J.A., et al., *Trace analyses for wastewaters.* Environ. Sci. Technol., 1981. **15**(12): p. 1426-1435.

50. Menzel, R., et al., *Inverse gas chromatography of as-received and modified carbon nanotubes.* Langmuir, 2009. **25**(14): p. 8340-8348.

51. Karwa, M. and M. Somenath, *Gas chromatography on self-assembled, single-walled carbon nanotubes.* Anal. Chem., 2006. **78**(6): p. 2064-2070.

C4 Supplementary Information

Table S.I.C4-1. Experiment block according to BBD. Four factors and three levels with five central points.

	Sample Plan			
Setting	S	F	T	D
1	-	-	0	0
2	+	-	0	0
3	-	+	0	0
4	+	+	0	0
5	0	0	-	-
6	0	0	+	-
7	0	0	-	+
8	0	0	+	+
9	-	0	0	-
10	+	0	0	-
11	-	0	0	+
12	+	0	0	+
13	0	-	-	0
14	0	+	-	0
15	0	-	+	0
16	0	+	+	0
17	-	0	-	0
18	+	0	-	0
19	-	0	+	0
20	+	0	+	0
21	0	-	0	-
22	0	+	0	-
23	0	-	0	+
24	0	+	0	+
25	0	0	0	0
26	0	0	0	0
27	0	0	0	0
28	0	0	0	0
29	0	0	0	0

Methods S.I.C4-1. Material characterization via IGC.

Reagents and materials

Natural gas obtained from an in-lab gas line was used as inert marker. It was stored in a one liter multi-layer foil gas sampling bag (Restek, Bad Homburg, Germany). Benzene (>99%), was purchased from Sigma-Aldrich. The probe was prepared with reagent water from a PURELAB Ultra Analytic water purification system (ELGA LabWater, Celle, Germany).

Stock and Sample Preparation

Amber 20-mL screw cap headspace vials (BGB Analytik AG, Böckten, Switzerland) closed with rubber-PTFE septa screw caps (BGB Analytik AG, Böckten, Switzerland) were used for sample preparation. From the benzene stock solution at 87.4 mg L^{-1}, samples were prepared at 3.49 mg L^{-1}. 10 mL were used as sample volume in the amber 20-mL headspace screw cap vial and closed with rubber-PTFE septa caps (BGB Analytik AG, Böckten, Switzerland).The stock and sample solutions were prepared daily. The samples were prepared at a concentration approaching the infinite dilution in the gas phase.

Inverse Gas Chromatography

Column

The ITEX needle packed with fullerenes (BGB Analytik AG, Böckten, Switzerland) was used as column. A 40 cm, 0.32 mm i. d. deactivated TSP FS-tubing (BGB Analytik AG, Böckten, Switzerland) was used to connect the column to the injector. On the side of the injector, the tubing was attached such as a usual GC column. The other side of the tubing was jointed to the ITEX needle (at the “top”, not the cannula end) with a Swagelok connector containing a 1/8 ” Teflon PTFE ferrule (Restek, Bad Homburg, Germany). The cannula from the ITEX was attached to the FID detector with the common ferrule and nut.

Apparatus and conditions

All measurements were performed using a Shimadzu 2014 gas chromatograph (GC) equipped with a flame ionization detector (FID) (Shimadzu, Duisburg, Germany). Injection was

performed in a split/splitless (S/SL) injector at 200 °C in split mode at a split ratio of 5. A VICI precision sampling pressure lok 0.5 mL (BGB Analytik AG, Böckten, Switzerland), was used to inject 20 µL of natural gas as inert marker, while a Hamilton syringe 1750 SL 500 µL (Hamilton AG, Bonaduz, Switzerland) was utilized to inject 500 µL of the probe's HS volume. N_2 of purity 5.0 (Air Liquide, Oberhausen, Germany) was used as carrier gas.

The thermodynamic parameters were determined at a constant column flow of 3 mL min^{-1} and the column temperature was varied from 393.15 to 453.15 K. The FID temperature was set at 260 °C with a sampling rate of 40 ms. Data reprocessing was performed with GCMS Solution, Microsoft Excel and Origin.

Each vial was used either for three temperature levels, each level was measured in triplicates. Before injection into the S/SL injector, the syringe was cleaned with the probe HS sample volume, afterwards another probe HS sample volume was injected for analysis.

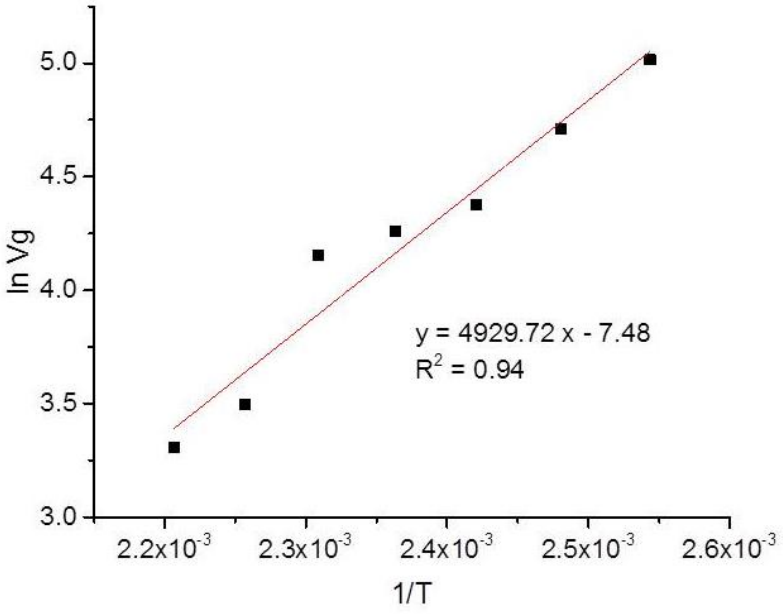

Figure S.I.C4-1. Graphical determination of *ΔHs* for benzene and fullerenes as sorbent (average of each temperature depicted)
The column flow was set to 3 mL min^{-1}. Benzene as probe compound, with a sample concentration (c_{sample}) of 3.49 mg L^{-1} in the liquid phase and a headspace injection volume of 500 µL.

$$V_g = \frac{273Fj\Delta t}{mT} \quad \text{in mL g}^{-1} \text{ Eq.1 [1]}$$

$$K_d = \frac{V_N}{V_P} \quad \text{Eq.2 [1]}$$

Here, V_N is the net retention volume and V_P that of the sorption phase.

Table S.I.C4-2. Sorbent extraction yield comparison with naphthalene. HS-ITEX-GC/MS method and a BBD, cPAHs = 50 µg L^{-1}.

	Naphthalene																
	Fullerenes			Tenax GR			MWCNTs-COOH			MWCNTs			Graphene platelets			Carbon nanohorns		
Setting	Average	St. dev.	CV / %	Average	St. dev.	CV / %	Average	St. dev.	CV / %	Average	St. dev.	CV / %	Average	St. dev.	CV / %	Average	St. dev.	CV / %
1	3.1E+07	8.3E+05	3	6.2E+05	8.2E+04	13	5.4E+06	7.7E+05	14	3.8E+07	3.4E+06	9	3.6E+06	8.4E+05	23	1.3E+05	8.6E+03	6
2	6.3E+07	3.5E+06	6	2.6E+06	4.4E+05	17	1.2E+08	3.1E+06	3	1.3E+08	5.2E+03	0.00	2.2E+07	1.3E+06	6	9.4E+05	9.7E+04	10
3	2.3E+07	6.1E+05	3	4.7E+05	2.7E+04	6	2.2E+06	1.3E+05	6	2.5E+07	4.9E+06	20	1.4E+06	4.5E+04	3	7.6E+04	1.3E+04	16
4	4.5E+07	2.0E+06	4	2.5E+06	5.5E+05	22	3.2E+07	6.2E+06	20	9.6E+07	3.8E+06	4	8.0E+06	6.2E+05	8	6.8E+05	1.6E+05	23
5	2.5E+07	2.7E+05	1	5.9E+05	1.5E+04	3	2.8E+06	1.4E+05	5	4.2E+07	1.7E+05	0.40	9.8E+05	8.5E+04	9	7.2E+04	9.3E+03	13
6	3.4E+07	2.7E+06	8	2.3E+06	6.5E+04	3	7.0E+07	7.0E+06	10	2.8E+07	2.6E+06	9	2.4E+07	4.0E+06	17	5.8E+05	4.1E+05	70
7	1.9E+07	2.4E+05	1	7.4E+05	8.4E+04	11	7.6E+06	5.0E+05	7	4.6E+07	5.4E+05	1	6.1E+06	6.5E+05	11	1.6E+05	4.5E+04	27
8	4.0E+07	2.3E+07	58	3.9E+06	3.0E+05	8	9.0E+07	1.8E+07	20	6.7E+07	6.0E+06	9	2.4E+07	1.9E+06	8	1.3E+06	2.4E+05	19
9	7.9E+06	1.5E+05	2	3.5E+05	1.9E+04	6	2.6E+06	2.3E+05	9	1.9E+07	3.5E+06	18	1.2E+06	1.1E+05	9	7.6E+04	1.1E+04	15
10	3.3E+07	3.2E+05	1	2.4E+06	2.8E+04	1	4.3E+07	6.2E+06	15	7.6E+07	5.9E+06	8	5.7E+06	3.2E+05	6	7.4E+05	1.0E+05	14
11	1.3E+07	7.0E+05	5	5.3E+05	2.8E+04	5	3.3E+06	7.6E+04	2	2.2E+07	1.8E+05	1	1.7E+06	9.4E+04	6	8.5E+04	1.5E+04	17
12	5.1E+07	4.3E+05	1	3.9E+06	1.3E+05	3	6.7E+07	5.6E+06	8	8.0E+07	5.4E+06	7	3.7E+07	2.4E+06	7	5.1E+05	4.1E+04	8
13	3.1E+07	6.3E+05	2	6.0E+05	1.7E+04	3	8.4E+06	3.5E+05	4	5.2E+07	3.4E+05	1	1.6E+07	1.7E+06	11	6.8E+04	8.2E+03	12
14	1.6E+07	2.1E+05	1	5.8E+05	3.6E+04	6	3.7E+06	1.1E+05	3	2.3E+07	3.6E+05	2	9.7E+06	1.4E+06	15	4.8E+04	1.4E+03	3
15	6.1E+07	2.7E+06	4	2.6E+06	2.3E+05	9	8.0E+07	1.9E+07	23	7.4E+07	1.8E+07	24	8.9E+07	3.6E+06	4	6.3E+05	1.5E+05	24
16	1.0E+08	2.9E+06	3	2.2E+06	8.3E+04	4	5.7E+07	1.8E+06	3	3.5E+07	1.0E+07	30	3.7E+07	1.8E+06	5	2.6E+05	3.1E+04	12
17	1.4E+07	1.5E+05	1	2.0E+05	3.3E+03	2	2.6E+06	1.4E+05	5	1.4E+07	6.2E+04	0.45	2.4E+06	1.2E+05	5	1.4E+04	1.8E+03	13
18	5.1E+07	2.4E+06	5	7.7E+05	2.0E+04	3	2.8E+07	3.5E+06	12	5.9E+07	1.8E+06	3	8.4E+06	8.4E+05	10	2.5E+04	1.2E+04	46
19	3.5E+07	2.1E+06	6	6.1E+05	3.9E+03	1	1.5E+07	1.7E+06	12	4.6E+07	6.1E+06	13	5.8E+06	7.0E+05	12	3.4E+04	1.9E+03	6
20	1.1E+08	2.0E+06	2	4.4E+06	2.0E+05	5	2.5E+08	2.1E+07	9	3.8E+07	2.7E+07	70	4.6E+07	1.4E+07	29	9.7E+04	9.9E+03	10
21	4.6E+07	8.4E+05	2	6.7E+05	5.4E+04	8	7.1E+07	2.8E+06	4	7.4E+07	9.5E+06	13	9.4E+06	1.3E+06	14	1.7E+04	3.1E+03	19
22	1.3E+07	9.4E+05	7	8.1E+05	2.1E+05	26	2.7E+07	2.8E+06	10	6.1E+07	1.8E+06	3	5.1E+06	4.4E+05	9	8.4E+03	5.4E+02	6
23	3.4E+07	5.7E+05	2	1.3E+06	1.3E+05	10	8.2E+07	6.2E+06	7	7.9E+07	1.0E+07	13	1.3E+07	1.1E+06	9	7.7E+03	3.6E+03	47
24	1.9E+07	1.0E+05	1	1.5E+06	9.7E+04	7	3.6E+07	9.2E+04	0.25	6.6E+07	2.5E+06	4	8.9E+06	1.1E+06	13	3.0E+04	5.8E+03	19
25	7.6E+07	1.3E+06	2	1.2E+06	1.4E+05	12	3.6E+07	1.3E+06	4	7.3E+07	3.5E+06	5	1.0E+07	1.6E+06	16	2.3E+05	4.4E+04	20
26	6.5E+07	2.7E+06	4	1.1E+06	7.7E+03	1	3.6E+07	3.3E+06	9	6.4E+07	9.1E+06	14	1.3E+07	5.3E+05	4	1.2E+05	8.2E+03	7
27	6.6E+07	9.2E+05	1	1.1E+06	1.1E+05	10	3.5E+07	2.3E+06	6	7.3E+07	1.7E+06	2	1.3E+07	9.3E+05	7	1.5E+05	1.3E+04	8
28	6.4E+07	1.1E+06	2	1.1E+06	8.2E+04	8	3.1E+07	1.0E+06	3	6.8E+07	1.0E+06	1	1.4E+07	2.2E+06	15	1.8E+05	5.6E+03	3
29	6.1E+07	1.6E+05	0.26	1.2E+06	1.1E+05	10	3.0E+07	2.5E+06	8	4.8E+07	8.6E+06	18	1.5E+07	3.4E+05	2	1.3E+05	2.5E+04	19

Table S.I.C4-3. Sorbent extraction yield comparison with pyrene. HS-ITEX-GC/MS method and a BBD, cPAHs = 50 µg L^{-1}.

	Pyrene																	
	Fullerenes			Tenax GR			MWCNTs-COOH			MWCNTs			Graphene platelets			Carbon nanohorns		
Setting	Average	St. Dev.	CV / %	Average	St. dev.	CV / %	Average	St. dev.	CV / %	Average	St. dev.	CV / %	Average	St. dev.	CV / %	Average	St. dev.	CV / %
1	9.5E+05	6.3E+04	7	4.4E+05	6.8E+04	16	8.6E+04	1.1E+04	13	6.1E+05	5.4E+04	9	4.0E+04	8.2E+03	20	1.5E+04	2.6E+03	17
2	7.8E+06	1.4E+05	2	2.7E+06	3.0E+05	11	6.1E+05	2.3E+04	4	4.2E+06	2.4E+05	6	1.1E+05	1.2E+04	11	4.9E+04	1.1E+04	22
3	7.3E+05	3.3E+04	5	2.4E+05	1.3E+03	1	9.9E+04	1.2E+04	12	4.9E+05	5.7E+04	12	2.8E+04	2.9E+03	10	1.5E+04	2.1E+03	14
4	5.7E+06	5.0E+05	9	1.9E+06	8.4E+03	0.4	4.2E+05	6.9E+04	17	3.6E+06	3.0E+05	8	1.3E+05	1.8E+04	14	5.4E+04	1.2E+04	23
5	4.9E+05	5.3E+04	11	1.2E+05	5.9E+03	5	3.3E+04	2.7E+03	8	3.6E+05	6.9E+03	2	1.6E+04	3.3E+03	21	7.5E+03	8.4E+02	11
6	4.3E+06	8.5E+05	20	2.2E+06	2.4E+05	11	1.5E+06	2.6E+05	17	2.1E+06	1.4E+05	7	1.0E+06	5.0E+04	5	6.2E+04	6.5E+04	105
7	9.1E+05	4.5E+04	5	2.5E+05	4.5E+04	18	7.4E+04	2.2E+03	3	3.0E+05	4.0E+04	13	8.3E+04	1.6E+04	19	8.8E+03	1.2E+03	13
8	1.1E+07	6.7E+05	6	3.7E+06	8.8E+04	2	2.8E+06	1.6E+05	6	3.3E+06	2.3E+05	7	8.3E+05	1.8E+04	2	1.6E+05	5.2E+04	32
9	2.6E+05	5.5E+04	21	5.6E+04	5.2E+03	9	8.5E+04	1.5E+04	18	1.5E+05	7.2E+03	5	4.7E+04	3.3E+03	7	1.0E+04	1.4E+03	14
10	2.6E+06	1.8E+05	7	1.2E+06	1.3E+05	11	4.8E+05	4.7E+04	10	2.3E+06	3.4E+05	15	1.6E+05	2.0E+04	12	4.1E+04	1.3E+04	30
11	7.6E+05	6.0E+04	8	2.2E+05	5.2E+04	23	1.1E+05	1.3E+04	11	1.9E+05	1.6E+04	8	5.6E+04	1.0E+04	18	1.3E+04	5.9E+03	47
12	6.5E+06	2.8E+05	4	1.1E+06	1.6E+05	14	7.6E+05	1.1E+05	15	3.6E+06	9.8E+04	3	1.1E+06	4.3E+04	4	8.7E+03	4.5E+02	5
13	4.5E+05	2.5E+04	6	9.5E+04	2.6E+04	27	8.0E+04	8.7E+03	11	9.1E+05	2.7E+04	3	3.2E+05	3.2E+04	10	2.5E+03	1.0E+03	42
14	4.2E+05	8.5E+03	2	5.8E+04	1.5E+04	25	6.2E+04	3.9E+03	6	5.1E+05	4.4E+04	9	3.1E+05	1.7E+04	6	2.5E+03	1.2E+03	50
15	6.4E+06	4.6E+05	7	2.0E+06	2.7E+05	13	1.3E+06	4.4E+05	33	4.1E+06	5.1E+05	12	2.8E+06	1.4E+05	5	4.3E+04	1.1E+04	27
16	6.3E+06	3.4E+05	5	1.8E+06	3.0E+05	17	1.8E+06	2.3E+05	12	3.3E+06	6.5E+05	20	2.8E+06	4.1E+05	14	1.9E+04	3.9E+03	20
17	2.5E+05	1.7E+04	7	8.7E+03	1.7E+03	20	4.0E+04	4.7E+03	12	2.4E+05	2.7E+03	1.11	5.9E+04	2.7E+03	5			
18	1.3E+06	2.1E+05	16	1.2E+05	2.5E+04	21	1.5E+05	8.1E+03	5	9.0E+05	5.3E+04	6	1.6E+05	1.5E+04	9			
19	1.7E+06	1.9E+05	11	2.0E+05	1.4E+04	7	4.2E+05	6.3E+04	15	1.8E+06	2.2E+05	12	4.2E+05	2.7E+04	6			
20	8.1E+06	8.4E+05	10	4.1E+06	1.8E+05	4	4.6E+06	3.8E+05	8	3.6E+06	5.3E+05	15	2.9E+06	5.3E+05	18	1.2E+03	2.0E+02	16
21	1.8E+06	1.6E+05	9	4.0E+05	1.3E+05	33	2.8E+05	4.6E+04	16	1.1E+06	7.0E+04	7	2.7E+05	7.5E+04	27			
22	6.1E+05	8.4E+04	14	2.3E+05	6.8E+03	3	3.4E+05	5.1E+04	15	1.0E+06	1.6E+05	16	2.8E+05	3.0E+04	11			
23	2.5E+06	1.1E+05	5	7.3E+05	8.1E+04	11	3.9E+05	1.1E+04	3	1.6E+06	9.1E+04	6	2.7E+05	2.8E+04	11			
24	2.0E+06	3.7E+05	19	6.9E+05	5.0E+04	7	4.7E+05	5.9E+04	13	1.2E+06	1.5E+05	13	4.5E+05	8.0E+04	18	9.6E+03	4.3E+03	45
25	4.4E+06	3.1E+05	7	2.0E+05	2.1E+04	11	3.0E+05	1.9E+04	6	1.4E+06	1.8E+05	13	3.4E+05	6.2E+04	18	1.1E+05	1.6E+04	15
26	3.8E+06	3.0E+05	8	2.5E+05	4.7E+04	19	3.0E+05	3.7E+04	12	1.5E+06	9.2E+04	6	4.6E+05	5.5E+04	12	4.0E+04	6.4E+03	16
27	4.2E+06	1.6E+05	4	1.8E+05	3.9E+04	22	3.6E+05	6.1E+04	17	1.5E+06	1.8E+05	12	4.7E+05	3.4E+04	7	4.8E+04	3.8E+03	8
28	3.6E+06	2.1E+05	6	3.3E+05	2.0E+04	6	3.0E+05	1.9E+04	6	1.4E+06	3.7E+04	3	4.6E+05	2.2E+04	5	7.5E+04	1.2E+03	2
29	3.1E+06	2.2E+04	0.7	2.8E+05	7.4E+04	27	2.9E+05	1.2E+04	4	1.3E+06	3.7E+05	29	4.8E+05	8.7E+03	2	5.1E+04	5.1E+03	10

Table S.I.C4-4. Analyte gas phase concentration in equilibrium at the investigated extraction temperatures set for the BBD.

T / °C		25		40		55		70	
	$\Delta_f H_g^\circ$ / KJ mol^{-1}	K_{iaw} [2]	Ci_{air} in equilibrium / µg L^{-1}	K_{iaw}	Ci_{air} in equilibrium / µg L^{-1}	K_{iaw}	Ci_{air} in equilibrium / µg L^{-1}	K_{iaw}	Ci_{air} in equilibrium / µg L^{-1}
Naphthalene	150 [3]	1.82E-02	0.894	3.31E-01	12.445	5.13E+01	49.044	5.13E+01	49.044
Acenaphthylene	261 [4]	1.41E-02	0.695	2.20E+00	34.366	3.37E+04	49.999	1.42E+04	49.996
Acenaphthene	156 [5]	5.13E-03	0.255	1.05E-01	4.747	3.33E+01	48.542	1.99E+01	47.605
Fluorene	172 [6]	3.39E-03	0.169	9.45E-02	4.316	5.41E+01	49.093	3.07E+01	48.420
Phenanthrene	203 [7]	1.41E-03	0.070	7.16E-02	3.340	1.29E+02	49.615	6.58E+01	49.252
Anthracene	223 [8]	1.58E-03	0.079	1.18E-01	5.281	4.45E+02	49.888	2.13E+02	49.766
Fluoranthene	291 [9]	4.57E-04	0.023	1.27E-01	5.646	5.90E+03	49.992	2.26E+03	49.978
Pyrene	220 [10]	4.79E-04	0.024	3.38E-02	1.634	1.14E+02	49.565	5.50E+01	49.108

The Van´t Hoff equation, together with the enthalpy of the gas formation of each analyte at 25 °C, was applied to calculate the Kiaw at different temperatures. R = 8.314 J mol^{-1} K^{-1}.

$$ln\left(\frac{K_{iawT_1}}{K_{iawT_2}}\right) = \frac{-\Delta_f H_g^\circ}{2.3R}\left(\frac{1}{T_1} - \frac{1}{T_2}\right)$$

An example (without temperature change) for the calculation of the gas concentration in equilibrium is presented below:

$$K_{i12} = K_{naphthalene\ air\ water} = 1.82 \times 10^{-2}$$

$$r = \frac{V_{air}}{V_{water}} = \frac{10\ mL}{10\ mL}$$

$$f_{i2} = f_{naphthalene\ water} = \frac{1}{1 + K_{i12}r}$$

$$f_{i2} = f_{naphthalene\ water} = \frac{1}{1 + K_{i12}r} = \frac{1}{1 + (1.82 \times 10^{-2})1} = 0.982$$

$$f_{i1} = 1 - f_{i2} = 1 - 0.982 = 0.01787$$

$$c_{sample} = 0.05\ mg\ L^{-1}$$

$$m_{tot} = C_{sample} \times \left(\frac{1L \times 10mL}{1000mL}\right) = 0.0005\ mg$$

$$\therefore C_{air} = \frac{m_{tot} \times f_{i1}}{V_{air}} = \frac{0.0005\ mg \times 0.01787}{\frac{10\ mL}{1000\ mL}} = 8.9373 \times 10^{-4} mg\ L^{-1} = \underline{0.894\ \mu g\ L^{-1}}$$

Table S.I.C4-5. CNM BBD five point analysis.

	Peak area / AU					CV / %				
	MWCNTs	Fullerenes	MWCNTs-COOH	Graphene platelets	Carbon nanohorns	MWCNTs	Fullerenes	MWCNTs-COOH	Graphene platelets	Carbon nanohorns
Naphthalene	6.55E+07	6.64E+07	3.36E+07	1.31E+07	1.63E+05	16	8	9	14	25
Acenaphthylene	1.50E+07	2.41E+07	3.05E+06	8.73E+05	2.71E+04	14	4	4	10	58
Acenaphthene	1.36E+07	2.51E+07	4.41E+06	6.62E+05	2.62E+04	12	3	5	11	18
Fluorene	4.24E+06	1.67E+07	1.80E+06	4.28E+05	2.33E+04	9	3	4	10	50
Phenanthrene	8.95E+05	1.08E+07	6.26E+05	4.15E+05	2.03E+04	5	6	6	11	168
Anthracene	5.84E+06	1.17E+07	8.99E+05	8.56E+05	4.21E+04	7	8	4	11	47
Fluoroanthene	5.23E+05	4.57E+06	4.57E+06	3.19E+05	2.30E+04	6	13	12	11	66
Pyrene	1.41E+06	3.82E+06	3.10E+05	4.42E+05	6.49E+04	7	13	9	13	44

Methods S.I.C4-2. Material characterization via XPS.

X-ray photo-electron spectroscopy measurements (XPS) were conducted on a PHI VersaProbe II (Physical Electronics GmbH, Ismaning, Germany), using monochromatic Al K_α light at 1486.6 eV, an emission angle of 45 ° to determine the percentage of the elements found at the surface.

Figure S.I.C4-2 XPS spectra for MWCNTs.

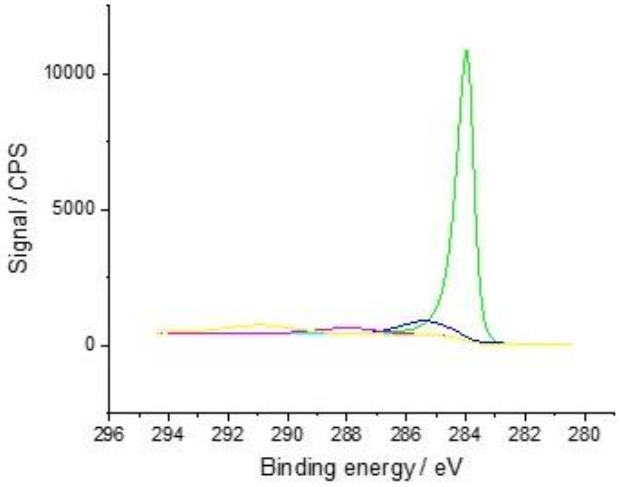

	Source energy: 1486.6 eV				
	Name	Position	FWHM	Area	LS
		eV		CPS eV	
	C 1s	283.96	0.54	8995.64	LA(1.6,3.
	C O	285.36	2	1243.3	SGL(25)
	C =O	286.86	1.33	116.52	SGL(25)
	C OOH	287.96	2.4	625.14	SGL(25)
	PiPi*	290.93	2.7	976.67	SGL(25)

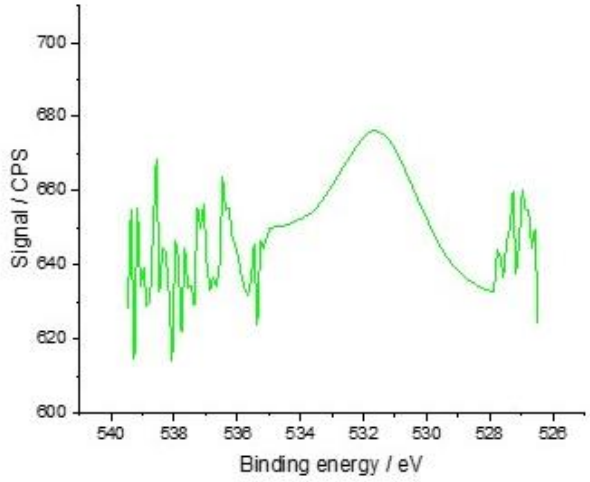

	Source energy: 1486.6 eV				
	Name	Position	FWHM	Area	LS
		eV		CPS eV	
	O 1s	531.44	2.84	122.96	SGL(25

Figure S.I.C4-3. XPS spectra for carbon nanohorns.

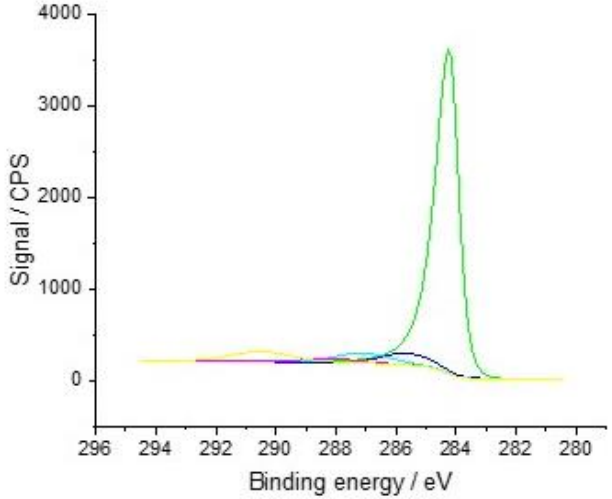

	Source energy: 1486.6 eV				
	Name	Position	FWHM	Area	LS
		eV		CPS eV	
	C 1s	284.22	0.73	3987.28	LA(1.6,3.
	C O	285.62	2	308.64	SGL(25)
	C =O	287.12	2.2	291.33	SGL(25)
	C OOH	288.22	2.4	122.53	SGL(25)
	PiPi*	290.47	2.43	316.07	SGL(25)

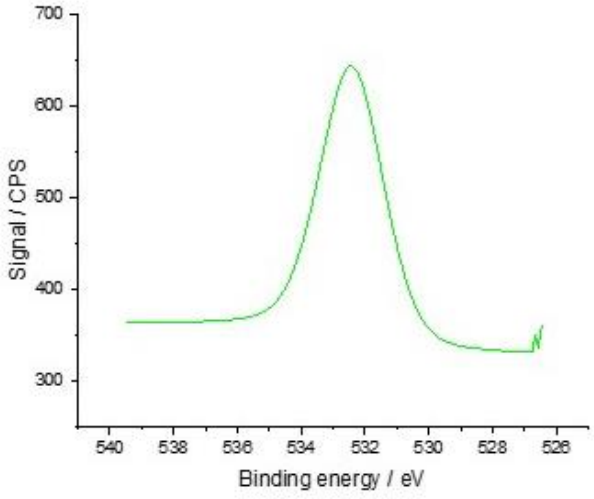

	Source energy: 1486.6 eV				
	Name	Position	FWHM	Area	LS
		eV		CPS eV	
	O 1s	532.41	2.35	839.7	SGL(25)

Figure S.I.C4-4. XPS spectra for graphene platelets.

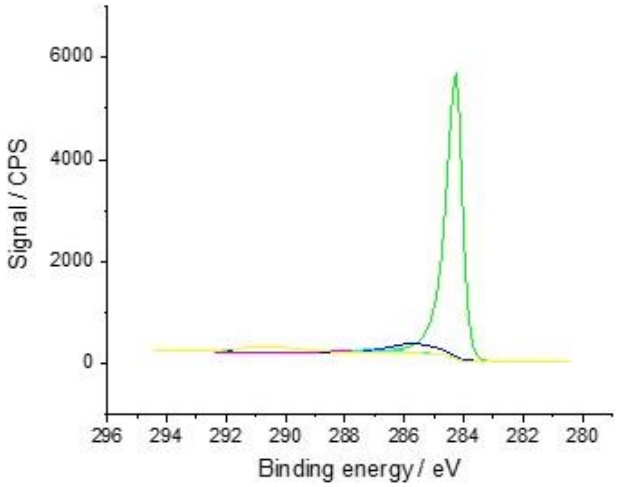

	Source energy: 1486.6 eV				
	Name	Position	FWHM	Area	LS
		eV		CPS eV	
	C 1s	284.26	0.49	4201.66	LA(1.6,3.
	C O	285.66	2	440.76	SGL(25)
	C =O	287.16	2.2	135.33	SGL(25)
	C OOH	288.26	1.08	37.15	SGL(25)
	PiPi*	290.66	2.34	295.45	SGL(25)

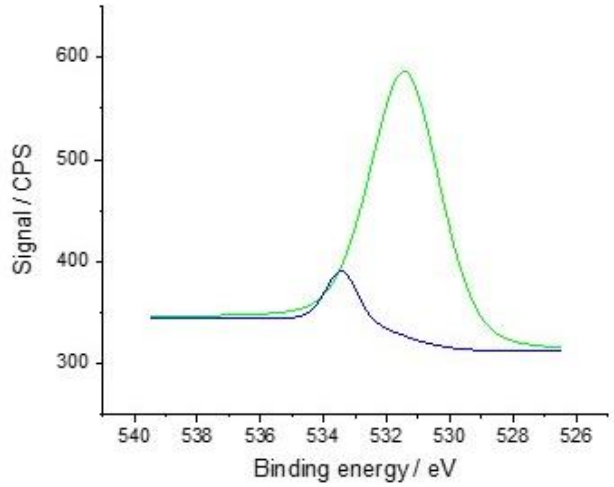

	Source energy: 1486.6 eV				
	Name	Position	FWHM	Area	LS
		eV		CPS eV	
	O 1s	531.41	2.6	806.62	SGL(25)
	O 1s	533.43	1.18	71.75	SGL(25)

Table S.I.C4-6. ANOVA for acenaphthene and phenanthrene with a BBD. HS-ITEX-GC/MS, fullerenes as sorbent.

	Acenaphthene				Phenanthrene			
	DF	*Adj. SS*	*F*-Value	*p*-Value	*DF*	*Adj. SS*	*F*-Value	*p*-Value
Model	14	2.60E+20	14.81	0.0000	14	16.7586	9.11	0.0000
Linear	4	1.78E+20	35.40	0.0000	4	13.2259	25.17	0.0000
T	1	1.07E+20	85.13	0.0000	1	4.7315	36.01	0.0000
S	1	6.34E+19	50.50	0.0000	1	6.8618	52.23	0.0000
F	1	4.08E+18	3.25	0.0930	1	0.3641	2.77	0.118
D	1	3.43E+18	2.74	0.1200	1	1.2685	9.66	0.008
Square	4	6.34E+19	12.62	0.0000	4	3.0887	5.88	0.005
T^2	1	4.91E+16	0.04	0.8460	1	0.4379	3.33	0.089
S^2	1	1.97E+19	15.74	0.0010	1	1.0921	8.31	0.012
F^2	1	1.55E+19	12.33	0.0030	1	0.6949	5.29	0.037
D^2	1	4.41E+19	35.18	0.0000	1	2.2496	17.12	0.001
2-Way interaction	6	1.92E+19	2.55	0.0700	6	0.4439	0.56	0.753
T×S	1	7.13E+18	5.68	0.0320	1	0.1156	0.88	0.364
T×F	1	2.19E+17	0.17	0.6830	1	0.0444	0.34	0.57
T×D	1	7.98E+18	6.34	0.0240	1	0.0848	0.65	0.435
S×F	1	8.42E+16	0.07	0.7990	1	0.0164	0.12	0.729
S×D	1	2.76E+18	2.20	0.1600	1	0.0119	0.09	0.768
F×D	1	1.01E+18	0.80	0.3850	1	0.1708	1.3	0.273
Error	14	1.76E+19			14	1.8394		
Lack -of-Fit	10	1.73E+19	29.99	0.0030	10	1.8254	52.17	0.001
Pure Error	4	5.78E+16			4	0.014		
Total	28	2.78E+20			28	19		

DF = Degrees of freedom. *Adj. SS* = Adjusted sum of squares. *F*-Value = Fisher´s value. *p*-Value = Result from the F-test for a lack of fit. T = Extraction temperature. S = Extraction strokes. F = Extraction flow. D = Desorption temperature.

References

1. Boutboul, A., et al., *Use of inverse gas chromatography to determine thermodynamic parameters of aroma–starch interactions.* J. Chromatogr. A, 2002. **969**(1-2): p. 9-16.

2. Schwarzenbach, R.P., P.M. Gschwend, and D.M. Imboden, *Environmental Organic Chemistry*. 2nd ed. 2005, New Jersey, USA: John Wiley & Sons, Inc.

3. *http://webbook.nist.gov/cgi/cbook.cgi?ID=C91203&Units=SI&Mask=1#Thermo-Gas (accessed: August 29th 2016).*

4. *http://webbook.nist.gov/cgi/cbook.cgi?ID=C208968&Units=SI&Mask=1#Thermo-Gas (accessed: August 29th 2016).*

5. *http://webbook.nist.gov/cgi/cbook.cgi?ID=C83329&Units=SI&Mask=1#Thermo-Gas (accessed: August 29th 2016).*

6. *http://webbook.nist.gov/cgi/cbook.cgi?ID=C86737&Units=SI&Mask=1#Thermo-Gas (accessed: August 29th 2016).*

7. *http://webbook.nist.gov/cgi/cbook.cgi?ID=C85018&Units=SI&Mask=1#Thermo-Gas (accessed: August 29th 2016).*

8. *http://webbook.nist.gov/cgi/cbook.cgi?ID=C120127&Units=SI&Mask=1#Thermo-Gas (accessed: August 29th 2016).*

9. *http://webbook.nist.gov/cgi/cbook.cgi?ID=C206440&Units=SI&Mask=1#Thermo-Gas (accessed: August 29th 2016).*

10. *http://webbook.nist.gov/cgi/cbook.cgi?ID=C129000&Units=SI&Mask=1#Thermo-Gas (accessed: August 29th 2016).*

Chapter 5 Polymeric ionic liquids as sorbent for in-tube extraction

Abstract

Polymeric ionic liquids (PIL) have gained attention in analytical chemistry, because their tune ability provide the opportunity to adapt the physicochemical properties of the sorbent to the application of interest. PIL are mainly applied in electrochemical devices and are emerging in the analytical chemistry field, making them an interesting material for analysis as sorbent in the microextraction technique field.

Two self-made silica PIL, Sil. PIL 1 and Sil. PIL 2, were synthesized for the investigation as sorbent material in the in-tube extraction (ITEX) technique. PIL have been used in solid phase microextraction (SPME), but coating the fiber generates further synthesis steps, which in the case of ITEX the material can be easily packed in the void volume of the syringe.

Multifunctional ionic liquid (IL) monomers were designed and synthesized from 1-vinylimidazole (VIm) and 2-acrylamido-2-methylpropane sulphonic acid (AMPS). This monomer was alternately copolymerized from surface radical transfer agent (3-mercaptopropyltrimethoxysilane) grafted silica core to obtain hybrid core-shell particles, namely Sil. PIL 1.

Sil. PIL 2 was synthesized with silica gel and 3-mercaptopropyl trimethoxysilane as surface initiator. N-vinylimidazolium Br monomer ([C_{10}VIm]Br) was modified via anion exchange to the *p*-styrenesulphonate. To the cation segment (1-vinylimidazolium) a C_{10} long alkyl chain is attached and the anion section (*p*-styrenesulphonate) is repeated 18 times.

Both PIL were applied in a headspace (HS)-ITEX-GC/MS method as sorbent. As preliminary test and to demonstrate that the PIL work as sorbent in ITEX, Sil. PIL 1 was tested with derivatized aldehydes (C_1 to C_{10}) and short chain alcohols. The results were compared against two commercial ITEX sorbents, PDMS and Tenax GR, respectively. Sil. PIL 1 proved to be a more suitable sorbent for the extraction of derivatized aldehydes than PDMS, while Tenax GR is a better option for the extraction alcohols than Sil. PIL 1. To this end, Sil. PIL 2 was investigated also with short chain alcohols to verify whether its analytical performance offered a better option than the commercial available materials. The extraction parameters were determined for Sil. PIL 2 and in some extent emulated to the ones reported in the literature. Sil. PIL 2 showed a linear range from 0.55 to 5,500 µg L^{-1} and detection limits between 0.3 to 15.1 µg L^{-1} for the aqueous standard samples. Analysis of the spiked beer samples for the recovery determinations, yielded poor results. Compared to the results of commercial sorbent materials like PDMS blue or Tenax TA, Sil. PIL 2 is not a recommendable sorbent for the investigated approach.

Partly redrafted from: Rahman, M.M., et al., *Core-shell hybrid particles by alternating copolymerization of ionic liquid monomers from silica as sorbent for solid phase microextraction.* Macromol. Mater. Eng., 2015. **300**(11): p. 1049-1056.

Introduction

Ionic liquids (ILs) are monomers, usually monovalent, where one or more polymerizable units are incorporated. [1] ILs characteristics are determined by the mutual fit of the cation and anion, size, geometry and charge distribution. Typical anions are halides, tetrafluoroborate, hexafluorophosphate and others, [2] but usually ILs are categorized by the type of cations into: 1) alkylammonia 2) phosphonium 3) dialkylimidazolium and 4) N-alkylpyridinium. [3]

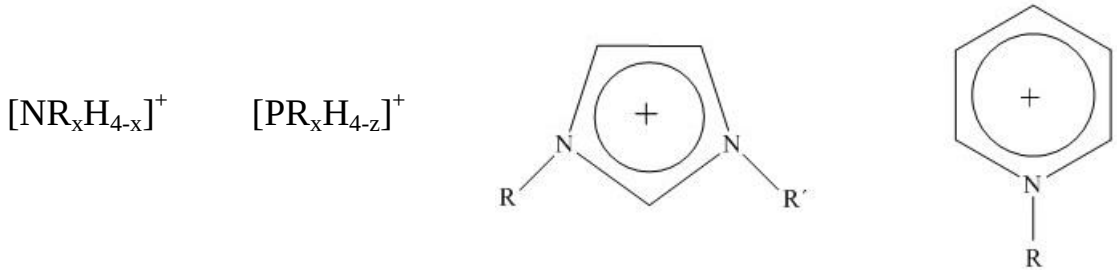

Figure 5-1. Typical cations categories for ILs. [3]

The selection of the cations and anions influences the temperature where they can be applied and the anion usually controls the water miscibility (hygroscopic character). [4] When the ILs are supported covalently linked to a polymer or organic surface, then supported ILs are produced, [5] called polymeric ionic liquids (PIL).

PIL refer to a special type of polyelectrolyte. [1] [2] This features an IL species in each repeating monomer, connected through a polymeric backbone to form a macromolecule. [6]

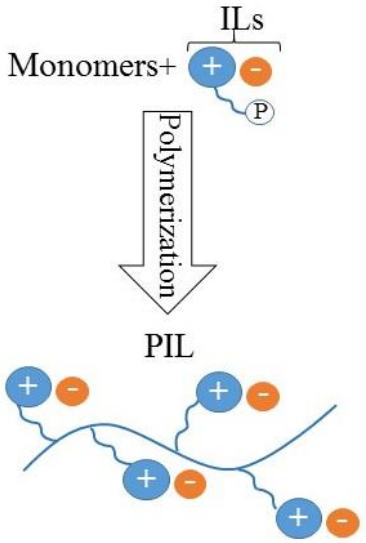

Figure 5-2. General PIL synthesis scheme. P = Polymerizable group. Redrafted from the literature. [6]

PIL can be synthesized by a) direct polymerization of IL monomers or b) chemical modification of existing polymers. N-vinylimidazolium-based (the imidazolium cation included into polymer backbones obtained from vinyl), [7] IL monomers for PIL are prepared via a simple quaternization reaction with a halo-alkane, which is the type of PIL applied as sorbent in this study (Sil. PIL 1 and 2). Free radical polymerization or anion exchange are efficient methods to modify the N-vinylimidazolium-based IL monomers. [1]

The major advantage of using PIL over ILs is the enhanced mechanical stability, improved durability [2] and broader (higher than room temperature or 100 °C [6]) glass transition temperatures (depending on the polymer backbone and cation). [7] As a rule of thumb, an increase at the cation in the branching on the alkyl chain increases the melting point of the PIL. [4] PIL are mainly applied for batteries and solar cells. [8] Another field of application of PIL is as surfactant in the synthesis of conductive polymer organic dispersion or for preparation of supramolecular polymer assembles. [7] In the analytical chemistry field, PIL are gaining interest as a selective coating for the detection of environmental contaminants in water using solid phase microextraction (SPME) coupled to gas chromatography (GC)-flame ionization detector (FID). [7]

An interesting approach is their application as sorbent for solventless microextraction techniques. These can be classified into: a) application of a coating in the surface of a rod or needle, b) sorbent material packed in a tube or needle. [9] Typical examples for category a) are SPME and stir bar sorptive extraction (SBSE), for b) in-tube extraction (ITEX) and needle trap (NT). [10]

To test the analytical performance, a PIL combined with gold as fiber in SPME and polycyclic aromatic hydrocarbons (PAHs) as model analytes was tested. [11] Other PIL were also evaluated with PAHs, benzene, toluene, ethylbenzene and xylenes (BTEX) or with non-halogenated hydrocarbons. [12] [13] [14] The overall advantage over SPME is the simple packing procedure. In contrast to ITEX, in SPME the fiber must be coated and occasionally extra synthesis procedures must be added. [12] [11]

Parts of this chapter have been published before, [15] as a first proof-of-concept for the application of Sil. PIL in the ITEX technique. Derivatized aldehydes and short chain alcohols, extracted from the headspace (HS) of aqueous samples, where used as probe compounds for the HS-ITEX-GC/MS method. To extend the previous work, the second PIL (Sil. PIL 2) was also investigated as sorbent in the HS-ITEX-GC/MS method, short chain alcohols were used as probe analytes.

The presented study, is the first one reported where PIL are packed as sorbent material in ITEX.

Experimental

5.1.1 Reagents and materials

Aldehydes

Formaldehyde (99 %), acetaldehyde (99.5 %) were purchased by Fluka. *n*-Propanal (97 %), *n*-Butanal (99 %), *n*-Pentanl (97 %), *n*-Hexanal (98 %), *n*-Heptanal (95 %), *n*-Octanal (99 %), and *n*-Decanal (98 %) were obtained from Sigma Aldrich. *n*-Nonanal (95 %) was purchased from Acros Organics. The derivatization reagent *o*-2,3,4,5,6-(pentafluorobenzyl)hydroxylamine hydrochloride (PFBHA, 99 %), as well as surrogates and internal standards, 2,4,5-trifluoroacetophenone (99 %) and 1,2-dibromopropane were purchased from Alfa Aesar (Karlsruhe, Germany). Potassium hydrogen phthalate (99.5 %) was obtained from Riedel-de Haën, sulfuric acid (96%) from Merck.

Alcohols

Tert-butanol (> 99.9 %), 1-hexanol (> 99.9 %), 3-methyl-1-butanol (> 99.8 %), 2-methyl-1-propanol (> 99.8 %) and 1-pentanol (> 99.8 %) were purchased from Fluka (Sigma-Aldrich, Steinheim, Germany). 1-butanol (99.9%) and 2-propanol (99.5%) were obtained from Sigma-Aldrich (Germany). König Pilsener (König-Brauerei GmbH, Duisburg, Germany) was bought for recovery measurements.

Water was obtained from a PURELAB Ultra Analytic water purification system (ELGA LabWater, Celle, Germany).

5.1.2 Stock and Sample Preparation

Aldehydes

Stock solutions for aldehydes were prepared with analytical grade PURELAB Ultra Analytic water by injection of 2.9×10^{-5} mol of each aldehyde with Hamilton syringes (Hamilton, Bonaduz, Switzerland) in 50-mL volumetric flasks. Secondary standard solutions were prepared in either 50- or 100-mL volumetric flasks. The derivatization of aldehydes was done by slight modification of a previously reported method. [16] In brief, pH was adjusted to 4 by adding 0.33 g of potassium hydrogen phthalate to 50 mL of the standard or sample solution. 10 mL as sample volume were pipetted into 20-mL headspace screw vials, containing a

magnetic stir bar (VWR International GmbH, Darmstadt, Germany) and closed with rubber-PTFE septa caps (BGB Analytik AG, Böckten, Switzerland). To each vial, 6.6 µL of 2,4,5-trifluoroacetophenone (20 µg mL^{-1}) and 200 µL of PFBHA (9.01 mg mL^{-1}) were added. The samples were then introduced in the water bath and left for 1 h and 45 min at 45ºC. Afterwards, samples were cooled for 10 minutes at room temperature. Finally, two drops of sulphuric acid were added to the derivatized aldehydes mixture.

Alcohols

For the proof-of-concept with Sil. PIL 1, an aqueous stock solution containing each alcohol (2-methyl-1-propanol, 3-methyl-1-butanol, 1-butanol, 1-pentanol, 1-hexanol and 2-propanol) at 1000 mg L^{-1} was prepared. A secondary aqueous stock solution at 0.1 mg L^{-1} was used for the experiments.

For the Sil. PIL 2 analysis as sorbent, an aqueous stock solution containing each alcohol (2-methyl-1-propanol, *tert*-butanol, 3-methyl-1-butanol, 1-pentanol and 1-hexanol) at 1000 mg L^{-1} was prepared.

To determine the linear range, also a secondary aqueous stock solution at 0.1 mg L^{-1} (from the 1000 mg L^{-1} stock solution applied with the Sil. PIL 2) was prepared to measure the concentrations ranging from 0.01 to 5.5 µg L^{-1}. From 10 to 10,000 µg L^{-1} the first stock solution, at 1000 mg L^{-1}, was used for preparation. For determination of the limit of detection a concentration range from 0.25 to 550 µg L^{-1} was prepared. For concentrations lower than 10 µg L^{-1} the secondary stock solution was applied and for concentrations larger than 10 µg L^{-1} the first stock solution was used. For recovery determination, a procedure reported in literature was followed. [17] 10 g of beer were weighed in a 100-mL volumetric flask, water from the water purification system was added, then the spike was added to reach a concentration of 321 µg L^{-1} and finally the remaining water was filled to the mark.

10 mL were used as sample volume in amber 20-mL headspace screw cap vials, containing a magnetic stir bar (VWR International GmbH, Darmstadt, Germany) and closed with rubber-PTFE septa caps (BGB Analytik AG, Böckten, Switzerland).

The stock solutions were prepared every 2-3 months and stored at 4 °C. The samples were prepared daily.

5.1.3 GC/MS instrument parameters and injection

All measurements were performed with a Trace GC 2000 (Thermo, Milan, Italy) coupled to a Polaris Q ion trap mass spectrometer (Finnigan, Bremen, Germany). The GC was equipped with a PAL COMBI-xt autosampler (Axel Semrau, Sprockhövel, Germany) and a split/splitless (S/SL) injector. It was also equipped with a TrayCooler for 20-mL headspace vials and single magnet mixer (SSM; Chromtech, Idstein, Germany). The ITEX option for the PAL COMBI-xt was obtained from CTC Analytics (Zwingen, Switerzerland), which consists of a heated syringe holder, a 1.3 mL gas tight Hamilton syringe with side port (Hamilton, Bonaduz, Switzerland) and a trap heater around the ITEX needle.

For the derivatized aldehydes a Varian VF-5ms column (60 m × 0.25 mm × 0.25 μm) from Agilent (Agilent, Waldbronn, Germany) was used for separation.

The S/SL injector was set to 250 °C and operated in splitless mode. 500 μL of helium were aspirated as desorption gas and injected at 50 μL s^{-1} for analysis. After the transfer time, the split was opened at 10 mL min^{-1}. Helium was used as carrier gas and a constant flow of 1 mL min^{-1} (Air Liquide, Oberhausen, Germany) was maintained. The initial GC oven temperature was 50 °C for 1 min, continued by a 4 °C min^{-1} ramp to 220 °C. Finally, a 20 °C min^{-1} ramp was set to reach 250 °C and held for 10 min.

The temperature of the MS ion source and transfer line were 200 and 300 °C, respectively. The mass spectrometer was set to electron ionization (EI), in full scan mode (*m/z* range from 55 to 355) with 0.39 scans per second.

For the alcohols, a Stabilwax-DA column (60 m × 0.32 mm × 1 μm) from Restek (Restek GmbH, Bad Homburg, Germany) was used for separation.

The S/SL injector was set to 250 °C and operated in splitless mode. 250 μL of helium were aspirated as desorption gas and injected at 50 μL s^{-1} for analysis. After the transfer time, the split was opened at 10 mL min^{-1}. Helium was used as carrier gas and a constant flow of 1.5 mL min^{-1} (Air Liquide, Oberhausen, Germany) was maintained. The initial GC oven temperature was 38 °C for 5 min, continued by a 5 °C min^{-1} ramp to 110 °C, held for 2 min. Finally, a 10 °C min^{-1} ramp was set to reach 200 °C and held for 10 min.

The temperature of the MS ion source and transfer line were 200 and 250 °C, respectively. The mass spectrometer was set to electron ionization (EI), in full scan mode (*m/z* range from 30 to 200) with 0.31 scans per second.

Data were processed via the Xcalibur software (Thermo, Bremen, Germany).

5.1.4 ITEX

5.1.4.1 Sorbent

5.1.4.1.1 Sil. PIL 1 synthesis

In a typical process, 2-acrylamido-2-methylpropane sulphonic acid (AMPS) was neutralized by 1-vinylimidazole by dissolving it in water at room temperature. Evaporation of the water gave a yellowish transparent viscous liquid with high yield and purity. The IL monomers (1) were then polymerized from initiator grafted silica surface. This process can be broken down in two steps (Figure 5-3): (i) immobilization of surface initiator on silica particles and (ii) radical transfer polymerization reaction from initiator-grafted silica. The reaction between the surface-accessible OH groups of silica and the anchoring group of the initiator (-Si $(OCH_3)_3$) resulted in the formation of a chemical bond between the silica surface and initiator, 3-mercaptopropyl trimethoxysilane (MPS) to form (2). Surface initiated polymerization was carried out by using (2) as a macroinitiator suspended in the mixture of monomer (1) in toluene and azobisisobutyronitrile (AIBN) as free radical initiator. After the polymerization process, the resulting material is Sil. PIL 1. The Sil. PIL is initially washed and purified with toluene/chloroform followed by methanol and successive washing with warm water. A final washing with methanol and diethyl ether proceeds, to conclude with a drying step under vacuum conditions. Further details of the synthesis method are found in the literature. [15]

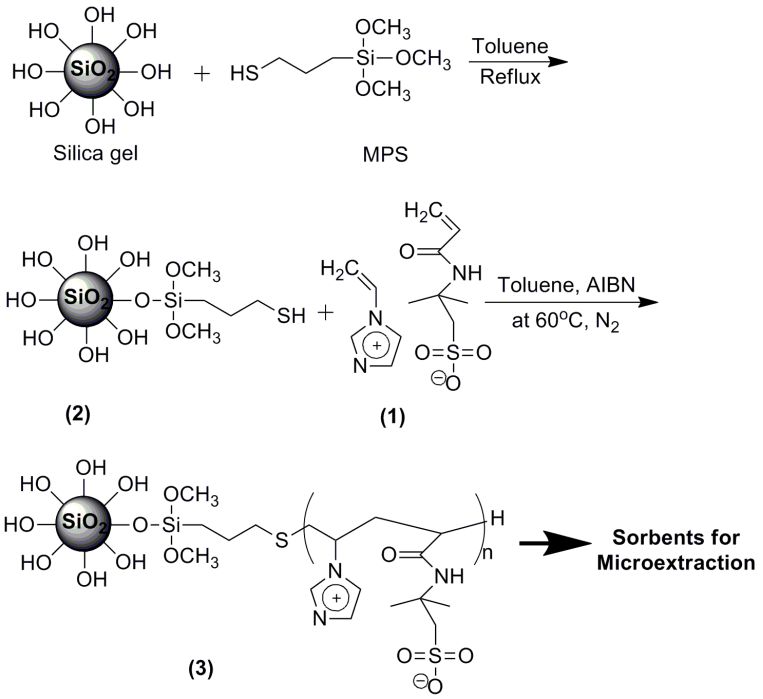

Figure 5-3. Grafting of cationic and anionic monomers from silica core which was previously modified by radical transfer agent (MPS). (1) = Monomeric IL consisting of VIm-AMPS. (2) = MPS modified silica. (3) = Sil. PIL 1 copolymerized functionalized silica. [15]

5.1.4.1.2 Sil. PIL 2 synthesis

6.0 g of silica gel with 3.0 g of 3-mercaptopropyl trimethoxysilane (MPS) were dispersed in 30 mL of toluene and refluxed for 36 hr. The suspension was filtered and the solid was washed with toluene, methanol, water, methanol and diethyl ether successively. N-vinylimidazolium Br monomer ([C_{10}VIm]Br) was modified via anion exchange to be *p*-styrenesulphonate. At last, [C_{10}VIm] SS was grafted onto Silica-MPS through a surface radical chain-transfer reaction. Silica-MPS (2.8 g) was added to a three-neck round-bottomed container. [C_{18}VIm]Br (5.0 g) was mixed with excess sodium *p*-styrenesulphonate (2.5 g) in 50 ml of water. 2.0 g of [C_{10}VIm] SS dissolved in chloroform and 1% of azobisisobutyronitrile (AIBN) was added into the container. The mixture was stirred in nitrogen atmosphere at 60 °C for 30 h. The precipitates were filtered and washed with chloroform, methanol, and diethyl ether. After being dried under vacuum, Sil. PIL 2 was used as sorbent in ITEX. Figure 5-4 depicts the PIL applied as sorbent in this study:

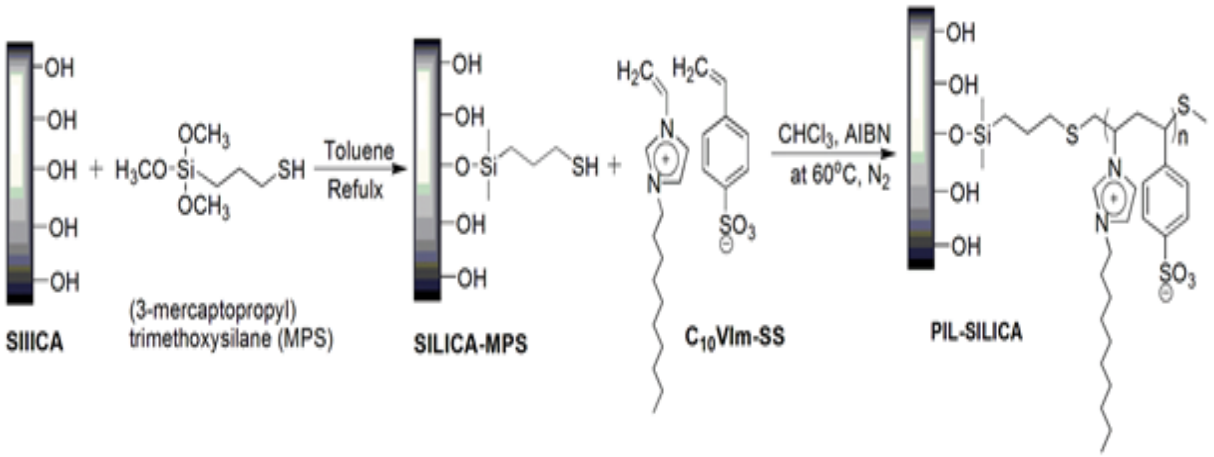

Figure 5-4. Synthesis step and Sil. PIL 2 end product.
1-vinylimidazolium as cation, attached a C_{10} alkyl chain and *p*-styrenesulphonate as anion. [18]

5.1.4.1.3 Sorbent characterization for Sil. PIL 1 and Sil. PIL 2

X-ray photo-electron spectroscopy measurements (XPS) were conducted on a PHI VersaProbe II (Physical Electronics GmbH, Ismaning, Germany), using monochromatic Al K_α light at 1486.6 eV, an emission angle of 45 ° and at room temperature to determine the percentage of the elements found at the surface.

5.1.4.2 Packing

A N 820.3 FT.40.18 vacuum pump (KNF Neuberger GmbH, Freiburg, Germany) was connected with a rubber tubing (6 mm i.d.) to an adapter where the ITEX needle was inserted for packing. The adapter consists of a stainless steel tube fitting, union ½ ” o.d. (Swagelok). One nut contained an 11 mm septa (Auto-Sep 11 from SGE), to position the ITEX needle for packing. To the other nut, a 2 cm stainless steel tube (3 mm i.d. and 6 mm o.d.) covered with PTFE thread seal tape, was attached to fit the hose and ensure vacuum during the packing procedure. This part is fixed in a 45 ° stainlees steel plaque. On the right side of Figure 5-4, the described adapter is depicted.

Stainless steel frits, 4.6 mm, 2 µm, PEEK-encased 0.25 x 0.062 ” thick (VICI Jour, Switzerland), were laser cut to fit the inner diameter of the ITEX syringe. Only the stainless steel section was used.

After inserting the frit, 1 cm of glass wool was added. With the help of an Allen wrench (with a nominal size of 1 and 2.53 ” as length of the long arm), the glass wool was compressed. Afterwards, 3 cm (± 0.2 cm) of the ITEX body were packed with PIL. The body of the

syringe had to be taped while it was filled. To ensure the length of the packed column, the Allen wrench was inserted before and after filling the PIL into the ITEX. The pump was turned off and the ITEX needle removed from the adapter. 1 cm of glass wool were added at the top, compressed again with the Allen wrench and a stainless steel "v" shaped piece was inserted to fix the material. Finally, the pump was turned on, the ITEX needle plugged in and the pump was left on for another minute on. The left side of Figure 5-5 provides a scheme of the packed ITEX needle. The specifications of the packing procedure are explained in Figure S.I.C5-1 of the Supplementary Information.

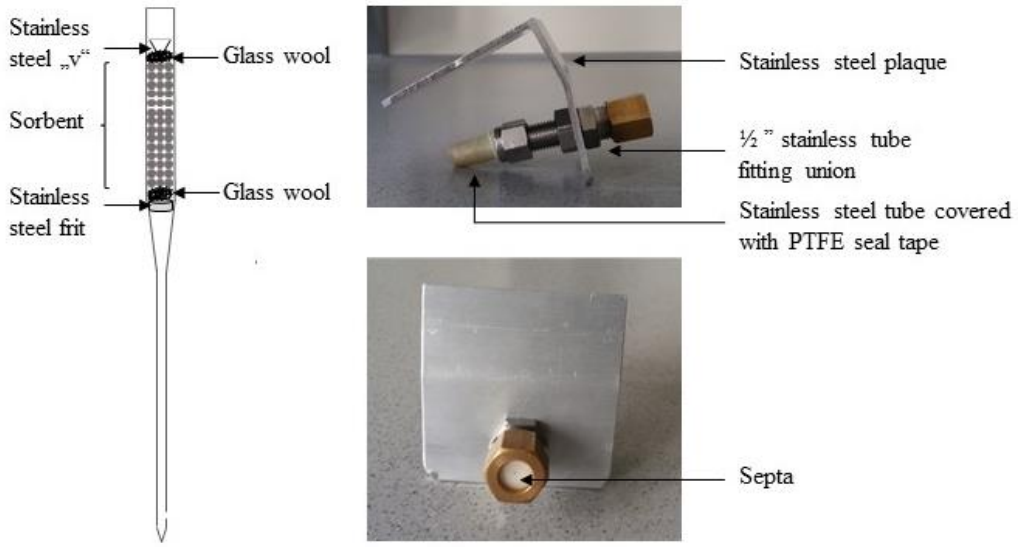

Figure 5-5. Left: Scheme of ITEX packing content for Sil. PIL 1 and Sil. PIL 2 as sorbent. Right: Description of the adapter used during the packing procedure with ITEX needles.

5.1.5 Extraction parameters

For the derivatized aldehydes, after placing the samples on the TrayCooler, the vials were transported to the SMM, where they were heated at 80 °C and stirred at 500 rpm for 10 min. 50 strokes at 100 µL s^{-1} were applied for extraction. Following the extraction, 500 µL of helium were aspirated as desorption gas from the S/SL. Thermal desorption, 150 °C for Sil. PIL 1 and 250 °C for PDMS, was performed at the S/SL injector with 50 µL s^{-1} as desorption flow. To avoid carry-over, the trap was flushed with nitrogen for 15 min. heated at 180 °C for Sil. PIL 1 and at 300 °C for PDMS.

For the experiments with the short chain alcohols, with Sil. PIL 1, Sil. PIL 2 and Tenax GR as sorbent, after the samples were placed on the TrayCooler, the vials were transported to the SMM, where they were heated at 70 °C and stirred at 500 rpm for 15 min. 60 strokes at 100 µL s^{-1} were applied for extraction. Following the extraction, 250 µL of helium were aspirated

as desorption gas from the S/SL. Thermal desorption at 150 °C was performed at the S/SL injector with 50 µL s^{-1} as desorption flow. To avoid carry-over, the trap was flushed with nitrogen for 15 min and heated at 180 °C.

The ITEX procedure was controlled by manufacturer supplied macros, customized in the PAL Cycle Composer (CTC Analytics, Zwingen, Switzerland).

Results and Discussion

5.1.6 Sorbent characterization and application in ITEX

XPS measurements were performed to determine whether the grafting onto the silica gel was successfully performed. The statement was confirmed by comparing silica to the end product (Sil. PIL 1 and Sil. PIL 2). In contrast to bare silica, where carbon and oxygen are only present, the end products should also contain nitrogen and sulphur. This is due to the type of cation and anion used for their synthesis. The peak positions, in terms of binding energy, provide information about the chemical state and type of element. [19] See Figures S.I.C5-2 and S.I.C5-4 of the Supplementary Information for the XPS spectra of silica, Sil. PIL 1 and Sil. PIL 2, respectively.

In order to quantify the peak area at the corresponding binding energy (amount of material present), relative sensitivity factors are applied. [19] Table 5-1 presents the results of the elements of interest for silica, Sil. PIL 1 and Sil. PIL 2:

Table 5-1. Element amount comparison of silica and two self-made PIL (Sil. PIL1 and sil. PIL 2) via XPS measurements.

	Cation (%)		Anion (%)		Other elements (%)		
	Azide[20]	Amide	Sulphone	Sulphide/ Thiol	O	Si	C
Silica	-	-	-		62.36	30.34	5.65
Sil. PIL 1	2.76	2.99	3.45	2.24	33.49	16.99	18.43
Sil. PIL 2	5.45	0.48	4.89	0.34	7.46	1.75	52.26

The grafting of the ionic liquids was successfully performed, as can be seen from the XPS data in Table 5-1 where no nitrogen nor sulphur is present in the bare silica, while both PIL (Sil. PIL 1 and Sil. PIL 2) do.

Sil. PIL 1 should have a larger amount of amide groups than Sil. PIL 2 (Figures 5-2 and 5-3), also confirmed by the XPS measurements.

In ITEX a thermo- resistant and stable sorbent is of advantage, due to the thermodesorption procedure applied in this technique. For Sil. PIL 1, the temperature reported where

degradation could start was 225 °C (determined via a thermogravimetric analysis, the experimental details are explained in the literature [15]), so potentially the thermal desorption could be applied at 220 °C. Reported in the literature, an increase in the branching on the alkyl chain at the cation increases the melting point. [4] From the C percentage in Table 5-1. and the structure on Figures 5-3 and 5-4, it would be assumed that Sil. PIL 2 is more thermostable than Sil. PIL 1. By this, Sil. PIL 2 represents a more suitable sorbent to be applied in ITEX.

Preliminary tests with Sil. PIL 1 as sorbent, with a thermodesorption temperature of 200 °C, were run to check the material. After measuring 44 samples, an unexpected material degradation was observed. Figure 5-6 presents the damaged sorbent material, as well as the contaminated GC-liner:

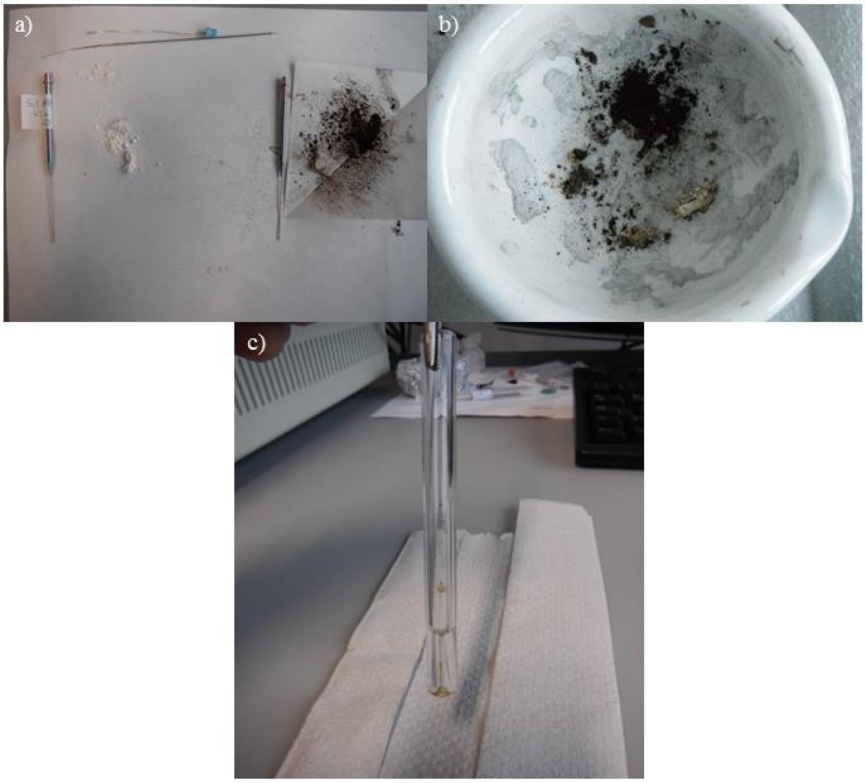

Figure 5-6. Sil. PIL 1 degradation after applying 200 °C as desorption temperature.
On the left from panel a) pristine Sil. PIL 1, no damages. On the right side panel from a) damaged Sil. PIL 1. b) Extracted Sil. PIL 1 from the ITEX needle, after its application at 200 °C. In clockwise direction, at five o´clock some undamaged Sil. PIL 1 material, at six o´clock until twelve o´clock the colorization and increased degradation are found. c) Affected GC-liner due to material loss.

Black powder was found on the parts of the autosampler too. The chromatograms were revised and a peak at a *m/z* equal to 94, corresponding to vynilimidazole, was detected.

In order to be cautious and avoid further equipment damages a larger particle size (> 3 µm) for Sil. PIL 2 was synthesized. As well as the thermodesorption and cleaning temperatures were set lower than 200 °C to protect the instruments (150 °C for thermodesorption and 180 °C for the trap cleaning) from further disturbances. The vynilimidazole peak was also monitored along the sample runs.

5.1.7 Proof-of-concept with Sil. PIl 1

In order to demonstrate the high potential of Sil-PIL.1 as a sorbent material in microextraction techniques, low molecular weight aldehydes (C_1-C_{10}) and short chain alcohols (C_3-C_6) were used as probe compounds. The evaluation of new sorbent materials for microextraction requires information on both kinetic and thermodynamic aspects of phase partitioning of probe compounds. For the former, extraction profiles are good indicators of the performance of the sorbent. To that end, the extraction profiles of Sil. PIL 1 (at 150°C desorption temperature) and PDMS (at 250°C desorption temperature) were generated for the derivatized low molecular weight aldehydes (C_1-C_{10}) at a concentration of 2.34 µmol L^{-1}. The peak area is plotted against the extraction strokes and the equilibrium is reached when a plateau is observed. [9] Concerning the proper number of strokes for extraction, 50 strokes are suitable for both materials, because near-equilibrium partitioning for all the derivatized aldehydes was achieved.

An example for the derivatized formaldehyde and *n*-Decanal are shown in Figure 5-7.

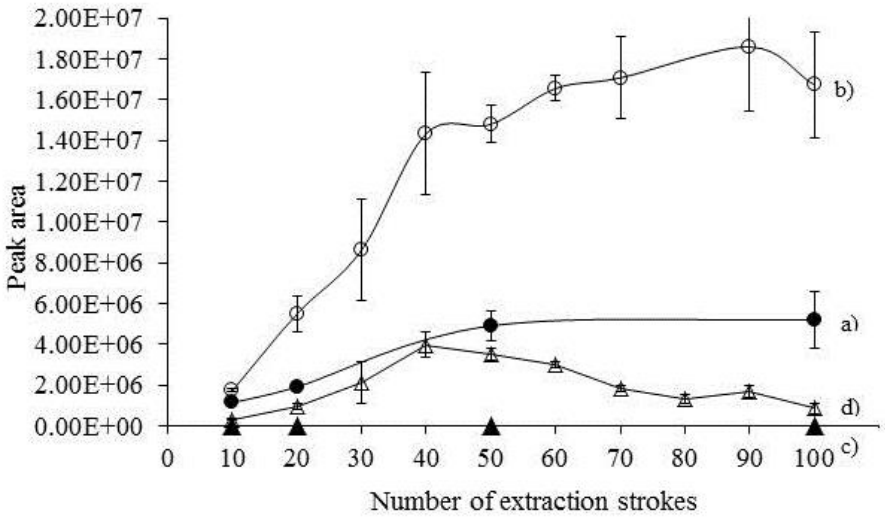

Figure 5-7. Extraction profiles of derivatized aldehydes at a concentration of 2.34 µmol L^{-1}. a) formaldehyde, c) *n*-Decanal for PDMS sorbent (desorption temperature: 250°C), b) formaldehyde, d) *n*-Decanal for Sil. PIL 1 as sorbent material (desorption temperature: 150°C).

Sil. PIL 1 showed a higher extraction efficiency than PDMS. The chromatogram of the separated aldehyde derivatives with the same y-axis scale for both materials is presented in Figure 5-8.

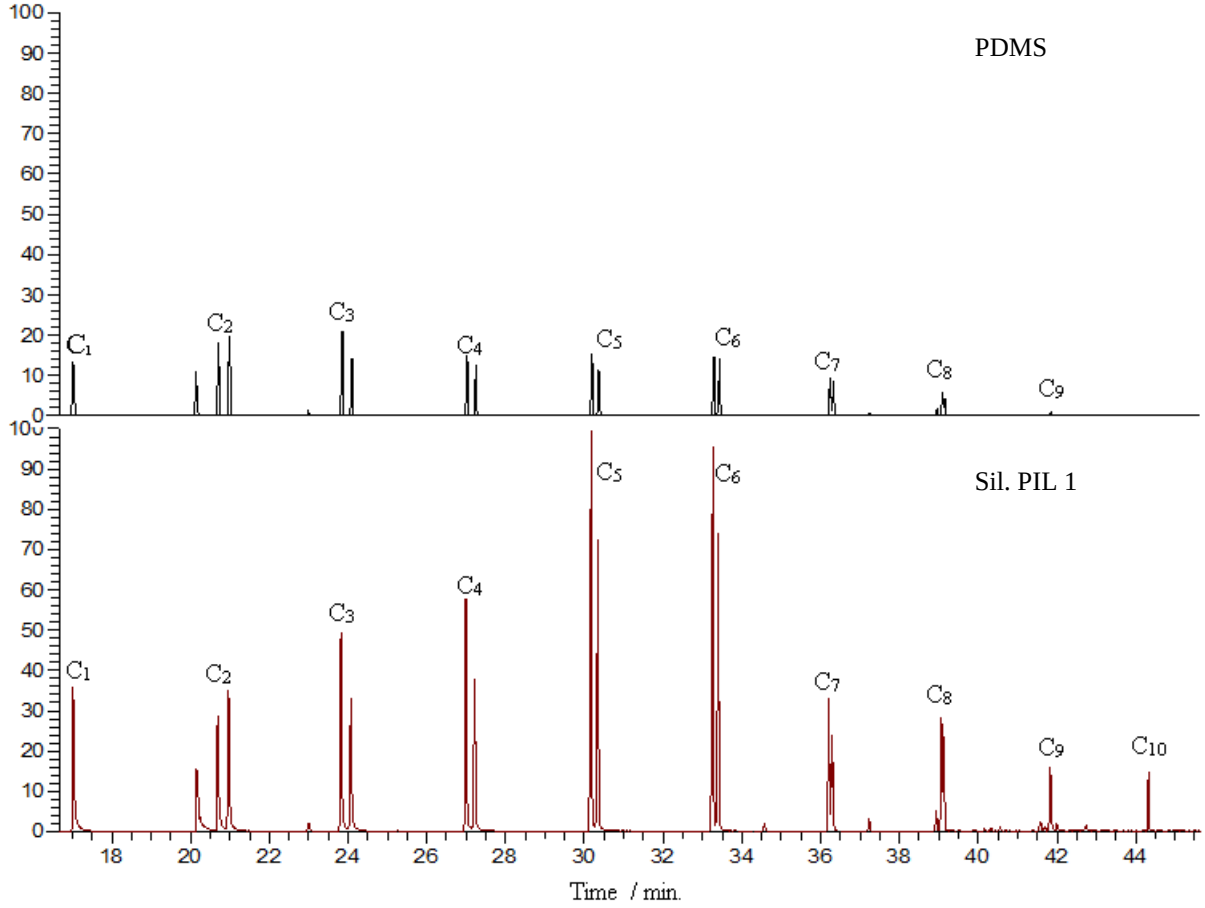

Figure 5-8. Chromatograms of derivatized aldehydes.
Normalized at max. intensity 1.13×10^{7}, concentration = 2.34 µmol L^{-1}, mass trace *m/z* = 181. Top: PDMS as sorbent material, 250°C as desorption temperature. Bottom: Sil. PIL.1 as sorbent material, 150°C as desorption temperature.

Sil. PIL 1 apparently yielded significantly larger peak areas than PDMS that had previously been found to be the most efficient commercial sorbent (data not shown). A quantitative comparison of both materials at optimum number of extraction strokes showed that the extraction efficiencies for derivatized aldehydes indicated by peak areas of the Sil. PIL 1 sorbent material were up to 200 times higher than of commercial PDMS (as shown in Table 5-2), which revealed its very promising preconcentration performance for the analyzed probe compounds.

In addition to the extraction performance of Sil. PIL 1 with derivatized aldehydes, also several short chained aliphatic alcohols, shown in Figure 5-9 were measured. The results were compared with Tenax GR and an improvement as with derivatized aldehydes was not observed.

Table 5-2. Increase of the extraction yield for Sil. PIL 1:PDMS with PFBHA derivatized aldehydes (C_1-C_{10}). Given as ratio of peak areas obtained by Sil. PIL 1 and PDMS.

Derivatized aldehyde	Peak area ratio (Sil. PIL 1: PDMS)
Formaldehyde	3.0
Acetaldehyde	2.3
n-Propanal	2.8
n-Butanal	3.5
n-Pentanal	5.9
n-Hexanal	5.3
n-Heptanal	3.2
n-Octanal	4.9
n-Nonanal	17
n-Decanal	230

Sil. PIL 2 was also investigated with the same short chain alcohols as with Sil. PIL 1 and the material yielded promising results, Figure 5-10. Thus, it was decided to perform a method validation with Sil. PIL 2 as sorbent and compare its analytical performance with the literature.

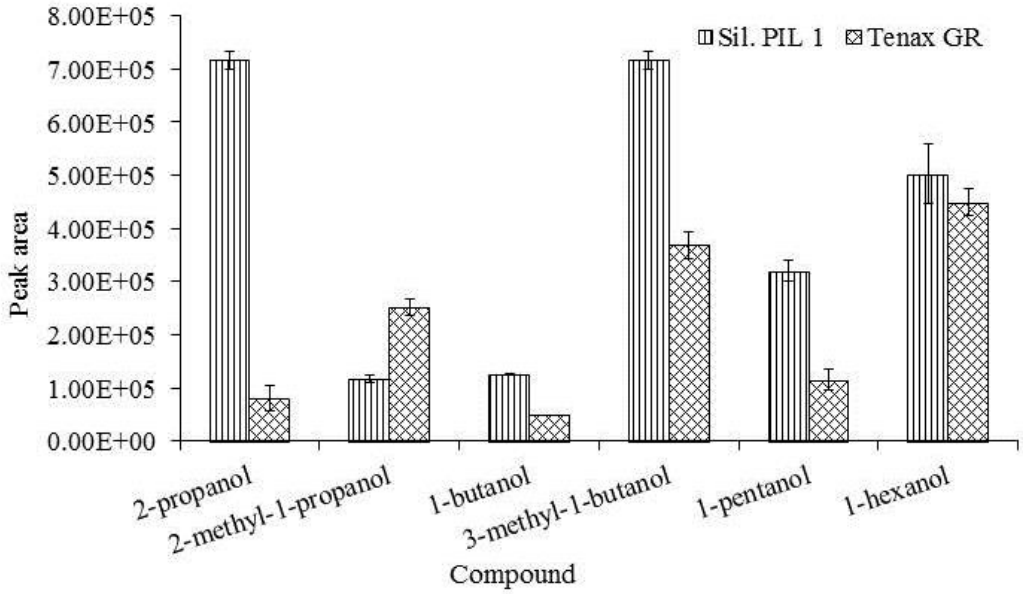

Figure 5-9. Extraction yield comparison between Sil. PIL 1 and Tenax GR for short chained aliphatic alcohols, concentration = 0.1 mg L^{-1} and 150 °C as desorption temperature.

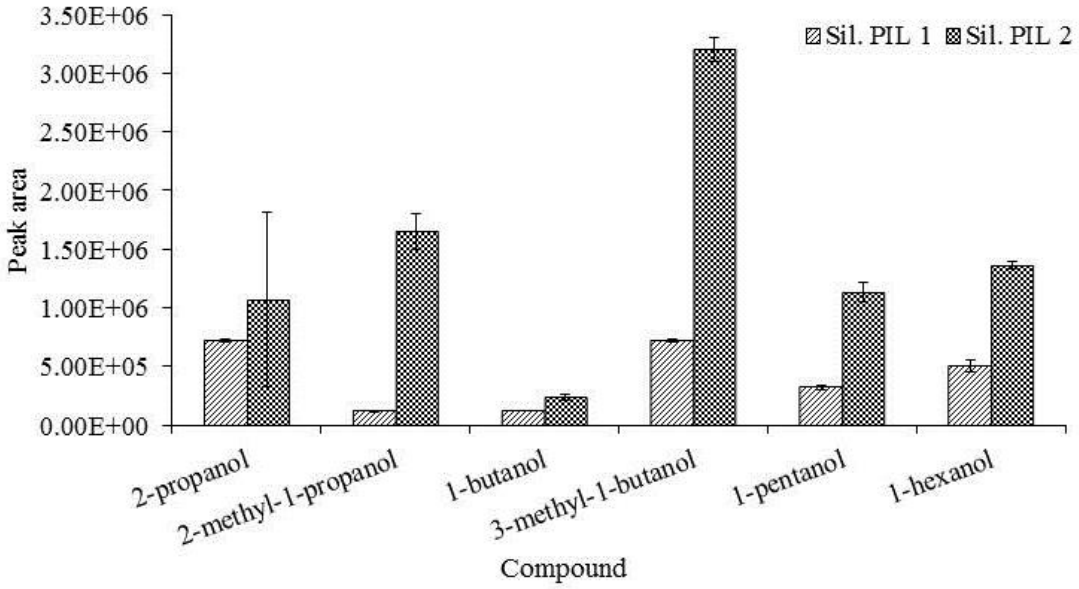

Figure 5-10. Extraction yield comparison between Sil. PIL 1 and Sil. PIL 2 for short chained aliphatic alcohols, concentration = 0.1 mg L^{-1} and 150 °C as desorption temperature.

5.1.8 Extraction parameter optimization ad figures of merit with Sil. PIL 2

In this study, the extraction temperature (during sample conditioning) was taken from the literature, because (to some extent) the same type of analytes where used. [17] The number of strokes, was similar to the ones reported in the literature. [17] 60 strokes instead of 65 where applied, since with 60 strokes the equilibrium was already established and the application of further strokes is not necessary. The extraction flow emulates the one from the source at 100 µL s^{-1}. [17] As mentioned in section 3.1, the application of high thermodesoprtion temperatures, damaged the Sil. PIL as well as the instruments. For this reason it was decided to set a lower desorption temperature, 150 °C. Finally the cleaning procedure, was performed at 180 °C. The thermodesorption and cleaning temperature were set lower than for commercial materials, [10] [21] [22] due to the previous facts mentioned

For method validation, the linear range, method detection limit (MDL), precision and recovery were determined. The linear range consisted on a 10 point calibration, each level measured in triplicate. To identify the linear range a change in the calibration slope arises and to this end the limits of the range, Figure 5-11 depicts the calibration range for each compound. On Tables S.I.C5-1 and S.I.C5-2 of the Supplementary Information the extraction yield as well as the parameters of the calibration curves are presented.

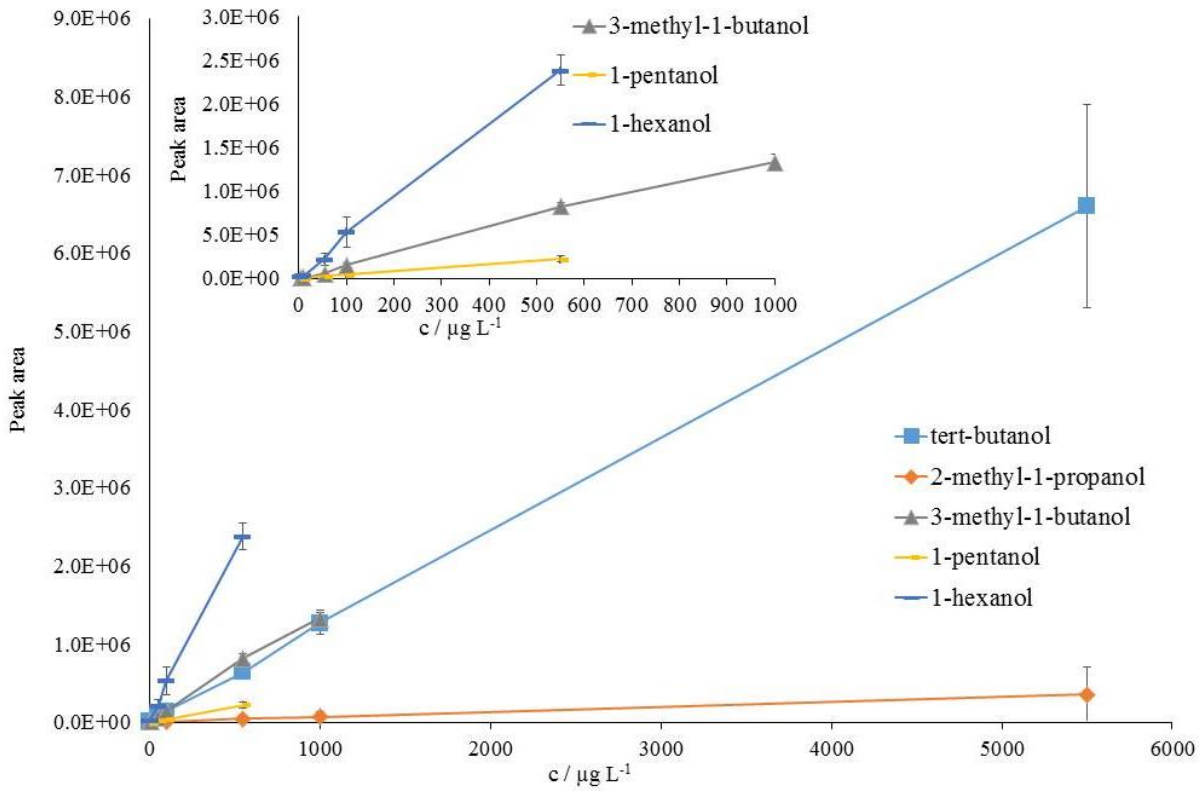

Figure 5-11. Calibration curves in the linear range for all the short chain alcohols applying Sil. PIL 2 as sorbent. For a more clear data presentation, three alcohols (3-methyl-1-butanol, 1-pentanol and 1-hexnaol) are ploted on the top at the left side corner of the graphic.

The precision was calculated as the average of the RSD within the calibration range. [17] The MDL was obtained according to Eq. 1.:

$$MDL = t_{(N-1,1-\alpha=99\%)}\, s_c \qquad \text{Eq.1. [23]}$$

Where *t* is the student's t value for the one-tailed test with a confidence level of 99% and six degrees of freedom multiplied by the standard deviation of seven replicates (s_c) at a concentration that corresponds to an instrument signal to noise (S/N) in the range of 2.5 to 5. In Table 5-3 the figures of merit as well as a literature comparison is presented.

An improved linear range with Sil. PIL 2 in comparison to the commercial materials is shown, enabling the measurement of a broader concentration range. This is of interest, because a larger range of analytes could be measured and during sample preparation, as reported in the literature, the dilution of the real sample could be avoided. [17] For the remaining validation parameters, the commercial materials yielded a better performance than Sil. PIL 2. Though, the results from the literature in Table 5-3 were generated with a cryofocusing unit, which influences the response and higher desorption temperatures were applied.

Table 5-3. Figures of merit comparison for Sil. PIL 2 as sorbent against Tenax TA and PDMS in a HS-ITEX-GC/MS method.

	Sorbent										
	Linear range / µg L^{-1}			MDL / µg L^{-1}			Precision / %			Recovery / %	
Compound	Sil. PIL 2[a)]	Tenax TA [17]	PDMS blue [17]	Sil. PIL 2[a)]	Tenax TA [17]	PDMS blue [17]	Sil. PIL 2[a)]	Tenax TA [17]	PDMS blue [17]	Sil. PIL 2[a)]	PDMS blue [17]
tert-butanol	0.55-5500	0.6−47	2.3−146	0.3	0.3	2.2	16	8.9	4.5		104.5
2-methyl-1-propanol	100-5500	3.2−241	50.1−3208	15.1	1.6	13	17	9.7	8.8	6	105.8
3-methyl-1-butanol	5.5 - 1000	0.3−24	6.3−3236	4.8	0.1	3	26	7.4	4.2	45	110.4
1-pentanol	5.5-550	0.2−81	6.4−204	0.8	0.2	1.4	23	7.1	7.6		100
1-hexanol	5.5-550	0.2−16.3	1.6−1627	0.8	0.08	1.1	31	6.9	3.5	0.1	117.3

a) n = 3. All MDL were estimated according to Eq.1.

Conclusions

A self-made PIL was synthesized and applied for the first time as sorbent in ITEX. The versatility of ITEX was proven, because several types of sorbents can be packed and material loss can be simply solved by inserting a frit.

PIL seems a promising sorbent material in ITEX, but further improvement for the PIL as sorbent, is needed. A more thermostable material and more hydrophobic feature, could help to reach a similar analytical performance as with the commercial materials.

Furthermore, once the PIL has been improved, it would be appealing to perform the measurements applying a cryofocusing unit and determine whether PIL gained an enhanced.

Acknowledgement

We would like to thank Prof. Mohammed M. Rahman for the synthesis of both PIL (Sil. PIL 1 and Sil. PIL 2) and Dr. Ulrich Hagemann for performing the XPS measurements.

Nomenclature

S_c Standard deviation

t Student’s t value

References

1. Yuan, J. and M. Antonietti, *Poly(ionic liquid)s: polymers expanding classical property profiles.* Polymer, 2011. **52**(7): p. 1469-1482.

2. Yuan, J. and M. Antonietti, *Poly(ionic liquid) latexes prepared by dispersion polymerization of ionic liquid monomers.* Macromolecules, 2011. **44**(4): p. 744-750.

3. Ghandi, K., *A review of ionic liquids, their limits and applications.* GSC, 2014. **4**(1): p. 44-53.

4. Keskin, S., et al., *A review of ionic liquids towards supercritical fluid applications.* J. Supercrit. Fluid 2007. **43**(1): p. 150-180.

5. Lu, J., F. Yan, and J. Texter, *Advanced applications of ionic liquids in polymer science.* Prog. Polym. Sci. , 2009. **34**(5): p. 431-448.

6. Yuan, J., D. Mecerreyes, and M. Antonietti, *Poly(ionic liquid)s: an update.* Prog. Polym. Sci., 2013. **38**(7): p. 1009-1036.

7. Mecerreyes, D., *Polymeric ionic liquids: broadening the properties and applications of polyelectrolytes.* Prog. Polym. Sci., 2011. **36**(12): p. 1629-1648.

8. Panniello, A., et al., *Nanocomposites based on luminescent colloidal nanocrystals and polymeric ionic liquids towards optoelectronic applications.* Materials, 2014. **7**(1): p. 591.

9. Jochmann, M.A., et al., *In-tube extraction for enrichment of volatile organic hydrocarbons from aqueous samples.* J. Chromatogr. A, 2008. **1179**(2): p. 96-105.

10. Laaks, J., et al., *In-tube extraction of volatile organic compounds from aqueous samples: an economical alternative to purge and trap enrichment.* Anal. Chem., 2010. **82**(18): p. 7641-7648.

11. Pang, L. and J.F. Liu, *Development of a solid-phase microextraction fiber by chemical binding of polymeric ionic liquid on a silica coated stainless steel wire.* J. Chromatogr. A, 2012. **1230**(23 March 2012): p. 8-14.

12. Feng, J., et al., *A novel aromatically functional polymeric ionic liquid as sorbent material for solid-phase microextraction.* J. Chromatogr. A, 2012. **1227**(2 March 2012): p. 54-59.

13. Feng, J., et al., *Preparation of a polymeric ionic liquid-coated solid-phase microextraction fiber by surface radical chain-transfer polymerization with stainless steel wire as support.* J. Chromatogr. A, 2011. **1218**(43): p. 7758-7764.

14. Ho, T.D., et al., *Selective extraction of genotoxic impurities and structurally alerting compounds using polymeric ionic liquid sorbent coatings in solid-phase microextraction: alkyl halides and aromatics.* J. Chromatogr. A, 2012. **1240**(1 June 2012): p. 29-44.

15. Rahman, M.M., et al., *Core-shell hybrid particles by alternating copolymerization of ionic liquid monomers from silica as sorbent for solid phase microextraction.* Macromol. Mater. Eng., 2015. **300**(11): p. 1049-1056.

16. Cancho, B., F. Ventura, and M.T. Galceran, *Determination of aldehydes in drinking water using pentafluorobenzylhydroxylamine derivatization and solid-phase microextraction.* J. Chromatogr. A, 2002. **943**(1): p. 1-13.

17. Laaks, J., et al., *In-tube extraction-GC-MS as a high-capacity enrichment technique for the analysis of alcoholic beverages.* J. Agric. Food Chem., 2014. **62**(14): p. 3081-3091.

18. Rahman, M.M., *Personal communication*. 2013.

19. XPS, C., *XPS spectra*. 2012. p. 77.

20. Zorn, G., et al., *X-ray photoelectron spectroscopy investigation of the nitrogen species in photoactive perfluorophenylazide-modified surfaces.* J. Phys. Chem. C Nanomater. Interfaces, 2014. **118**(1): p. 376-383.

21. David, F. and C. Devos, *Analysis of volatile organic compounds in beer using ITEX headspace sampling.* CTC Analytics. **ITEX Application Note #04**.

22. Rasanen, I., et al., *Headspace in-tube extraction gas chromatography– mass spectrometry for the analysis of hydroxylic methyl-derivatized and volatile organic compounds in blood and urine.* J. Anal. Toxicol., 2010. **34**(3): p. 113-121.

23. Glaser, J.A., et al., *Trace analyses for wastewaters.* Environ. Sci. Technol., 1981. **15**(12): p. 1426-1435.

C5 Supplementary Information

Figure S.I.C5-1 Materials and ITEX packing procedure.

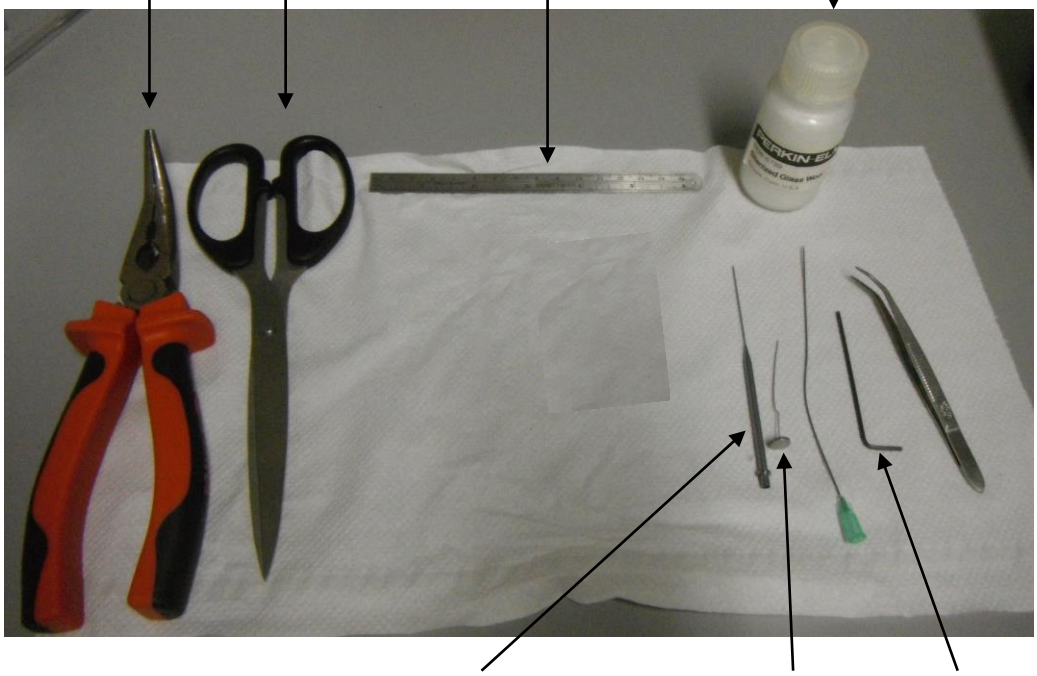

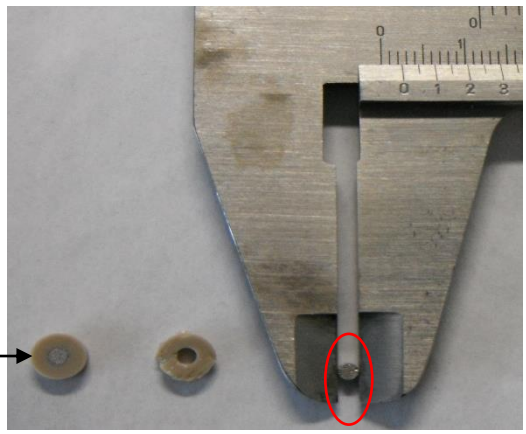

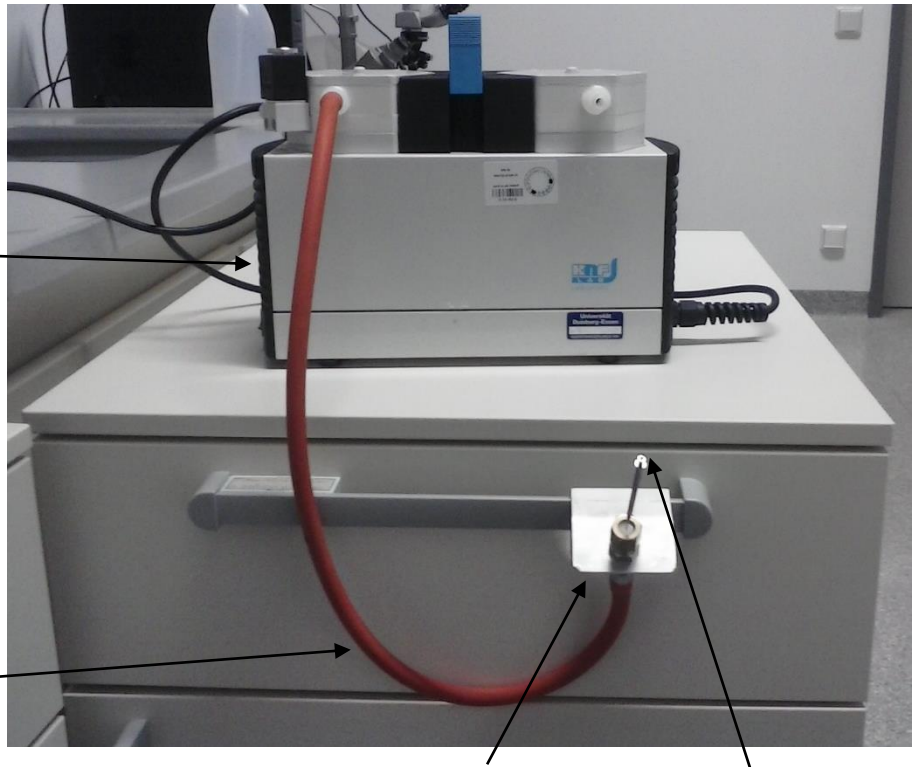

1) Gather material.
2) Insert the frit in the ITEX needle.
3) Insert 1 cm of glass wool and compress it with the Allen wrench.
4) With weigh paper form a funnel to fit into the top of the ITEX needle.
5) Attach the ITEX needle to the pump.
6) Measure with the Allen wrench the depth (approx. 5 cm) and write it down. In the end 3 cm should be packed, thus the depth of the Allen wrench (once finished) should be 2 cm.
7) Turn the pump on.
8) Check that vacuum is generated.
9) Attach the ITEX needle.
10) With the spatula pour the material through the funnel into the ITEX needle.
11) Tap the stainless steel body of the ITEX to have an homogeneous packing.
12) Insert the Allen wrench carfully to compact the material.
13) Fill in more material and repeat steps 12 and 13 until 3 cm (± 0.2 cm) are packed.
14) Turn the vacuum pump off.
15) Remove the ITEX needle of the adapter.
16) Cut with the tweezers two “v” shaped pieces.
17) Insert 1 cm of glass wool.
18) Compact it with the Allen wrench.
19) Insert one “v” piece to fix the material. Carefully, otherwise the piece may act as a spring and might be easyly lost. If that is the case, then insert the other one.
20) Insert the packed ITEX needle to the pump.
21) Turn it on and let it run for one minute.

Figure S.I.C5-2 XPS silica spectra.

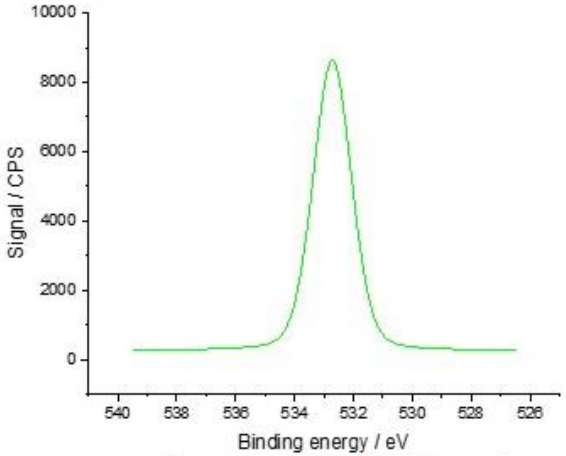

Source energy: 1486.6 eV					
	Name	Position	FWHM	Area	LS
		eV		CPS eV	
	O 1s	532.72	1.52	14908.	SGL(20)

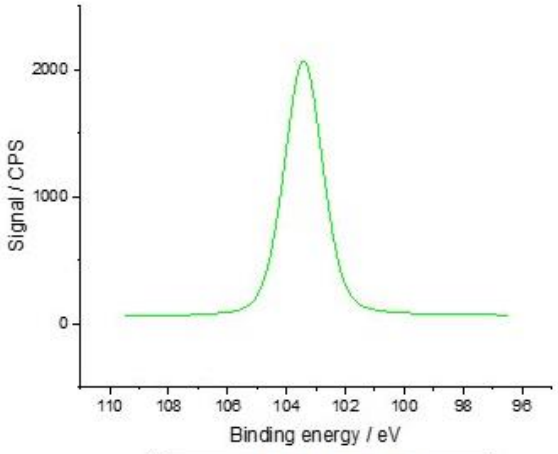

Source energy: 1486.6 eV					
	Name	Position	FWHM	Area	LS
		eV		CPS eV	
	Si 2p	103.42	1.52	3641.1	SGL(25)

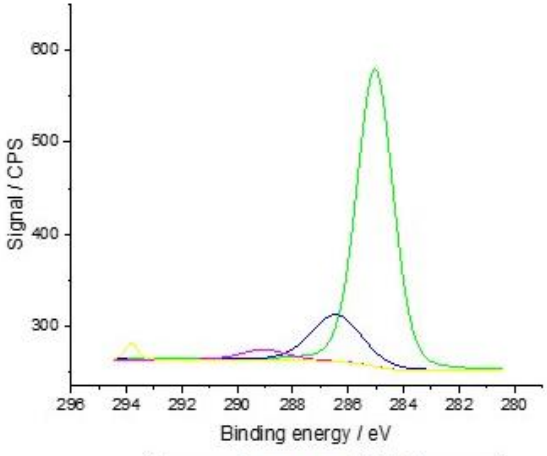

Source energy: 1486.6 eV					
	Name	Position	FWHM	Area	LS
		eV		CPS eV	
	C 1s	285.03	1.53	578.56	SGL(20)
	C O	286.43	2.15	130.62	SGL(25)
	C =O	287.93	2.2	0	SGL(25)
	C OOH	289.03	1.98	27.31	SGL(25)
	PiPi*	293.82	0.51	10.82	SGL(25)

Figure S.I.C5-3 XPS Sil. PIL 1 spectra.

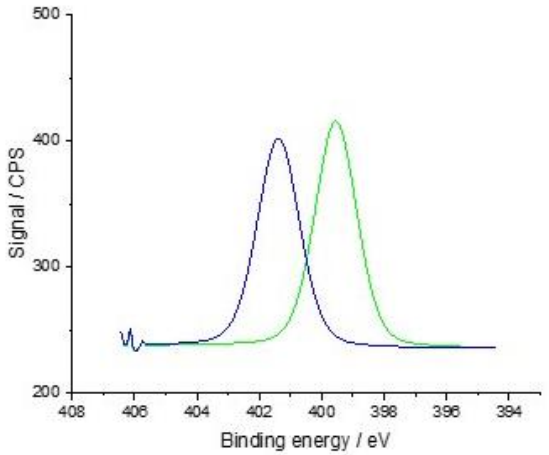

	Source energy: 1486.6 eV				
	Name	Position	FWHM	Area	LS
		eV		CPS eV	
	Amide	399.55	1.58	340.11	SGL(25)
	N 1s	401.39	1.59	313.64	SGL(25)

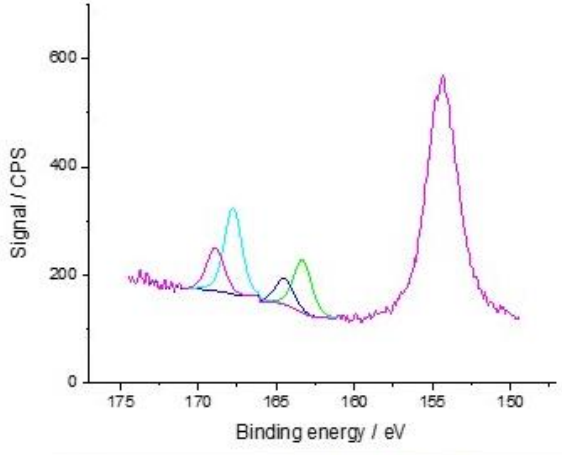

	Source energy: 1486.6 eV				
	Name	Position	FWHM	Area	LS
		eV		CPS eV	
	Sulfide / Thiol	163.32	1.37	160.23	SGL(25)
	Sulfide / Thiol	164.48	1.37	80.11	SGL(25)
	Sulphone 3/2	167.77	1.31	251.23	SGL(25)
	Sulphone 1/2	168.9	1.31	125.62	SGL(25)

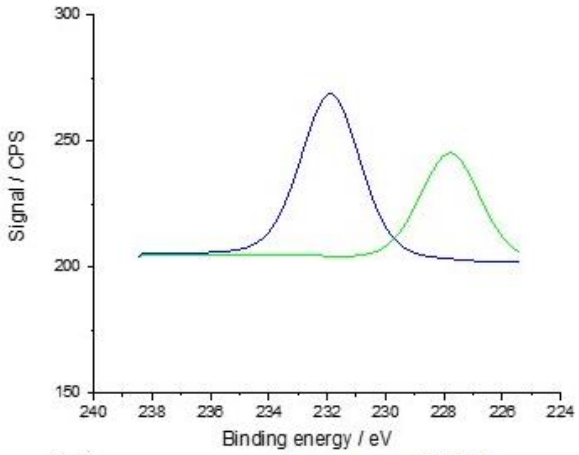

	Source energy: 1486.6 eV				
	Name	Position	FWHM	Area	LS
		eV		CPS eV	
	Sulfide / Thiol	227.78	2.42	125.03	SGL(25)
	Sulphone	231.88	2.39	185.99	SGL(25)

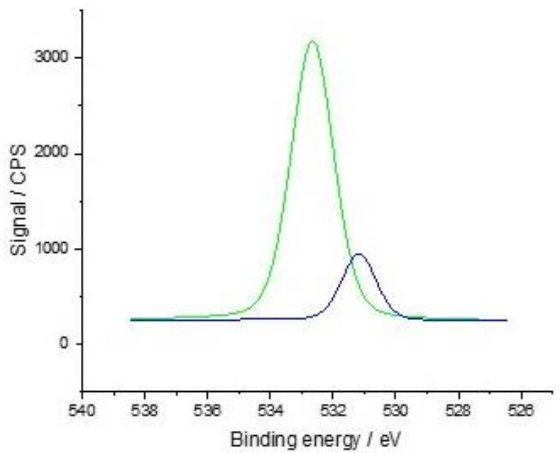

	Source energy: 1486.6 eV				
	Name	Position	FWHM	Area	LS
		eV		CPS eV	
	O 1s of S	532.65	1.6	5586.98	SGL(25)
	O 1s	531.17	1.3	1087.97	SGL(25)

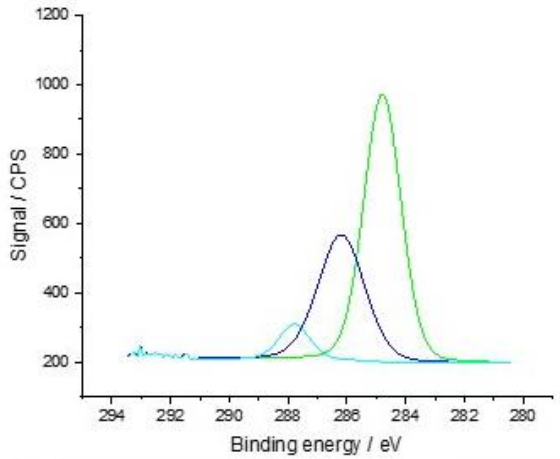

	Source energy: 1486.6 eV				
	Name	Position	FWHM	Area	LS
		eV		CPS eV	
	C 1s	284.79	1.49	1317.53	SGL(15)
	C -N / C-O	286.19	1.86	788.76	SGL(20)
	C=O/O-C-O/	287.79	1.23	149.48	SGL(25)

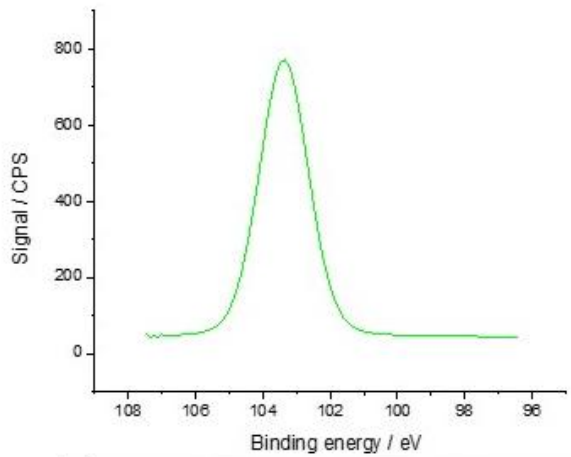

	Source energy: 1486.6 eV				
	Name	Position	FWHM	Area	LS
		eV		CPS eV	
	Si 2p of	103.38	1.71	1422.97	SGL(15)

Figure S.I.C5-4 XPS Sil. PIL 2 spectra.

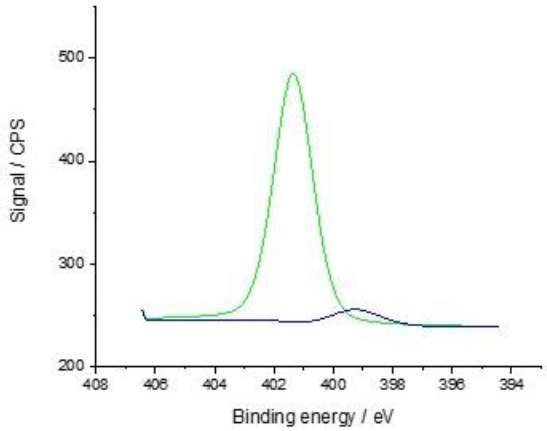

	Source energy: 1486.6 eV				
	Name	Position	FWHM	Area	LS
		eV		CPS eV	
	N 1s	401.35	1.53	444.65	SGL(25)
	Amide?	399.25	2	39.18	SGL(25)

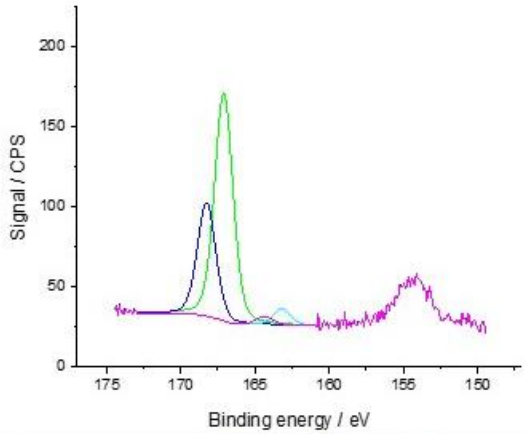

	Source energy: 1486.6 eV				
	Name	Position	FWHM	Area	LS
		eV		CPS eV	
	Sulphone 3/2	167.1	1.44	245.48	SGL(25)
	Sulphone 1/2	168.26	1.44	122.74	SGL(25)
	Sulfide / Thiol	163.19	1.37	17.39	SGL(25)
	Sulfide / Thiol	164.35	1.37	8.69	SGL(25)

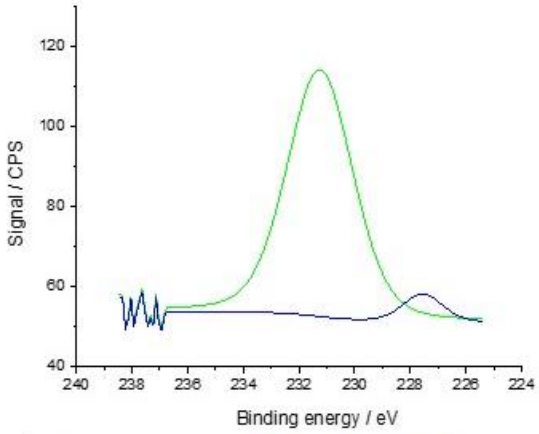

	Source energy: 1486.6 eV				
	Name	Position	FWHM	Area	LS
		eV		CPS eV	
	Sulphone	231.25	2.78	204.98	SGL(25)
	Sulfide / Thiol	227.55	1.69	14.06	SGL(25)

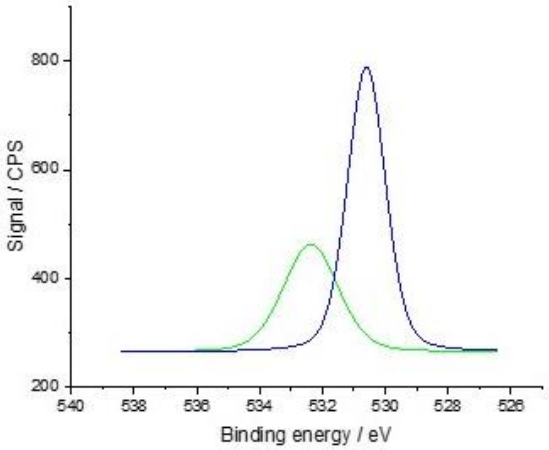

	Source energy: 1486.6 eV				
	Name	Position	FWHM	Area	LS
		eV		CPS eV	
	O 1s of	532.37	2.07	491.9	SGL(25)
	O 1s	530.6	1.43	895.18	SGL(25)

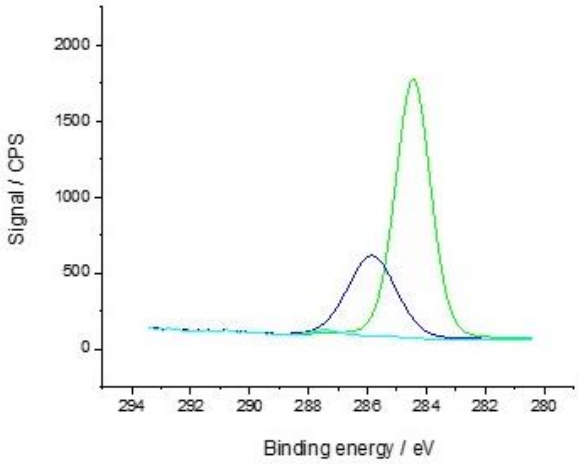

	Source energy: 1486.6 eV				
	Name	Position	FWHM	Area	LS
		eV		CPS eV	
	C 1s	284.45	1.38	2684.9	SGL(15)
	C -N / C-O	285.85	1.9	1150.26	SGL(15)
	C=O/C-C-O	287.45	1.1	45.79	SGL(25)

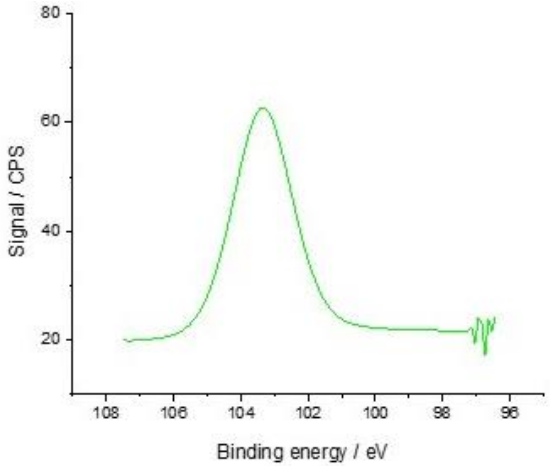

	Source energy: 1486.6 eV				
	Name	Positio	FWHM	Area	LS
		eV		CPS eV	
	Si 2p	103.36	2.08	105.29	SGL(25

Table S.I.C5-1 Linear range and extraction yield for each shrot chain alcohol. Sil. PIL 2 as sorbent, applied in a HS-ITEX-GC/MS method.

	tert-butanol			2-methyl-1-propanol			3-methyl-1-butanol			1-pentanol			1-hexanol		
c / µg L^{-1}	Peak area	Std. dev.	CV / %	Peak area	Std. dev.	CV / %	Peak area	Std. dev.	CV / %	Peak area	Std. dev.	CV / %	Peak area	Std. dev.	CV / %
0.55	1.0E+03	7.2E+01	7.1												
1	2.1E+03	1.2E+02	5.6												
5.5	9.4E+03	2.7E+03	28.9				6.6E+03	5.6E+02	8.5	1.2E+03	1.6E+02	13.6	2.8E+04	1.6E+03	5.9
10	1.6E+04	8.2E+02	5.0				8.0E+03	4.6E+02	5.7	2.2E+03	5.2E+02	23.5	3.2E+04	5.1E+03	15.7
55	9.7E+04	1.8E+04	18.1				5.7E+04	7.7E+03	13.5	2.4E+04	2.1E+03	8.5	2.2E+05	6.9E+04	31.8
100	1.4E+05	3.3E+04	24.5	8.2E+03	6.6E+01	0.8	1.5E+05	3.1E+04	21.1	4.1E+04	6.8E+03	16.6	5.3E+05	1.7E+05	32.7
550	6.4E+05	9.6E+04	14.9	4.7E+04	6.2E+03	13.1	8.2E+05	5.2E+04	6.3	2.2E+05	3.3E+04	15.0	2.4E+06	1.7E+05	7.1
1000	1.3E+06	1.4E+05	10.9	6.7E+04	7.4E+03	11.0	1.3E+06	1.0E+05	7.5						
5500	6.6E+06	1.3E+06	19.6	3.5E+05	6.3E+04	18.1									

Table S.I.C5-2 Para meters of the calibration curve in the linear range. Sil. PIL 2 as sorbent, applied in a HS-ITEX-GC/MS method.

Compound	m	b	R^2
tert-butanol	1198.6	12335	0.99
2-methyl-1-propanol	62.7	6203	0.99
3-methyl-1-butanol	1358.1	4947.5	0.99
1-pentanol	402.7	-21.6	0.99
1-hexanol	4324.1	15001	0.99

Chapter 6 General conclusions and outlook

The goal to achieve a fast, reliable, robust and high throughput method is an ongoing topic in analytical chemistry. [1] [2]

The workflow in analytical chemistry consists of mainly five steps, namely sample collection, sampling pretreatment/preparation, data acquisition, data analysis and report presentation. [3] [4] [5] Sample preparation consumes about 60 % of the analytical workflow time to generate a proper final method development. [5] In the case of ITEX, sorbent selection and optimization of extraction parameters are the key issues for a reliable and successful sample preparation.

To accelerate the sorbent selection, material characterization is required. Three commercial available sorbents for ITEX were investigated via inverse gas chromatography. Tenax TA proved to be the most suitable material. The thermodynamic data for PDMS, generated via inverse gas chromatography together with the experimental set-up presented in this work, compared to the reported literature [6] [7] [8], proved to be a realiable tool for material characterization. The literature comparison is limited, not many studies have characterized Tenax TA nor Carbopack C, but it opens a field to confirm/improve the data found in this thesis.

The measurements of the kinetic parameters at higher temperatures than the one reported here, would help to elucidate how these parameters vary according to the Arrhenius equation. [9]

A great variety of materials can be packed in ITEX, for this reason Carbopack B can be the next material to set under investigation. This graphitized carbon black is recommended as sorbent for analytes ranging between C_5 and $C_{12.}$ [10] With the future results, it would be possible to compare the data with the ones generated here and present a clearer difference among the sorbents used in this work. Carbopack B was not considered in this thesis because the focus here was on the characterization of ITEX sorbent materials offered by the manufacturer. The results from Chapter 3, could be applied as boundary values in a mathematical model to simulate the extraction procedure in ITEX. The extraction yield, according to the sorbent and analytes, could be estimated/predicted and by this the sorbent selection accelerated.

An interesting approach to apply inverse gas chromatography and the experiments in the range of infinite dilution, would be to verify air-water partitioning constants of solutes. In this

work, the 10 mL water samples stored in 20-mL HS vials were prepared at a concentration approaching the infinite dilution in the gas phase. To calculate this concentration, the air-water partition constants are needed. Aqueous samples containing pyridine were prepared to characterize Tenax GR. The results of this study, in order to perform inverse gas chromatography experiments in the range of infinite dilution, indicated that the gas phase concentration in equilibrium should be between 0.3 to 1 mg L^{-1}. The first run of experiments with the aqueous pyridine samples were prepared to reach the 0.3 to 1 mg L^{-1} gas phase concentration with an air-water partition constant equal to 4.4×10^{-4} , according to the first reference [11] [12], and recalculated with the Van´t Hoff equation for temperature correction (20 °C instead of 25 °C, yielding an air-water partition constant equal to 1.7×10^{-4}). The headspace of the aqueous pyridine samples was injected to the gas chromatograph and no signal was obtained. The procedure of preparing aqueous pyridine samples, to reach the gas phase equilibrium concentration was repeated, but with another literature source. [13] The air air-water partition constant reported equaled this time 1.1×10^{-2}. The first aqueous pyridine samples (at 29 mg L^{-1}) prepared to reach a 0.3 mg L^{-1} gas phase equilibrium concentration, did not yield any signal either. Then the aqueous samples were prepared again (at 50 mg L^{-1}), but to reach a gas phase concentration of 0.56 mg L^{-1}, under these conditions it was possible to obtain a signal and characterize the material with pyridine as probe compound. By this, checking and confirming the correct air-water partition constant that should be applied for the experiments.

The ITEX needle installed in a common gas chromatograph coupled to an FID, proved to be a versatile experimental set-up for material characterization.

The peaks obtained via inverse gas chromatography have a strong tailing. For this reason, the retention time of the peaks is estimated with the half mass point method. The raw data, triplicates, are converted into a text file and pasted to a numerical processor (excel). In the excel sheet an average of the measured triplicates is created (numerical representation of the chromatogram). This average is then transferred to another software (OriginPro) for analysis (manual integration). With the manual integration tool of the software, the retention time according to the half mass point method is estimated. This time is used to correct the retention from each of the measured peaks (the probe and the inert marker). Finally, it is possible to continue with the thermodynamic calculations and data interpretation. The technique yields accurate results, but the evaluation can be time consuming. With further knowledge of the software (setting a macro to estimate the retention time) and automated sample injection, the method can be improved.

The goal to apply new sorbents in microextraction techniques is of growing interest, because more selective materials with higher adsorption capacity than the commercial ones, is of great interest. [3] In Chapter 4 it was possible to investigate carbon based-nanomaterials as sorbent and polycyclic aromatic hydrocarbons as model analytes, in combination with design of experiments. Due to raw data amount, it is recommendable to apply mathematical models for analysis. [14] A large number of samples were measured and the optimal conditions were set within a short time frame. Once the most influential parameters have been selected, a Box-Behnken design, Central Composite design or Doehlert Matrix should be applied to determine the optimal conditions. [15] [16] The Box-Behnken design requires only three levels for the experimental plan, in comparison to a Central Composite design where five levels are needed, thus reducing the sample number and achieving sufficient data for the determination of the optimal parameters. Also, since it is not intended to predict extreme conditions, then the Box-Behnken design is a proper alternative over a Central Composite design for the determination of optimal parameters. [15] A Doehlert Matrix design has a comparable efficiency to a Box-Behnken design. [16] As a next approach, the Doehlert Matrix design could be applied and determine whether for the ITEX system represents a more suitable optimization procedure then a Box-Behnken design. The application of these surface response methodologies, represent a step further to improve sample preparation, because the optimal extraction conditions were established in a faster fashion, than with the common one-step-at-the-time optimization. [17] It was also observed, that especially fullerenes are a suitable sorbent for extraction of large polycyclic aromatic hydrocarbons and that carbon nanohorns or graphene sheets are preferable not applied. A rolled material, e.g.: fullerenes, MWCNTs or MWCNTs-COOH, seems a more suitable sorbent for extraction of large polycyclic aromatic hydrocarbons than materials organized in lattices like graphene. The sorption strength of the PAHs towards the carbon based-nanomaterials was not influenced by the oxygen amount on the surface. The larger PAHs, e.g.: pyrene over naphthalene, will have a stronger sorption during extraction, displacing the smaller PAHs and yielding higher method detection limits for the small PAHs. Tenax GR, with a 30% content of graphitized carbon and 70% of porous polymer, [18] was also applied as sorbent. The results revealed, that it does not offer enough contact sorption strength as sorbent for the extraction of the here studied polycyclic aromatic hydrocarbons. The application of carbon based-nanomaterials packed in ITEX and used as sorbent for the enrichment of samples out of the headspace is not a common extraction approach. They have proven to work [19] and with the results of this thesis, their use has been

broadened and would be recommended as sorbent for the extraction of polycyclic aromatic hydrocarbons.

For sorbent materials, where the thermostability is not clearly indicated and particle diameters smaller than 3 µm are present, a frit/filter should be included during the packing procedure. This is needed to avoid material loss and damage in the subsequent instruments. For initial experiments, low desorption temperatures (120 to 150 °C) should be set and only if no changes are observed after at least 90 samples (which is the number of samples run for the estimation of the extraction profile from 10 to 100 strokes at two low desorption temperatures), then the desorption temperature can increased stepwise. It is recommended after every run, to dismount the ITEX needle from the autosampler and tap the upper cannula body against a red/white surface to assure that no material loss happened. In Chapter 5, the packing procedure for unconventional sorbents such as polymeric ionic liquids, was described. In contrast to solid phase microextraction, in ITEX the material can be easily filled, which avoids extra preparative steps for bonding to the support, as in solid phase microextraction. [20] [21] The figures of merit obtained were in some occasions similar to commercial sorbent materials, but in others worse. The analytical performance of the polymeric ionic liquids, could be changed into a more hydrophobic character with a larger alkyl chain and other type of anion. [22] It would be also appealing to measure the same polycyclic aromatic hydrocarbons, as with the carbon based-nanomaterials, but with the polymeric ionic liquids as sorbent and compare them against the available literature. [20] As a further step, material characterization via inverse gas chromatography could also be performed to gain information about the sorbent.

The sorbent characterization and application of the ITEX technique was described in this work, as well as its versatility and meaningful use as a microextraction technique and as column in the inverse gas chromatography field. From the knowledge learned and the technology, facilities, opportunities that are at our reach, we are committed to transform them into solutions, to help and improve our constant changing world.

References

1. *http://www.chromatographyonline.com/overview-sample-preparation (accessed: April 27th 2016).*

2. Sampson, M.M., et al., *Simultaneous analysis of 22 volatile organic compounds in cigarette smoke using gas sampling bags for high-throughput solid-phase microextraction.* Anal. Chem., 2014. **86**(14): p. 7088-7095.

3. Fumes, B.H., et al., *Recent advances and future trends in new materials for sample preparation.* Trends Anal. Chem., 2015. **71**: p. 9-25.

4. Raterink, R.J., et al., *Recent developments in sample-pretreatment techniques for mass spectrometry-based metabolomics.* Trends Anal. Chem., 2014. **61**: p. 157-167.

5. Majors, R.E., *Sample preparation fundamentals for chromatography The measure of confidence.* Agilent Technologies, Inc. , 2013. **5991-3326EN**.

6. Sprunger, L., et al., *Characterization of the sorption of gaseous and organic solutes onto polydimethyl siloxane solid-phase microextraction surfaces using the Abraham model.* J. Chromatogr. A, 2007. **1175**(2): p. 162-173.

7. Pawliszyn, J., *Solid phase microextraction theory and practice*. 1997, Canada: Wiley-VCH. 1-247.

8. Endo, S., et al., *UFZ-LSER database v 2.1 [Internet], Leipzig, Germany, Helmholtz Centre for Environmental Research-UFZ. 2015. Available from https://www.ufz.de/index.php?en=31698&contentonly=1&m=0&lserd_data[mvc]=Public/start (accessed: June 4th 2016).*

9. Zhao, C., J. Li, and C. Zeng, *Determination of the infinite dilution diffusion and activity coefficients of alkanes in polypropylene by inverse gas chromatography.* J. Appl. Polym. Sci., 2006. **101**(3): p. 1925-1930.

10. Sigma-Aldrich, *Supelco specialty carbon adsorbents.* 2015(MQR 82950/T410081 1045).

11. Hawthorne, S.B., R.E. Sievers, and R.M. Barkley, *Organic emissions from shale oil wastewaters and their implications for air quality.* Environ. Sci. Technol. , 1985. **19**(10): p. 992-997.

12. *http://esc.syrres.com/fatepointer/webprop.asp?CAS=110861 (accessed: July 21st 2016).*

13. Staudinger, J. and P.V. Roberts, *A critical compilation of Henry's law constant temperature dependence relations for organic compounds in dilute aqueous solutions.* Chemosphere, 2001. **44**(4): p. 561-576.

14. Vogel, M.e.a., *Trendbericht Analytische Chemie 2014/2015.* Nachrichten aus der Chemie, 2016. **64**(Mai 2016): p. 491-594.

15. Wu, L., et al., *Application of the Box–Behnken design to the optimization of process parameters in foam cup molding.* Expert Syst. Appl., 2012. **39**(9): p. 8059–8065.

16. Ferreira, S.L.C., et al., *Box-Behnken design: an alternative for the optimization of analytical methods.* Anal. Chim. Acta, 2007. **597**(2): p. 179–186.

17. Bezerra, M.A., et al., *Response surface methodology (RSM) as a tool for optimization in analytical chemistry.* Talanta, 2008. **76**(5): p. 965-977.

18. Laaks, J., et al., *Optimization strategies of in-tube extraction (ITEX) methods.* Anal. Bioanal. Chem., 2015. **407**(22): p. 6827-6838.

19. Hüffer, T., et al., *Multi-walled carbon nanotubes as sorptive material for solventless in-tube microextraction (ITEX2)—a factorial design study.* Anal. Bioanal. Chem., 2013. **405**(26): p. 8387-8395.

20. Pang, L. and J.F. Liu, *Development of a solid-phase microextraction fiber by chemical binding of polymeric ionic liquid on a silica coated stainless steel wire.* J. Chromatogr. A, 2012. **1230**(23 March 2012): p. 8-14.

21. Feng, J., et al., *A novel aromatically functional polymeric ionic liquid as sorbent material for solid-phase microextraction.* J. Chromatogr. A, 2012. **1227**(2 March 2012): p. 54-59.

22. Panniello, A., et al., *Nanocomposites based on luminescent colloidal nanocrystals and polymeric ionic liquids towards optoelectronic applications.* Materials, 2014. **7**(1): p. 591.

Chapter 7 Appendix

List of Figures

List of Tables, Calculations and Methods

List of Abbreviations and Symbols

Adj. SS	Adjusted sum of squares
AIBN	Azobisisobutyronitrile
AMPS	2-acrylamido-2-methylpropane sulphonic acid
ANOVA	Analysis of variance
BBD	Box-Behnken design
BTEX	Benzene, toluene, ethylbenzene and xylenes
CCD (Introduction section 1.1 and Chapter 4.)	Central Composite design
CCD (Introduction section 1.2.4)	Charged-coupled device
CNM	Carbon based-nanomaterials
CNTs	Carbon nanotubes
CV	Coefficient of variation
DF	Degrees of freedom
DoE	Design of experiments
EI	Electron ionization
ETBE	Ethyl *tert*-butyl ether
EP	Elution plateau
FA	Frontal analysis
FACP	Frontal analysis by a characteristic point
FC	Finite concentration
FID	Flame ionization detector
GC	Gas chromatography
HPLC	High-performance liquid chromatography
HS	Headspace
HSSE	High-capacity headspace sorptive extraction
IGC	Inverse gas chromatography
ILs	Ionic liquids
ITEX	In-tube extraction
K	Partition constant/Henry constant
LC	Liquid chromatography
MDL	Method detection limit
MPS	3-mercaptopropyl trimethoxysilane
MS	Mass spectrometry
MTBE	Methyl *tert*-butyl ether
MWCNTs	Multi-walled carbon nanotubes
MWCNTs-COOH	Functionalized multi-walled carbon nanotubes
N	Number of experiments/runs according to the Design of Experiments

NT	Needle trap
PAHs	Polycyclic aromatic hydrocarbons
PDMS	Polydimethylsiloxane
PFBHA	*o*-2,3,4,5,6-(pentafluorobenzyl)hydroxylamine hydrochloride
PIL	Polymeric ionic liquids
PTFE	Polytetrafluoroethylene
RSD	Relative standard deviation
RSM	Response surface methodology
SBSE	Stir bar sorptive extraction
SEM	Scanning electron microscopy
S/N	Signal-to-noise ratio
Sil. PIL 1 or 2	Silica polymeric ionic liquid 1 or 2
SSA	Specific surface area
SSM	Single magnet mixer
SPDE	Solid phase dynamic extraction
SPE	Solid phase extraction
SPMTE	Solid phase membrane tip extraction
SPME	Solid phase microextraction
SPNE	Solid phase nanoextraction
S/SL	Split/Splitless injector
Std. dev.	Standard deviation
SWCNTs	Single-walled carbon nanotubes
TGA	Thermal gravimetric analysis
TEM	Transmission electron microscopy
UV	Ultraviolet detector
VIm	Vinylimidazole
XRD	X-ray diffraction
XPS	X-ray spectroscopy

A	Surface area of sorbent
b	y-axis intercept
C	Slope from the linear section of the van Deemter plot
c_p	Central points
D	Desorption temperature
D^{∞}	Diffusion coefficient in the sorbent
D*	Dispersion coefficient
d	Peak width at half height maximum
d_p	Particle diameter
F (Chapter 3)	Column flow
F (Chapter 4)	Extraction flow
F-value	Fisher´s value
f_{i1}, f_{i2}	Fraction of the analyte (i) in the corresponding phase (1 or 2)
H	Plate Height

ΔHs	Sorption enthalpy
$\Delta_f H$	Gas formation enthalpy
j	James-Martin compressibility factor
k (Introduction 1.1)	Number of factors in a response surface methodology
k (Chapter 3)	Partition ratio
K_d	Partitioning constant between the solid and gas phase
l	Length of the packed sorbent material
m	Slope
m	Mass of the sorbent or stationary phase
n	Repeated units of the material
PA	Polyacrylate
P	Ratio between inlet and outlet pressure
P_{app}	Apparent permeability
p-Value	Result from the F-test for a lack of fit
p_0	Outlet pressure (atmospheric)
R	Gas constant
R^2	R-squared
S	Extraction strokes
S_c	Standard deviation
T (Chapter 3)	Column temperature
T (Chapter 4)	Extraction temperature
t	Student's t value
t_0	Inert marker retention time
t_r	Probe retention time
v_{cg}	Mobile phase velocity
V_g	Specific retention volume
V_N	Net retention volume
V_P	Volume of the stationary phase
y_0	Mole fraction of the solute in the gas phase
d_q/d_c	Slope of the adsoprtion isotherm at the corresponding concentration
$\Delta t = t_r - t_0$	Time difference between the probe (t_r) and the inert marker (t_0)
η	Dynamic viscosity of the mobile phase
ρ	Density of the mobile phase

List of Publications

Articles

Rahman, M.M., Osorio Barajas, X. L., Luján Hermosillo, J. L., Jochmann, M. A., Mayer, C., Schmidt, T. C., *Core-shell hybrid particles by alternating copolymerization of ionic liquid monomers from silica as sorbent for solid phase microextraction.* Macromol. Mater. Eng., 2015. 300(11): p. 1049-1056.

Weigold, P., Ruecker, A., Jochmann, M., Osorio Barajas, X. L., Lege, S., Zwiener, C., Kappler, A., Behrens, S., *Formation of chloroform and tetrachloroethene by Sinorhizobium meliloti strain 1021*. Lett. Appl. Microbiol., 2015. 61(4): p. 346-353.

Ruecker, A., Weigold, P., Behrens, S., Jochmann, M., Osorio Barajas, X. L., Kappler, A., *Halogenated hydrocarbon formation in a moderately acidic salt lake in Western Australia - Role of abiotic and biotic processes.* Environ. Chem., 2015. 12(4): p. 406-414.

Hüffer, T., Osorio, X. L., Jochmann, M. A., Schilling, B., Schmidt, T. C., *Multi-walled carbon nanotubes as sorptive material for solventless in-tube microextraction (ITEX2)—a factorial design study*. Anal. Bioanal. Chem., 2013. 405(26): p. 8387-8395.

Poster presentations

Osorio Barajas, X. L., Hüffer, T., Mettig, P., Schilling, B., Jochmann, M. A., Schmidt, T. C. *DoE application for the investigation of carbon based-nanomaterials as sorbent via headspace in-tube extraction*, Analytica, May 10th to 13th 2016, Munich, Germany.

Osorio Barajas, X. L., Hüffer, T., Jochmann, M. A., Schmidt, T. C. *In-Tube Microextraction (ITEX) and carbon-based nanomaterials (CNM) in combination with Design of Experiments: Determination of Polycyclic Aromatic Hydrocarbons (PAHs)*, ANAKON 2015, March 23rd to 26th 2015, Graz, Austria.

Oral presentations

Osorio Barajas, X. L., Jochmann, M. A., Schilling, B., Hüffer, T., Schmidt, T. C., *Inverse Gaschromatographie zur Charakterisierung von Sorbenzien in Mikroextraktionstechniken*, Doktorandenseminar Hohenroda, January 10th to 12th 2016, Hohenroda, Germany.

Osorio Barajas, X. L., Jochmann, M. A., Schilling, B., T., Schmidt, T. C., *Inverse Gaschromatographie zur Charakterisierung von Sorbenzien in Mikroextraktionstechniken*, Doktorandenseminar „Adsorption", August 25th to 26th 2015, Magdeburg, Germany.

Curriculum Vitae

Erklärung

Hiermit versichere ich, dass ich die vorliegende Arbeit mit dem Titel

„Sorbent characterization and application of the in-tube microextraction technique"

selbst verfasst und keine außer den angegebenen Hilfsmitteln und Quellen benutzt habe, und dass die Arbeit in dieser oder ähnlicher Form noch bei keiner anderen Universität eingereicht wurde.

Essen, 12. September 2016

Danksagung

Mein Herzlicher Dank gilt Herrn Prof. Dr. Torsten C. Schmidt, für die Zeit, Nettigkeit, Aufmerksamkeit, Hilfe, Mühe und Vertrauen, damit diese Arbeit und mein Aufenthalt möglich waren. Vielen Dank, dass ich von Dir lernen durfte und für alle die Möglichkeiten, die daraus entstanden sind.
Ich möchte Herrn PD Dr. Hans-Georg Schmarr für die Übernahme des Zweitgutachtens bedanken, sowie für die interessante Gaschromatographie Kurse und für die Leidenschaft der Önologie. An Herrn Dr. Maik A. Jochmann, für die nette Betreuung, Hilfsbereitschaft und Ratschläge.

Meinen besten Dank gilt auch an Herrn Dr. Thorsten Hüffer, für die tolle Zusammenarbeit über Jahren, Geduld, harter Arbeit, Zeit und Mühe. Ein Grundstein für diese Arbeit.
Herrn Beat Schilling, herzlichen Dank für Deine Hilfe in alle möglichen Gebiete, Verständniss und Nettigkeit.
Ich möchte Herrn Dr. Alexander Rücker bedanken, für die schöne Zeit im Labor und der Zusammenarbeit.

Frau Lydia Vaaßen und Frau Claudia Ullrich, lieben Dank für Eure Unterstützung (nicht nur beruflich) und Bereitschaft.

Dr. Thomas Bahners und Dr. Hansjörg Majer, gehört mein Dank für die Erweiterung meines Wissens und für die persönliche nette Unterstützung bei Fragen. Danke sehr.

Vielen Dank an der gesamten Abteilung der Instrumentelle Analytische Chemie, in der ich wichtige Jahre meiner persönliche Entwicklung verbracht habe und viel von allen und alles gelernt habe. Vielen und lieben Dank an meinen Freundschaften.

Mi querida Mamá y querido Papá, increíble todo lo que han hecho por nosotras. Invaluable su apoyo, amor, fuerza y paciencia, los quiero mucho y Muchas gracias por Todo. Querida Toch y familia, en especial a las lindas de Vale y Sofi. Lo hemos logrado.